THESIS

EVALUATION OF ADVANCED AIR-FUEL RATIO CONTROL STRATEGIES AND THEIR EFFECTS ON THREE-WAY CATALYSTS IN A STOICHIOMETRIC, SPARK IGNITED, NATURAL GAS ENGINE

Submitted by

Andrew Lawrence Jones

Department of Mechanical Engineering

In partial fulfillment of the requirements

For the Degree of Master of Science

Colorado State University

Fort Collins, Colorado

Spring 2021

Master's Committee:

Advisor: Daniel B. Olsen

Anthony Marchese
Jerry Johnson

ABSTRACT

EVALUATION OF ADVANCED AIR-FUEL RATIO CONTROL STRATEGIES AND THEIR EFFECTS ON THREE-WAY CATALYSTS IN A STOICHIOMETRIC, SPARK IGNITED, NATURAL GAS ENGINE

Engine emissions are a growing concern in the 21st century. As the world works to combat rising pollution levels, engine emissions are under scrutiny. Natural gas engines are increasing in popularity over diesel engines, due to the high availability of fuel and fewer pollutant emissions than comparable diesel engines. Pollutants such as NOx, CO, and THCs (total hydrocarbons) are harmful to the environment and are currently regulated, and limits for these pollutants are expected to decrease further in the future. A three-way catalyst (TWC) is a cost-effective exhaust after treatment system can be used to reduce pollutant emissions through a series of reactions that are catalyzed by special conditions within the catalyst. Using TWCs, emissions can be drastically reduced using simple chemical reactions, without affecting engine performance. Air-fuel ratio dithering is a strategy that can be used to increase catalyst reduction efficiency by utilizing the oxygen storing properties of ceria, a material in the catalyst washcoat. Dithering is a method of periodically varying the air-fuel ratio of the engine around an optimum point. The focus of this work is understanding how dithering affects oxygen storage in a catalyst, as well as how dithering amplitude and frequency can be tuned to maximize catalyst efficiency. Experiments were performed on a CAT CG137-8, a stationary natural gas engine used for gas compression. Three different catalysts were tested, including the standard catalyst for the test engine, a custom catalyst with one half of the oxygen storage capability of the standard catalyst,

and the standard catalyst artificially aged to 16,000 hours. Emissions data were collected across a dithering parameter sweep where a large number of amplitude and frequency combinations were tested. Additionally, steady state and dithering air-fuel ratio sweeps were performed to investigate the emissions window of compliance across a wide range of air-fuel ratios.

It was found that dithering with optimized amplitude and frequency can significantly reduce pollutant emissions with a fresh catalyst. However, dithering does not have a large effect on aged catalysts. Additionally, dithering was shown to improve the window of emissions compliance on a standard catalyst by 100% but showed a smaller improvement on a catalyst with ½ oxygen storage capability. The window of compliance with an aged catalyst was unimproved by dithering. Optimized dithering has the potential to significantly reduce engine emissions, allowing for compliance with more stringent emissions requirements or for less expensive catalysts to be used.

ACKNOWLEDGEMENTS

I would like to recognize the people and groups who supported during the work presented in this Thesis. Caterpillar for sponsoring and funding this study. My advisor, Dr. Daniel B. Olsen, for his support throughout my graduate studies and allowing me to work within his research group. Dr. Anthony Marchese for his interest in this work, for the time he invested on my behalf, and for the guidance he provided me throughout this process. I would also like to thank Dave Montgomery, Jas Singh, Ron Silver, Eric Fierson from Caterpillar Inc. for their support throughout the whole project, from providing advice at every turn. Along with Greg Hampson from Woodward Inc. for his assistance with data processing and installation of their donated LECM on the CFR engine test cell. Additionally, Jeffrey Carlson for his help with programming and troubleshooting the LECM in the engine test cell. To my lab intern Rachel Lorenzen, who helped with countless tasks and issues in the engine test cell, as well as helped process and create figures from the mountains of data that were collected. The powerhouse staff – Mark, Kirk, and James, who guided me through months of troubleshooting and engine test cell development. I would also like to thank many others who assisted me – Scott, Alex, and Mars. Finally, my parents Anne and Larry along with the rest of my friends and family, who endlessly supported me every step of the way.

TABLE OF CONTENTS

LIST OF TABLES

LIST OF FIGURES

CHAPTER 1: INTRODUCTION

1.1 BACKGROUND AND MOTIVATION

Reducing internal combustion engine emissions is an important goal as concerns about climate change and pollution grow in the 21st century. Engine manufacturers must consider both current and future emissions regulations when designing engines. In addition to meeting cost and performance targets, engines must also meet limits on emissions of harmful pollutants such as NOx and CO. In industrial applications, natural gas (NG) is becoming widely used as a replacement for other fossil fuels such as diesel and gasoline [1]. Spark ignited (SI) natural gas fueled engines produce fewer pollutants than comparable diesel engines, while emitting less CO_2 than all other equivalent engines [2].

Stationary natural gas engines are used for natural gas compression and power generation across the United States and are subject to federal emissions regulations. Compression stations are typically in remote locations, used to ensure adequate gas pressure along transmission lines. Engines in these stations must be incredibly durable, as service intervals are long and they operate continuously in all conditions. Stochiometric engines are typically used in this application because of their simplicity and reliability. Stoichiometric engines operate at an air-fuel ratio where there is exactly enough air to burn with the fuel. Stochiometric engines are often referred to as rich burn engines because their point of lowest emissions is slightly rich of the stoichiometric point. This is in contrast to lean burn engines which operate with a significant amount of excess air.

Small and medium sized stoichiometric engines are subject to the EPA "Quad J" regulations. Stationary natural gas engines over 100 hp must comply with the NSPS Title 40, Part 60, Subpart JJJJ rules. State and local governments often have stricter emissions regulations, the strictest being the Pennsylvania GP5 regulations.

Table 1: Local and state emissions levels are often stricter than federal emissions regulations. EPA JJJJ is the current federal emissions limit for stationary gas engines above 100 hp, while the PA GP5 regulation is the strictest local regulation.

	g/kW-hr (g/bhp-hr)		
	NOx	CO	VOC
EPA JJJJ	1.3 (1.0)	2.6 (2.0)	0.92 (0.7)
PA GP5	0.325 (0.25)	0.39 (0.3)	0.26 (0.2)

Emissions from stoichiometric natural gas engines can be effectively minimized with the use of a three-way catalyst (TWC) without negatively effecting engine performance. With the use of a TWC, NG engines have the potential to meet stringent requirements [3]. TWC performance has been studied extensively in SI gasoline engines, as is typical in automobiles. Advances have been made in catalyst materials as well as engine control strategies, but natural gas engines have not yet been studied with TWCs as extensively.

Precise air-fuel ratio (AFR) control is required on stoichiometric engines for TWCs to function properly. In stoichiometric exhaust conditions, there is a balance between oxidizing (NOx and O_2) and reducing (H_2, CO, HC) gases that results in near complete conversion of these gases into CO_2, N_2, and H_2O. There is a narrow window of AFRs around the stoichiometric point (λ=1, where $\lambda = AFR_{actual} / AFR_{stoich}$ and AFR refers to the air to fuel ratio) where adequate levels

of reducing and oxidizing species are present for the TWC to meet emissions requirements [4]. Lambda (λ) is typically used to normalize air fuel ratio and is defined as:

$$\lambda = \frac{AFR_{actual}}{AFR_{stoichiometric}} \quad (1)$$

TWC pollutant reduction efficiency is defined as:

$$Conversion\ Efficiency = \left(1 - \frac{pollutant\ emissions\ (postcat)}{pollutant\ emissions\ (precat)}\right) * 100 \quad (2)$$

1.2 LITERATURE REVIEW

Three-way catalysts have been used since the late 1970s to reduce NOx emissions from engines. They rely on complex reactions between exhaust species that are catalyzed by the platinum-group metals in the catalyst. The most prominent of these reactions are listed in Table 2.

The governing equations of the reaction are highly dependent on catalyst temperature, as well as oxygen content. When engine is running rich, there will be a shortage of oxygen, causing increased CO and THC emissions. When the engine is running lean, there is extra O_2 in the exhaust, which oxidizes CO and THCs more readily than NOx, resulting in increased NOx emissions. There is a minimum balance point between pre-catalyst CO and NOx emissions where their concentrations meet. This point occurs slightly on the rich side of stoichiometric. Figure 1 shows that the equivalence point for the CAT CG137-8 engine used in this test. NOx formation is exponentially related to peak combustion temperature, which is achieved right at

stochiometric, or just lean of stochiometric [5]. NOx formation is at a maximum in these conditions. As the air-fuel mixture becomes rich, NOx formation declines as combustion temperatures decrease. However, THCs and CO increase in concentration as byproducts of incomplete combustion. CO emissions increase rapidly as the mixture becomes rich because there is enough oxygen to convert the fuel to CO. THC emissions remain low as the mixture becomes rich because most of it is converted to CO in the scope of this lambda sweep.

Table 2: Major reactions occurring in a three-way catalyst for a natural gas engine.

$CO + \frac{1}{2}O_2 \leftrightarrow CO_2$	$H_2 + \frac{1}{2}CO_2 \leftrightarrow H_2O$
$C_xH_y + \left(x + \frac{y}{4}\right)O_2 \leftrightarrow xCO_2 + \frac{y}{2}H_2O$	$C_xH_y + xH_2O \leftrightarrow \left(x + \frac{y}{2}\right)H_2 + xCO$
$2NO + 2H_2 \leftrightarrow 2H_2O + N_2$	$NO + CO \rightarrow \frac{1}{2}N_2 + CO_2$
$2NO + 5CO + 3H_2O \rightarrow 2NH_3 + 5CO_2$	$2NO + CO \rightarrow N_2O + CO_2$
$NO + H_2 \rightarrow \frac{1}{2}N_2 + H_2O$	$2NO + 5H_2 \rightarrow N_2O + H_2O$

Methane (CH_4) is a relatively stable fuel, making it difficult to burn. Typical pipeline natural gas is usually between 85%-95% methane, meaning that methane is a large contributor to hydrocarbon emissions.

If stochiometric or near stochiometric conditions are not met in the engine, the concentrations of NOx, CO, and THC will not be present in the correct quantities in the catalyst to satisfy the equations in Table 2. At steady-state operating conditions, the TWC will have significantly reduced effectiveness, potentially allowing post-catalyst emissions to drift out of compliance. Figure 2 shows the operating window for a stoichiometric engine [6]. Engine

emissions increase significantly as the air-fuel ratio drifts away from a stoichiometric λ=1.00. As the mixture becomes rich, CO emissions climb dramatically, and as the mixture becomes lean, NOx emissions climb dramatically. For this reason, air-fuel ratio control is incredibly important for a stoichiometric engine with a three-way catalyst.

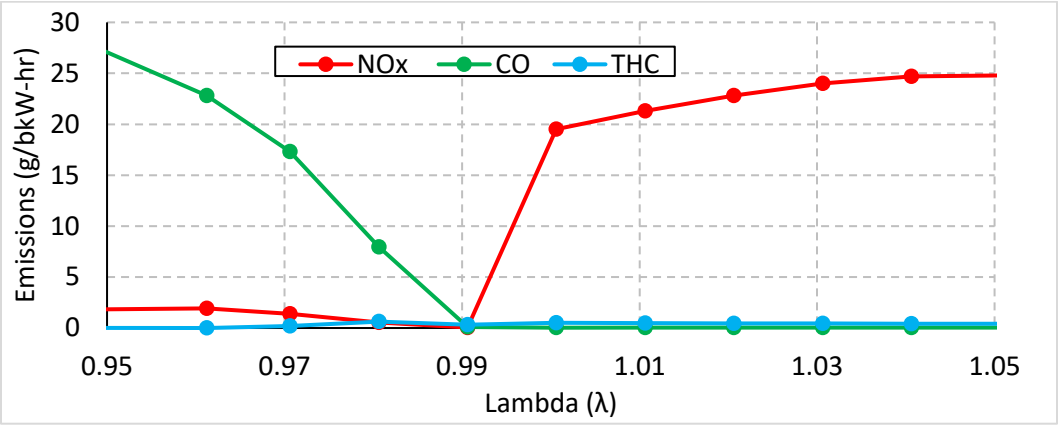

Figure 1: Post-catalyst emissions for the CAT CG137-8 natural gas engine are at a minimum at λ=0.990.

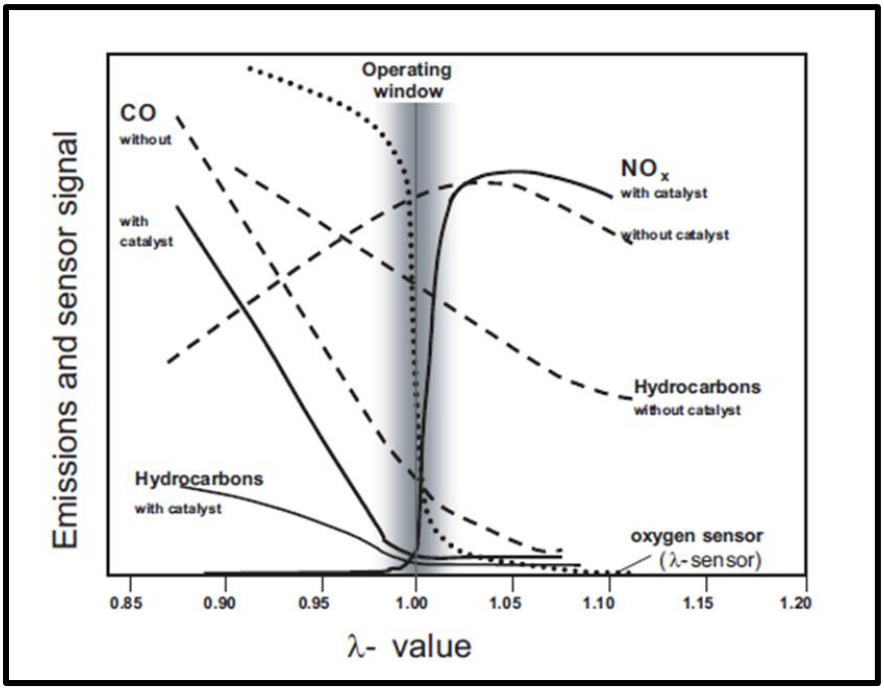

Figure 2: Three-way catalysts are only effective at reducing emissions close to a stoichiometric air-fuel ratio.

1.3 OXYGEN STORAGE AND DITHERING IN SI GASOLINE ENGINES

The narrow air-fuel ratio window for meeting emissions limits causes problems under transient conditions, when the air-fuel ratio cannot be precisely controlled. In automotive engines, these transients are introduced by rapidly changing engine loads and speeds. In a stationary industrial engine, the main transient is varying fuel composition, but other transients can be present, including the load. The role of the oxidation and reduction of the washcoat in the catalyst has been studied and modelled in automotive engines running on gasoline.

A catalyst is made of three important parts. The first is the outer shell, which often includes insulation for heat retention. Inside the outer shell is the substrate, a ceramic or metallic honeycomb that supports the washcoat. The washcoat covers the substrate and has a high surface area exposed to the passing exhaust gasses. Catalyst washcoats are made up of alumina, ceria, and precious metals such as platinum, rhodium and palladium, which function to catalyze the reactions described in Table 2

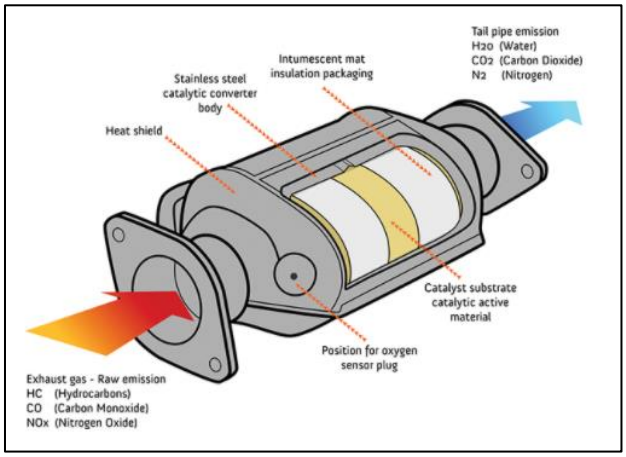

Figure 3: A three-way catalyst includes a housing, substrate, and washcoat on the substrate. The washcoat contains the compounds that catalyze the reactions.

Ceria (Ce_2O_3, CeO_2) and alumina (Al_2O_3, AlO_2) are used as a structural support in the washcoat of a three-way catalyst. Precious metals which perform that catalyzing reactions are absorbed into the ceria and alumina. These catalyzing metals include: rhodium (Rh), platinum (Pt), and palladium (Pd) [7].

Ceria makes up about 30% of the washcoat by mass and has multiple functions, which are stabilization of the washcoat layer, improvement of thermal resistance, enhancement of precious metal catalytic activity, and operation as an oxygen storage component [8]. The oxygen storage property of ceria in a catalyst is the primary area of interest for transient catalyst operation.

Under transient conditions, ceria can store oxygen while the engine is running lean, and then release oxygen while the engine is rich. It has been widely proven that intentional air-fuel ratio fluctuation or "dithering" can provide better transient response from catalysts. This effect was first studied on engines that had unintentional fluctuations at GM in 1983, and it was found that controlling the cyclic fluctuations allowed the engines to remain in emissions compliance in air-fuel ratio areas where they would usually be out of compliance in steady state operation [9].

In the study performed by GM, the air-fuel ratio was stepped from lean to rich, and rich to lean. When the ratio was stepped from lean to rich, it was expected that the post-catalyst emissions would contain large amounts of CO, a result of the rich air-fuel ratio. However, the post-catalyst CO emissions were lower than expected, directly after the shift. This same test was also run with a catalyst that did not contain cerium but was otherwise identical. The results for the non-cerium catalyst did not show the slower ramp of CO emissions, and more closely matched the expected steady-state result. The left side of Figure 4 shows the expected results for CO emissions during a lean-rich shift. The catalyst that did not contain cerium did not store

oxygen for release and CO reduction in an air fuel ratio shift. The right side shows the same air-fuel ratio shift from lean to rich and CO emissions from a catalyst containing cerium. As can be seen in the bottom left corner, the actual CO emissions trailed the predicted emissions due to oxygen release in the catalyst, allowing CO to be converted to CO_2. The catalyst that does not contain cerium does not store oxygen for release in an air fuel ratio shift. The reactions that occur with the ceria in the catalyst are more clearly defined in Table 3.

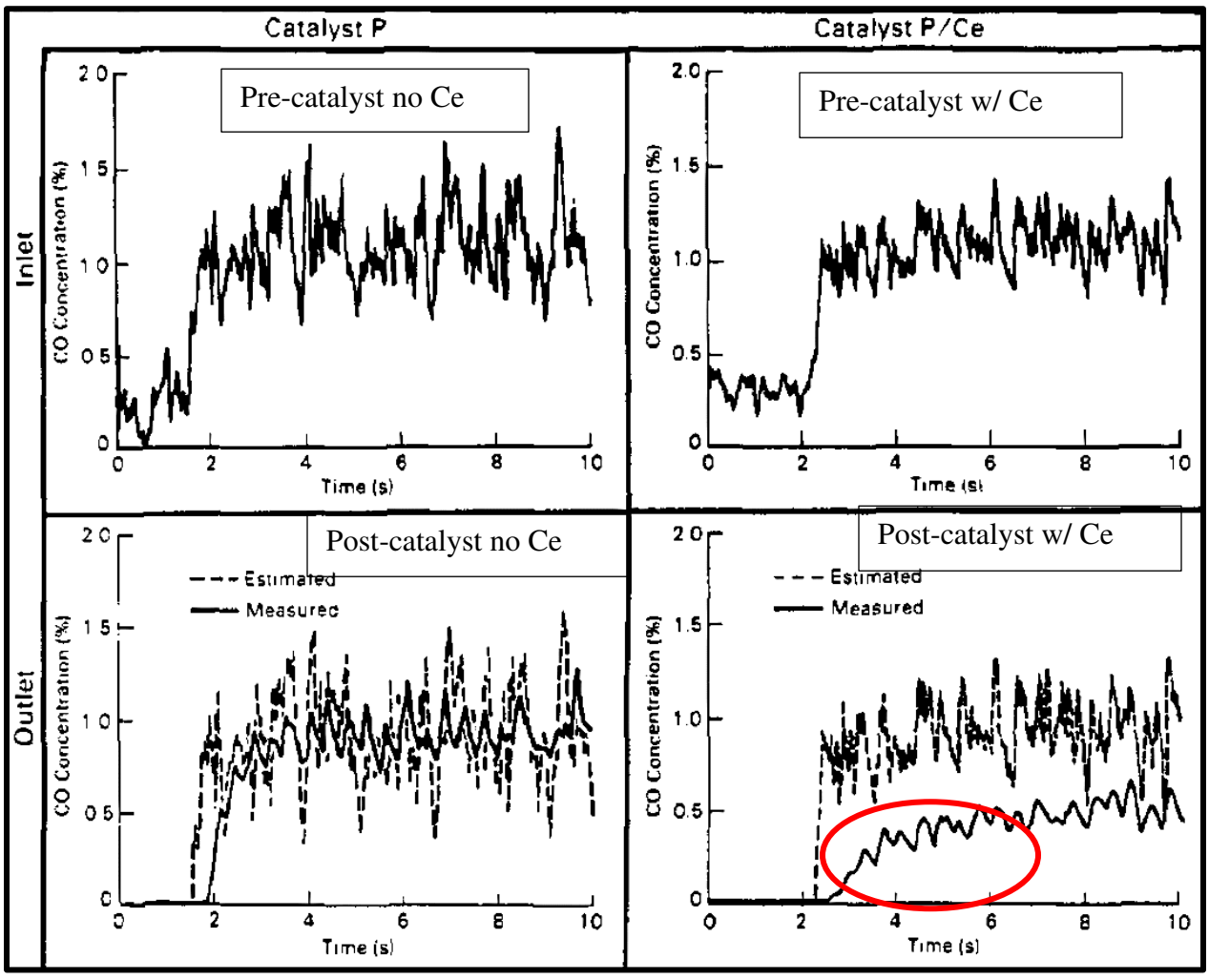

Figure 4: CO Emissions Pre and Post-Catalyst for a catalyst with and without Cerium. The red circle shows how the catalyst with cerium has lower than expected CO emissions during a lean-rich shift, due to oxygen release [10].

Table 3: Oxygen storage reactions with ceria

Rich (Oxygen Release)	Lean (Oxygen Storage)
$CO + 2CeO_2 \rightarrow Ce_2O_3 + CO_2$	$Ce_2O_3 + \frac{1}{2}O_2 \rightarrow 2CeO_2$
$H_2 + 2CeO_2 \rightarrow Ce_2O_3 + H_2O$	$Ce_2O_3 + NO \rightarrow 2CeO_2 + \frac{1}{2}N_2$

Equations shown in Table 3 are also highly dependent on temperature, with the oxygen storage happening more effectively at higher temperatures [11]. During steady state operation, the ceria will become either entirely saturated with oxygen or completely depleted, making the oxygen content of pre and post-catalyst exhaust flows equivalent. Then, if there is an air-fuel ratio shift, the oxygen storage capabilities may not be utilized. Additionally, average CO and NO conversion efficiency is higher when the air fuel ratio is oscillated periodically, due to the reduction and oxidation of the cerium in the catalyst [12]. These reactions in Table 3 supplement the steady state catalyst reactions in Table 1 .

1.4 OXYGEN STORAGE AND DITHERING IN SI NATURAL GAS ENGINES

The catalysts used on stationary natural gas engines are nearly identical to those used on gasoline engines, and accomplish the same task, which is to simultaneously reduce NOx, CO, and THC emissions. Three-way catalysts are used on stoichiometric engines and are most effective around a point slightly on the rich side of stoichiometric.

If no dithering strategy is applied (if the air-fuel ratio is held constant), there will be a small window of emissions compliance where both NOx and CO are converted effectively.

Figure 5 shows this window of compliance for certain conditions on an 80kW Cummins-Onan Genset. Emissions are limited on the left side by NOx regulations (2 g/bhp-hr for the Cummins-Onan Genset) and on the right side by CO regulations (4 g/bhp-hr for the Cummins-Onan Genset). On many engine/catalyst configurations, this window of emissions compliance can be extremely small, sometimes within equivalence ratio windows of 0.002 equivalence ratio [13].

In other experiments, the optimal air-fuel ratio for engine operation was found using an air-fuel ratio scan, where the ratio is varied from lean to rich in steps, and pre- and post- catalyst emissions data is recorded. It was found that on a natural gas engine, the optimal point for catalyst efficiency where NOx and CO removal efficiencies were near 95% was at an equivalence ratio of 1.014. This will vary between engines and catalysts, but this strategy can be used to find the optimal equivalence point.

Dithering strategies can then be applied to the fueling to further increase catalyst efficiency. With dithering, the air fuel ratio is oscillated periodically around the equivalence point that was previously determined. Both the frequency and amplitude of this wave form can be modulated, resulting in optimal oxygen storage and release within the catalyst. The amplitude and frequency must be determined experimentally for a given engine/catalyst system.

Shi et al performed testing of different dithering frequencies and amplitudes to find the optimal conditions for oxygen storage in their single cylinder CFR engine [14].

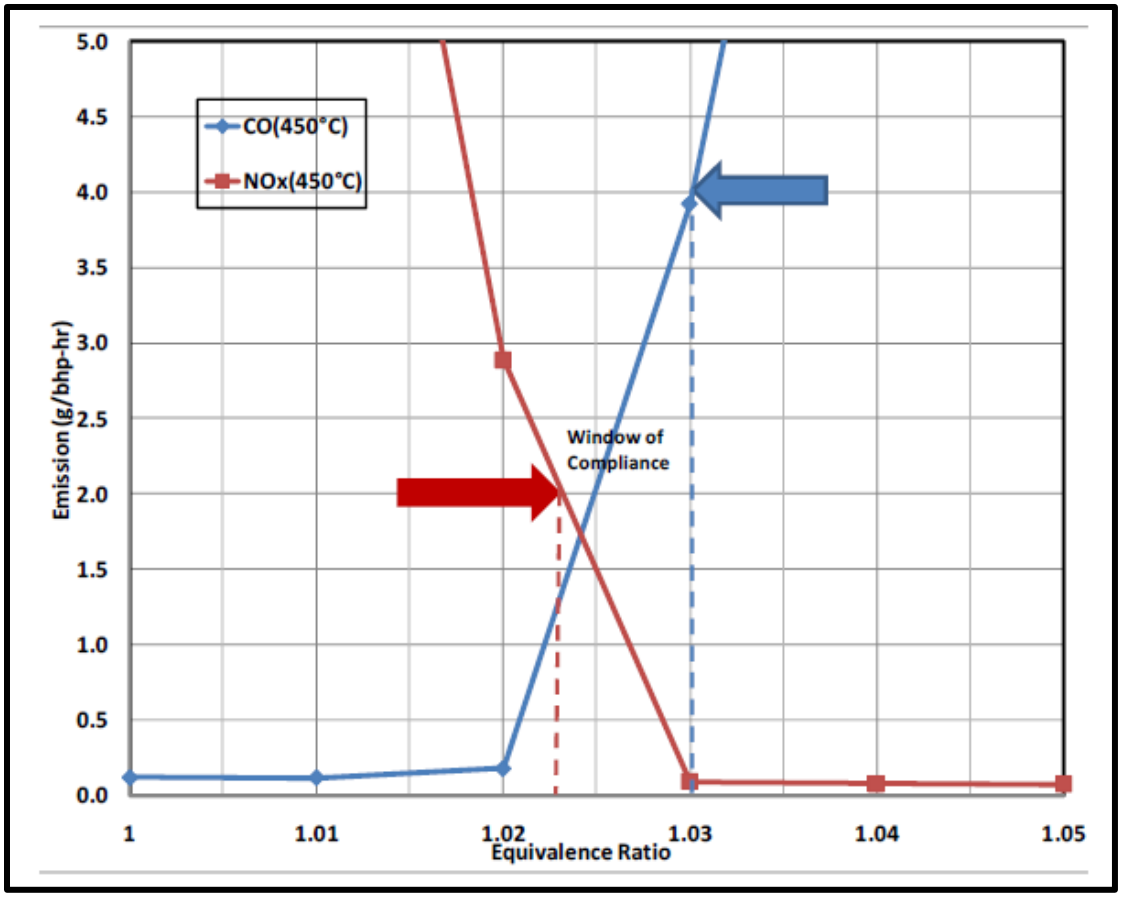

Figure 5: Window of Emissions Compliance for Cummins-Onan Genset. Window of compliant operation is bounded by NOx and CO emissions.

Frequency adjustments	Amplitude adjustments
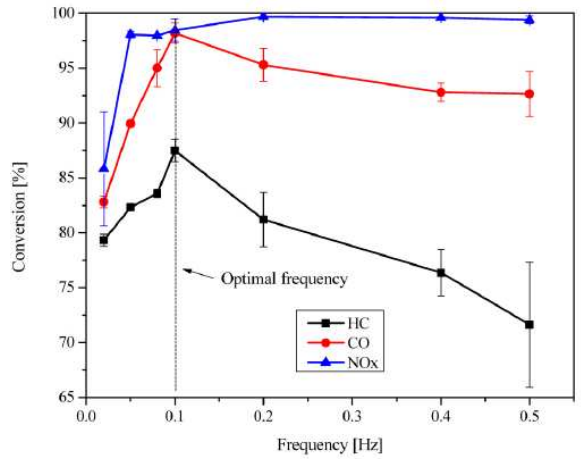	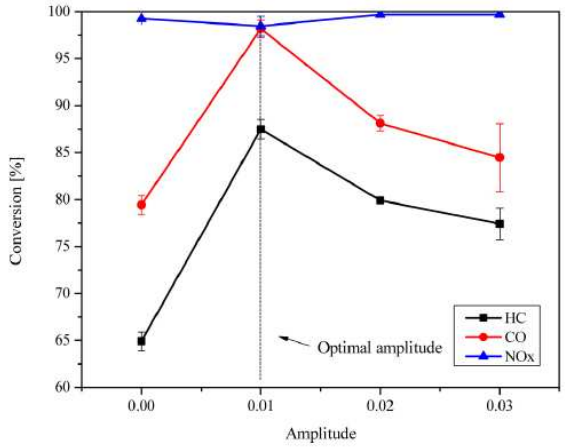

Figure 6: Dithering Amplitude and Frequency Adjustments and their Effect on Conversion Efficiency. This experiment found the optimal frequency for dithering was 0.1 Hz, with the optimal amplitude being 0.01λ.

Figure 6 shows that the optimal frequency was 0.1 Hz, and the optimal amplitude was 0.01λ. This corresponds closely with the findings of Defoort et al, as they settled on a frequency of 0.2 Hz and amplitude of 0.01 equivalence ratio for their engine. These closely matched results suggest that frequencies around 0.2 Hz and amplitudes of around 0.01 are a good place to start when fine tuning post-catalyst emissions to gain maximum possible conversion efficiency.

The time for a catalyst to become completely reduced or oxidized can vary, so the frequency must be adjusted accordingly. If the frequency is too high, the system will simply act like a rich burn steady state system would, because the oxidation and reduction reactions do not have time to complete. Additionally, periodic fluctuations in pre-catalyst exhaust will diffuse together between the exhaust port and the catalyst, effectively delivering a constant, average exhaust stream to the catalyst [15]. If the frequency is too slow, the catalyst will become entirely reduced or oxidized, resulting in the less efficient steady state operation until the mixture shifts back in the other direction.

There are many reactions occurring during oxygen storage and release, but they can be accurately simplified to the reactions shown in Table 3. When the engine is running lean, there is excess O_2. Usually, this would mean that NO is not reduced, but the oxygen from NO is stored in the catalyst washcoat. Then, when the engine oscillates to running rich, there would normally be a lack of oxygen to oxidize CO into CO_2. However, when the appropriate dithering conditions are met, oxygen to oxidize CO will be supplied from what is stored in the washcoat.

Figure 7 shows oxygen storage in the catalyst as observed by Gattoni and Olsen on a 7.5L Cummins-Onan rich-burn genset. This data shows optimized dithering, with oxygen storage and release keeping the oxygen concentration post-catalyst constant. The solid black line represents the pre-catalyst oxygen concentration, and the dotted line represents the post-catalyst oxygen concentration. The pre-catalyst oxygen concentration fluctuates with the fuel dithering, but the post-catalyst concentration remains relatively constant due to the oxygen storage and release.

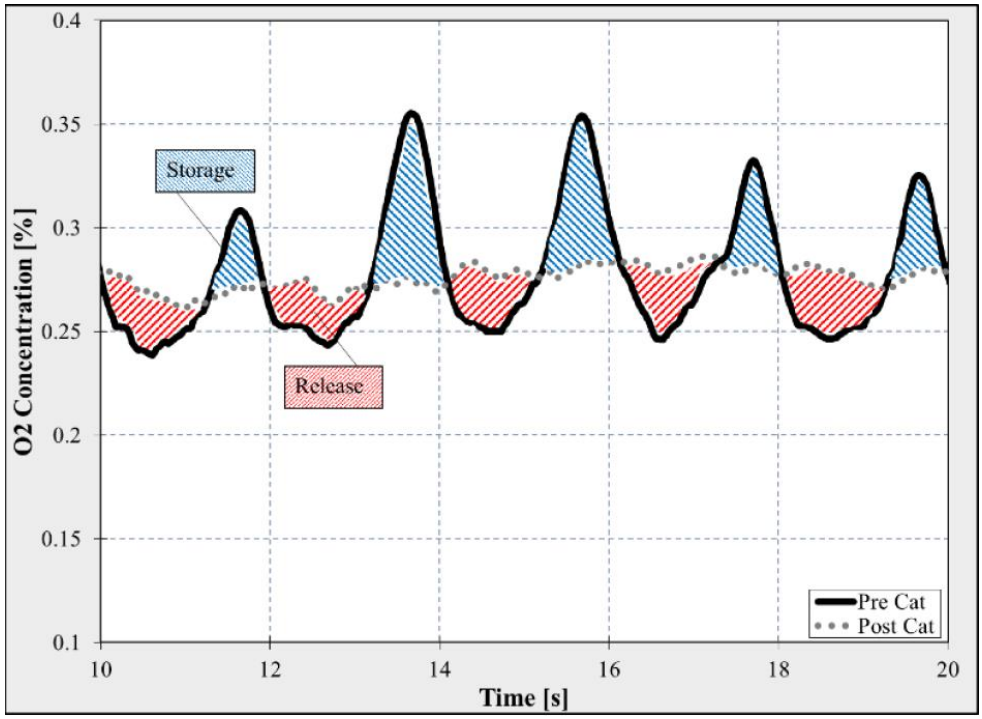

Figure 7: Oxygen Storage in a three-way catalyst, with pre- and post-catalyst oxygen sensors [16]. The post catalyst oxygen content remains constant while the pre-catalyst signal fluctuates, signaling optimized oxygen storage and release.

1.5 THESIS OVERVIEW

This study aims to better understand the effects of dithering on TWC reduction efficiency under multiple conditions. An optimal dithering midpoint will be selected based on the emissions results of a lambda sweep. Amplitude and frequencies will be swept in search of maximum catalyst reduction efficiency of NOx, CO, and HCs. The impact of catalyst age and composition on dithering performance will also be explored. Additionally, the window of emissions compliance will be explored with and without dithering. Specific research questions to be answered are as follows:

- How do dithering parameters such as midpoint, frequency, and amplitude affect emissions reduction efficiency and overall tailpipe-out emissions?
- How does catalyst age and chemical composition affect emissions with dithering?
- How can dithering parameters be adjusted to compensate for catalyst composition and age?

The thesis is organized in five chapters. In the first chapter, the engine control system and necessary modification will be described along with the DAQ equipment and emissions analyzers. In the second chapter, the results from symmetric dithering will be discussed and compared with steady state (non-dithering) results. In the third chapter, results from non-symmetric dithering will be discussed. In the fourth chapter, catalyst chemistry and age and its effects on required dithering parameters will be discussed. The fifth chapter will discuss the findings and give recommendations for dithering parameter selection, as well as describe potential next steps for experimentation.

CHAPTER 2: ENGINE EXPERIMENTAL METHODS

2.1 ENGINE CONFIGURATION AND CONTROL SYSTEM

Dithering testing will be performed on a 2015 Caterpillar CG137-8, an 18L industrial 4-stroke natural gas engine (S/N: WWF00318). It is an 8 cylinder, turbocharged, spark ignited natural gas engine with a 60 degree V8 head configuration. The engine exhaust system was designed to accommodate different aftertreatment systems. This is a stoichiometric engine, which uses a three-way catalyst to meet emissions regulations. These engines are used for power generation and natural gas gathering. Its specifications are shown in Table 1.

Table 4: CSU CAT CG137-8 Specifications

Engine	**CG137-8**
Displacement, L (in^3)	18.0 (1099)
Engine Power Output, kW (bhp)	298 (400)
BMEP, kPa (psi)	1100 (160)
Bore, mm (in)	137.16 (5.4)
Stroke, mm (in)	152.40 (6.0)
Compression Ratio	10.25:1
Lube Oil Capacity, L (gal)	147.63 (39)
Exhaust Gas Flow (Full Load) m^3/min (cfm)	15.64 (547.6)
Catalyst Space Velocity, h^{-1}	17095

The engine was initially commissioned at the CSU Powerhouse Engines and Energy Conversion Lab (EECL) with the stock Caterpillar ADEM A4 engine controller and was baseline tested using this system. The engine was then converted to a Woodward Large Engine Control Module (LECM) to allow for customization of engine control strategies. Engine control software was written using Woodward MotoHawk in collaboration with staff at Woodward. A human machine interface (HMI) created in Woodward Toolkit 3.0 was used to monitor engine control unit (ECU) parameters during tests. This software was installed on the desktop computer

ETS00258 located near the test cell at the Powerhouse. Licenses for Woodward MotoHawk and Toolkit were obtained through contact with Woodward. Figure 8 shows the CG137-8 engine test cell and points out key components.

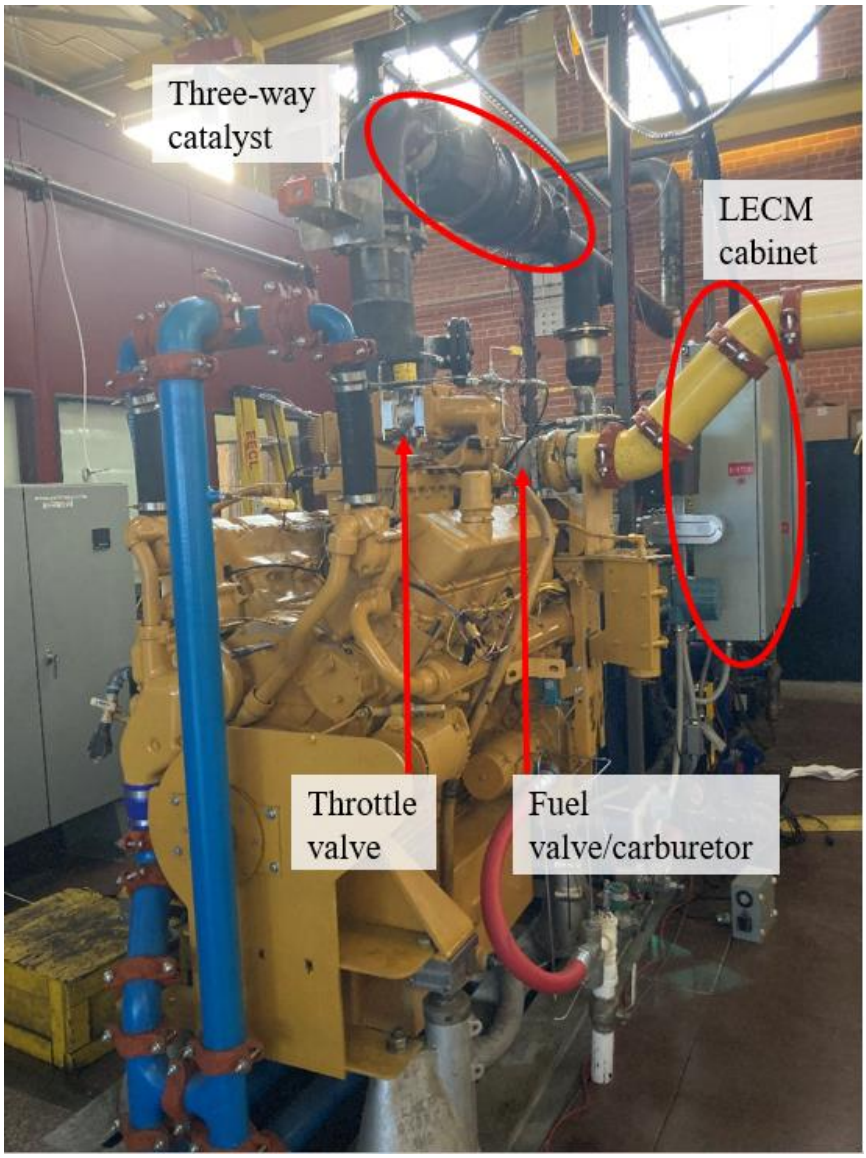

Figure 8: CG137-8 test cell at the CSU Powerhouse. The engine was converted to a full-authority Woodward control system for greater customizability.

The LECM runs a full-authority control system. It controls the throttle (engine air), carburetor fuel valve (engine fuel) and spark timing. Spark timing was controlled using Woodward Real Time Combustion and Detonation Control (RTCDC) which uses cylinder pressure feedback to provide optimal spark timing for combustion.

Data was recorded using an NI CompactRIO system that recorded pressure and temperature data for many key parameters. Additionally, an NI CompactDAQ with CAN cards was used to log data from the LECM. All engine and test cell parameters are viewed via a Labview HMI on the Powerhouse PEC-EECL-1 laptop. A complete list of LabView parameters logged during engine tests can be found in Appendix A.

The engine was also retrofitted with a Woodward EFR electronic carburetor and a Woodward F-series throttle valve. Through the LECM, the EFR electronic carburetor could be configured using Woodward computer tools to adjust AFR, providing control of dithering midpoint, amplitude, and frequency. Figure 9 shows the retrofitted engine actuators.

Figure 9: A top-down view of the engine shows the retrofitted Woodward actuators that will give the Woodward Large Engine Control Module (LECM) customizable control of engine operation.

Through the Woodward HMI, important parameters for dithering control could be adjusted. There were options for symmetrical sine, square, and triangle waves, as well as an option for creating a custom wave with non-symmetric dwell and rise. Amplitude and frequency could be controlled easily, and the midpoint could be adjusted to a desired AFR. Dithering was added to the fuel flow as a modulation of the fuel valve, after the steady state air-fuel ratio control PID. This means that during dithering operation, the air fuel ratio control was based on the average air fuel ratio. Figure 10 shows the LECM control system and how it is connected to key actuators and the plant LabView system.

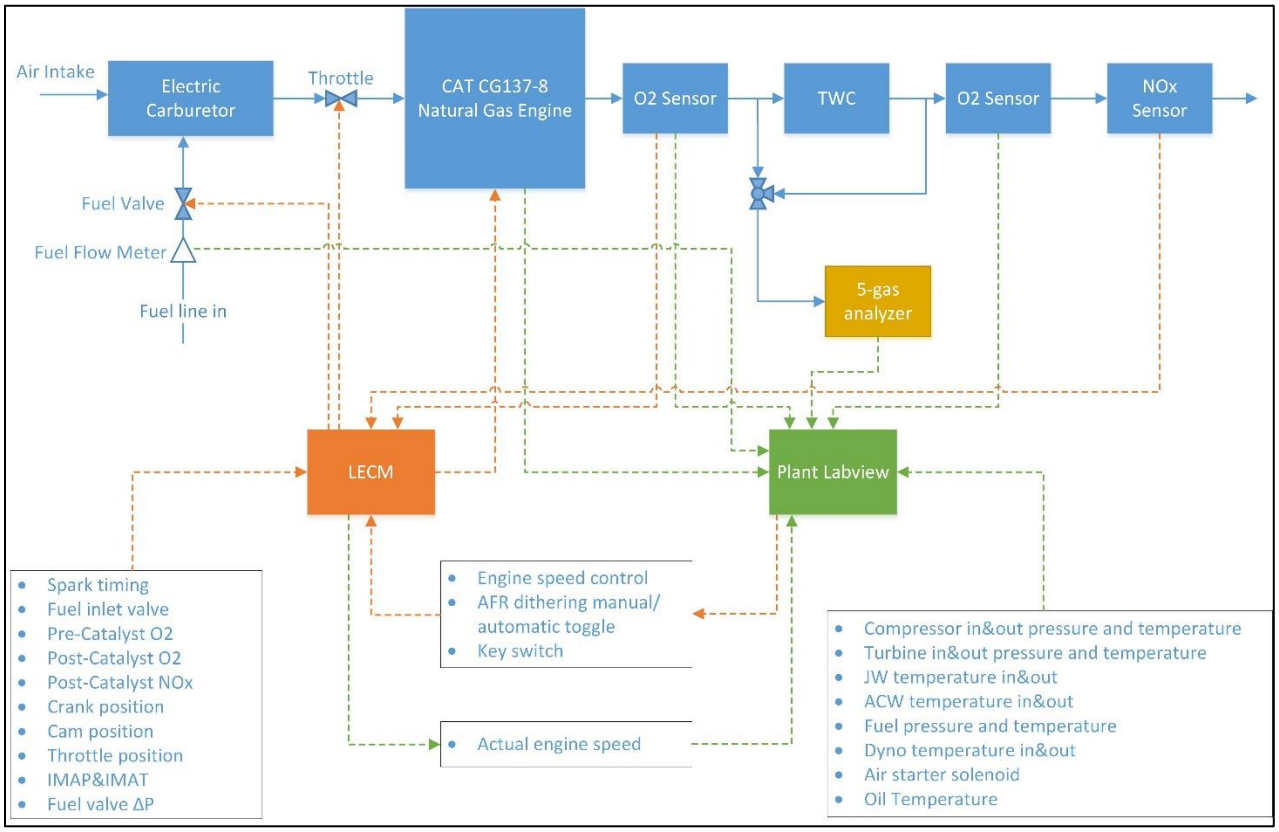

Figure 10: The LECM control system and LabView DAQ system schematic

THREE WAY CATALYST INFORMATION

Stoichiometric engines of this size use a three-way catalyst (TWC) to meet emissions limits. This study investigates the effects of air-fuel ratio dithering on a three-way catalyst, and also how catalyst age and chemical composition can change the effectiveness of dithering on emissions reduction. The three catalysts that will be used for this test are as follows: the stock CAT catalyst, a catalyst designed to have half the oxygen storage content of the standard catalysts, and the standard catalyst artificially aged to near end of life. Table 5 shows the different catalyst configurations that were used in testing.

Table 5: Testing was performed on three catalysts. The catalysts were identical other than the oxygen storage content and artificial aging.

	Catalyst Type	Cell Density	Space Velocity	Substrate Wall Thickness	Washcoat Layer Thickness
Catalyst 1	Standard CG137-8	100 cells/in^2	17095 h^{-1}	50 microns	100 microns
Catalyst 2	½ Ceria of Standard				
Catalyst 3	Standard aged to 16000 hrs				

Catalyst thermal aging was performed using a Scutt Automatic Kiln (Figure 11). For catalyst de-greening, it was set to 530°C for 24 hours, to simulate the first 24 hours in the exhaust stream. De-greening on the catalysts was performed to eliminate the effects of initial thermal aging that occurs in the first 24 hours of use.

The standard catalyst for the CG137-8 is comprised of two cylinder-shaped bricks. Each catalyst brick contains the metallic substrate with washcoat and catalytic materials. Figure 12 shows a catalyst brick before installation in the exhaust stream. Figure 13 shows the catalyst unit, which includes two catalyst bricks as well as adapters that bolt to the exhaust pipes and contain bosses for O2, NOx, and temperature sensors.

Figure 11: This Scutt automatic kiln was used for catalyst de-greening and aging.

Figure 12: Cross sectional view of a catalyst brick. Two bricks are used in the standard configuration.

Figure 13: The two catalyst bricks are clamped together and then bolted into the exhaust using a series of adapters.

The standard TWC designed for this class of engine is designed to meet 0.5g/bhp-hr emissions limits and is produced by Caterpillar catalyst supplier BASF. Two catalyst bricks were de-greened before installation.

The second catalyst is custom and was produced specifically for this project. The catalyst is made by BASF with the same chemical makeup as the stock catalyst other than the cerium oxygen storage content. This second catalyst has one half of the oxygen storage content as the stock catalyst.

For the third catalyst, the original catalyst was artificially aged to end of life condition, or 16,000 hours. The procedure used was based on EPA rules, assuming that the catalyst

experiences mostly thermal aging over its lifetime, and less chemical aging [17]. To accomplish this aging, the catalyst will be heated in a kiln at 800°C for 33 hours in the presence of 10% water. The tests with this catalyst will represent a stock catalyst on an engine that has been in the field for several years.

2.2 EMISSIONS ANALYZERS

Emissions concentrations were monitored by a Rosemount/Siemens 5-gas analyzer and a Nicolet 6700 Fourier Transform Infra-Red (FTIR) spectrometer. The 5-gas analyzer measured THC, NOx, O2, CO2, and CO concentrations. The FTIR was used to measure numerous exhaust species including formaldehyde, VOC's, and ammonia. A Varian CP-4900 micro gas chromatograph measured the fuel gas composition through C6. Detailed information about the gaseous emission sampling instruments can be found by referencing Davis [18].

AFR was monitored using Bosch LSU4.9 O_2 sensors both pre- and post- catalyst, and an Engine Control and Monitoring (ECM) Air Fuel Recorder 4800 was also installed pre-catalyst. The AFRecorder uses a SEGO wide band lambda sensor that responds to oxygen, hydrogen, and CO. An ECM NOx 5210 sensor was installed post-catalyst.

2.3 TEST PROCEDURE

During each test day, the engine was brought to operational steady state, given time to reach operational temperature and meet baseline conditions. At the beginning of each day, a baseline test was taken. Emissions analyzers were calibrated each morning before testing, and pipeline NG samples were analyzed continuously throughout the day.

The first set of tests is a lambda (λ) or AFR sweep. The LECM was programmed for a specific air-fuel ratio, and the engine was allowed to reach steady state, with the actual air-fuel ratio being monitored. Once AFR was steady, emissions and engine data were taken for 2 minutes at each point.

Table 6 shows the test plan for the wide AFR sweep. The data from this test was then analyzed, and a narrower test with 0.001λ resolution was run on either side of the emissions low point (NOx and CO).

Table 6: Test matrix for AFR sweep. This was used for steady state and dithering AFR sweeps.

Test Case	Engine Load	Lambda (λ)
1	298 kW	0.95
2	298 kW	0.96
3	298 kW	0.97
4	298 kW	0.98
5	298 kW	0.985
6	298 kW	0.987
7	298 kW	0.989
8	298 kW	0.990
9	298 kW	0.992
10	298 kW	0.994
11	298 kW	0.996
12	298 kW	0.998
13	298 kW	1.00
14	298 kW	1.01
15	298 kW	1.02
16	298 kW	1.03
17	298 kW	1.04
18	298 kW	1.05

The following phase of testing involves altering the dithering parameters around the CO and NOx emissions crossover found in the previous phase. Each test case can be found in Table 7. Each test case will be run for two minutes, with average catalyst reduction efficiency measured. The five-gas analyzer is not fast enough to analyze dithering exhaust in real time, and

there will be some amount of temporal mixing of exhaust gasses in the heated sample line to the analyzer.

Table 7: Test matrix for dithering parameter sweep

	Frequency			
Amplitude	0.1 Hz	0.2 Hz	0.5 Hz	1.0 Hz
0.000 λ	Test 1	-	-	-
0.005 λ	Test 2	Test 3	Test 4	Test 5
0.010 λ	Test 6	Test 7	Test 8	Test 9
0.015 λ	Test 10	Test 11	Test 12	Test 13
0.020 λ	Test 14	Test 15	Test 16	Test 17

Following the dithering parameter sweep, a dithering AFR sweep was performed using the test plan shown in Table 6. The optimal dithering parameters (amplitude and frequency) found in the dithering parameter sweep will be used while the midpoint AFR is swept. The final phase of this study is to investigate the optimal results from the test from Table 7 with a TWC with less oxygen storage material and on the aged TWC. Test cases for this phase will be the same as those listed in Table 6 and Table 7. The catalysts will be tested in phases, with all testing done on one catalyst before the next catalyst is installed. The phases and each corresponding catalyst are listed in Table 8.

Table 8: Three different catalysts will be tested.

Test Phase	Catalyst Number	Catalyst Type	Tests Performed
1	Catalyst 1	Standard CG137-8	Steady and dithering AFR sweep, dithering parameter sweep
2	Catalyst 2	½ Ceria of Standard	
3	Catalyst 3	Standard aged to 16000hrs	

CHAPTER 3: VALIDATION AND BASELINE TESTING

3.1 CSU TEST CELL BASELINE TESTING

When the CG137-8 was commissioned it was baseline tested with the stock CAT ADEM A4 control system to ensure that plant support systems could allow the engine to match its rated performance. The engine was originally used at a CAT test facility, so baseline data engine performance data was able to be obtained from engineers at CAT. The engine was then run at the same speed and load points to ensure engine performance matched the data from the CAT test cell. As can be seen in Figure 14, the engine was able to meet its rated power at different speeds in the new test cell, nearly identically matching the performance recorded in the CAT test cell. Additionally, important engine parameters such as intake manifold absolute pressure (IMAP), fuel flow, coolant temperatures, and exhaust temperatures were measured to ensure the health of internal components as well as plant support systems. Figure 15 shows some of these parameters compared between the two test cells. After consulting with engineers at CAT, it was concluded that all parameters were within acceptable normal ranges.

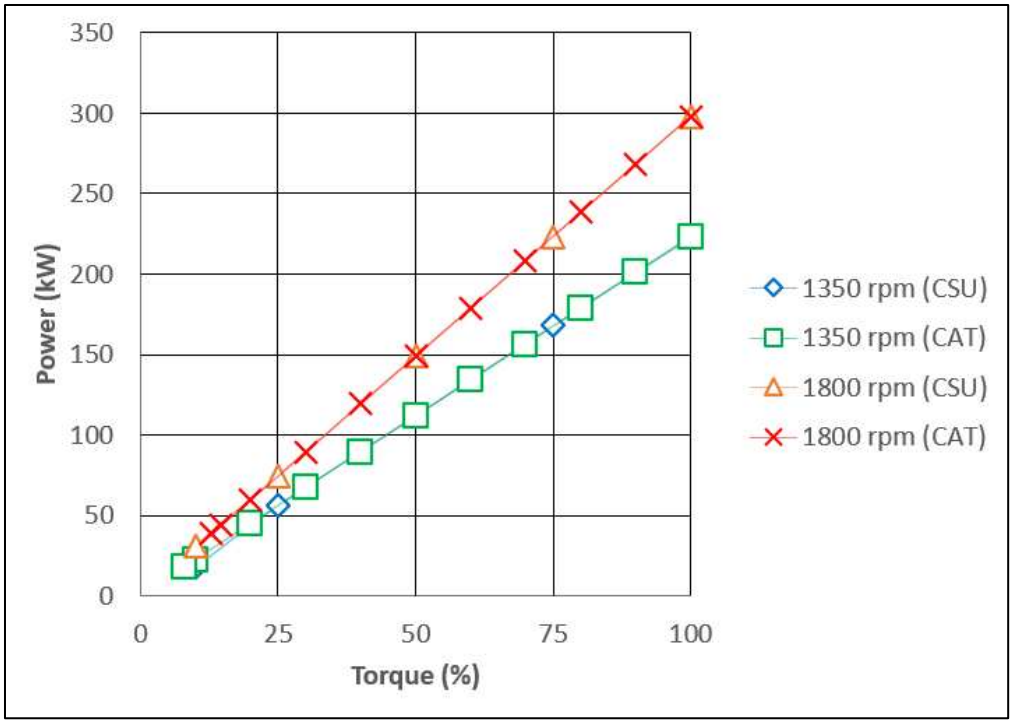

Figure 14: CAT test center baseline data compared with CSU data. Validation was performed to ensure engine could meet all desired speed and load points in the new test cell.

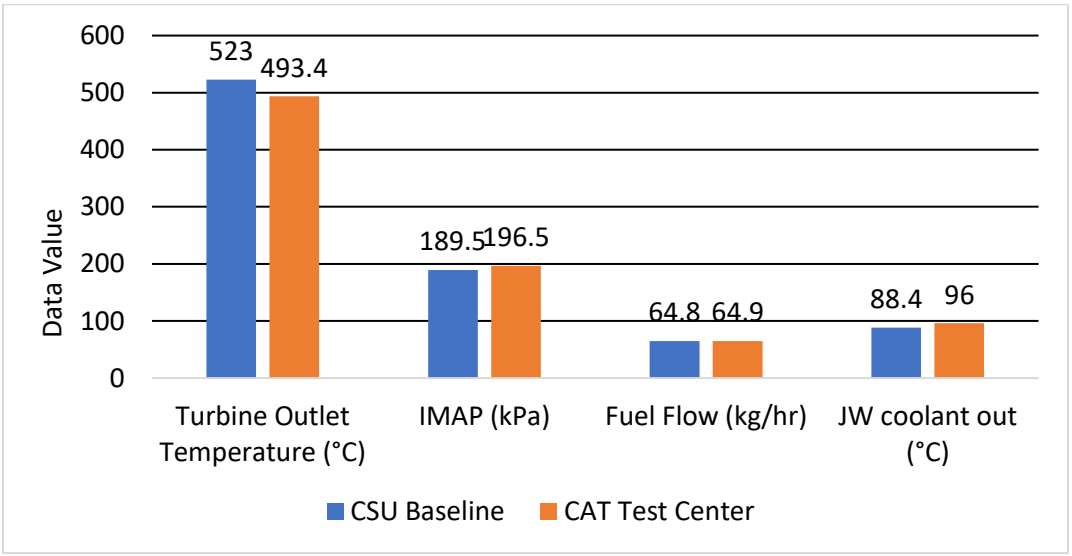

Figure 15: Key engine health parameters such as IMAP, fuel flow, coolant temperatures, and exhaust temperatures were monitored to ensure the engine and its support systems were functioning properly in the new test cell.

3.2 WOODWARD LECM BASELINE TESTING

Following the baseline test with the CAT ADEM A4 controller, the engine was converted to the Woodward LECM, as detailed in Chapter 2. Following a successful commissioning of the new control system, the same speed and load points were again run using the Woodward LECM, to verify the integrity of the new control system. The LECM on the engine runs a full-authority control system, controlling spark timing, fuel delivery, and speed control. Tuning was required to ensure that the control system was stable. Tuning consisted of PID manipulation and sensor range calibration. The air-fuel ratio and engine speed are controlled with PIDs, and it was important to ensure that these controllers did not interfere with one another. To accomplish this, the air-fuel ratio control was tuned to react to changes around an order of magnitude slower than the speed controller. This tuning method ensures that there will never be a feedback loop between the two controllers. Other parameters were checked to ensure controller stability including exhaust temperature, speed, and power. All parameters were stable and did not have any time-based fluctuation.

After tuning was completed, the same speed and load tests that were run on the ADEM A4 were run on the LECM. Figure 16 shows the LECM data compared to the ADEM A4 data. The new LECM control system was able to match the performance of the stock control system.

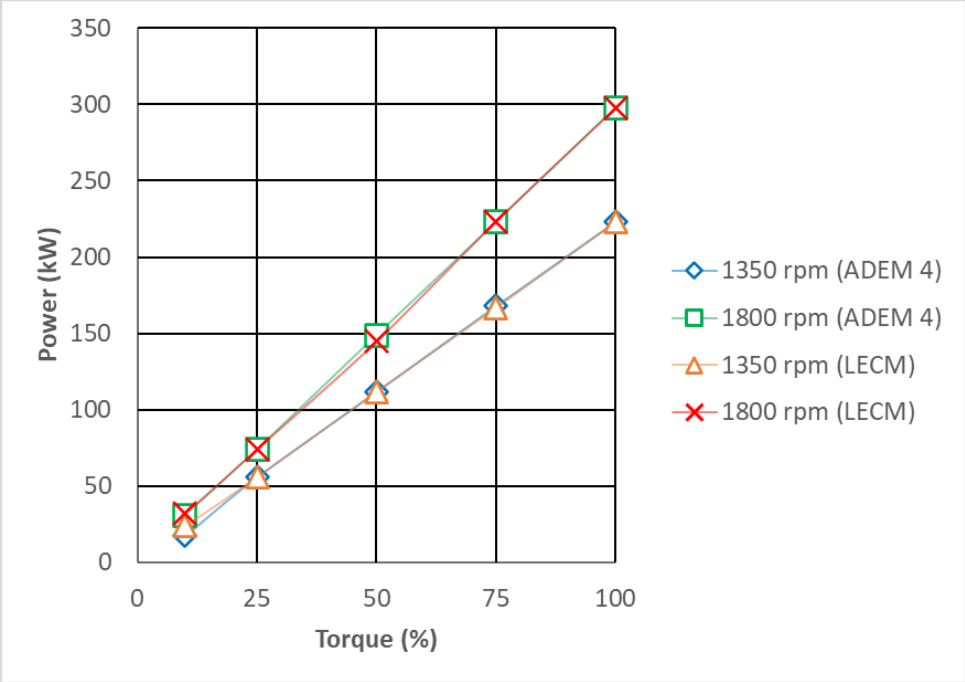

Figure 16: The LECM was able to meet the rated speed and load points for the CG137-8. This graph shows the points compared to the stock ADEM A4 controller.

3.3 BASELINE LAMBDA SWEEP TESTING

After it was verified that the LECM engine controller and plant system were able to adequately control the engine, a baseline lambda sweep was performed. During each point of the lambda sweep, lambda was controlled to a constant value. This sweep was carried out with the standard catalyst to analyze the emissions reduction performance of this catalyst for future comparison to other catalysts as well as dithering test cases. Lambda ($\lambda = AFR_{actual}/AFR_{stoich}$) was used as the control parameter to normalize the air-fuel ratio between different tests in which fuel composition may result in different stoichiometric air-fuel ratios. Catalyst reduction efficiency was calculated based on the pre-catalyst and post-catalyst species concentrations. Figure 17a

shows the post-catalyst NOx and CO emissions at various points in the lambda sweep. The catalyst followed the typical trends that can be expected for a stoichiometric engine with a three-way catalyst. At rich lambda values, CO emissions were high, while at lean lambda values, NOx emissions were high. There was a window between λ=0.987 and λ=0.992 where both NOx and CO emissions were relatively low. Figure 17b shows the same lambda sweep data for a narrower range of lambda values, highlighting the narrow margin where both NOx and CO emissions are at a minimum.

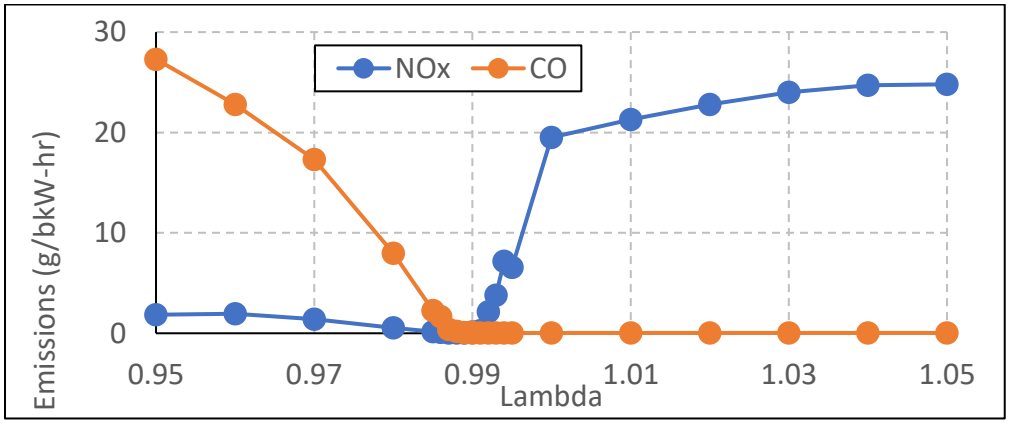

(a)

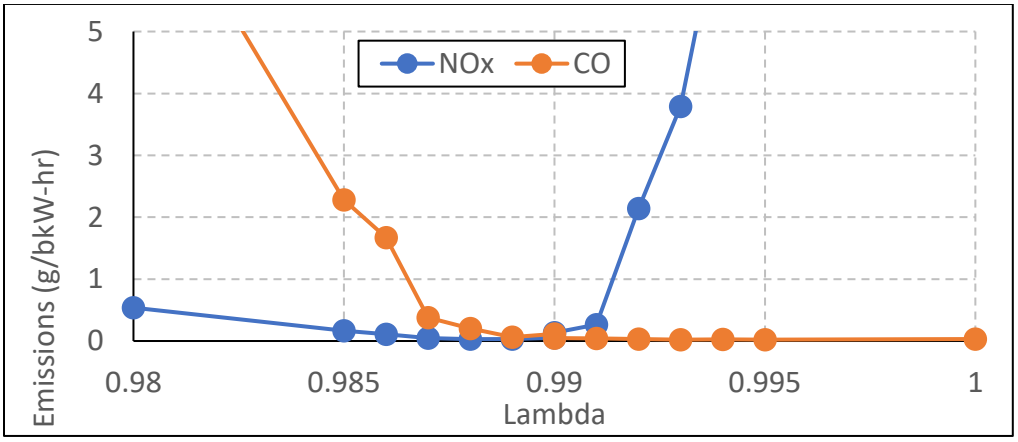

(b)

Figure 17: Baseline lambda sweep NOx and CO emissions (post-catalyst). (a) shows the range from λ=0.95 to λ=1.05, and (b) shows a subset of that range. There is a narrow window where both NOx and CO emissions are low. ($\lambda=AFR_{actual}/AFR_{stoich}$)

Figure 18 shows the reduction efficiency for the standard catalyst during the baseline lambda sweep. There is a small window of reduction efficiencies between λ=0.987 and λ=0.992 where the reduction efficiency for both NOx and CO is near 100%. Outside of that range, the appropriate chemistry is not present in the catalyst for proper reduction of both pollutants.

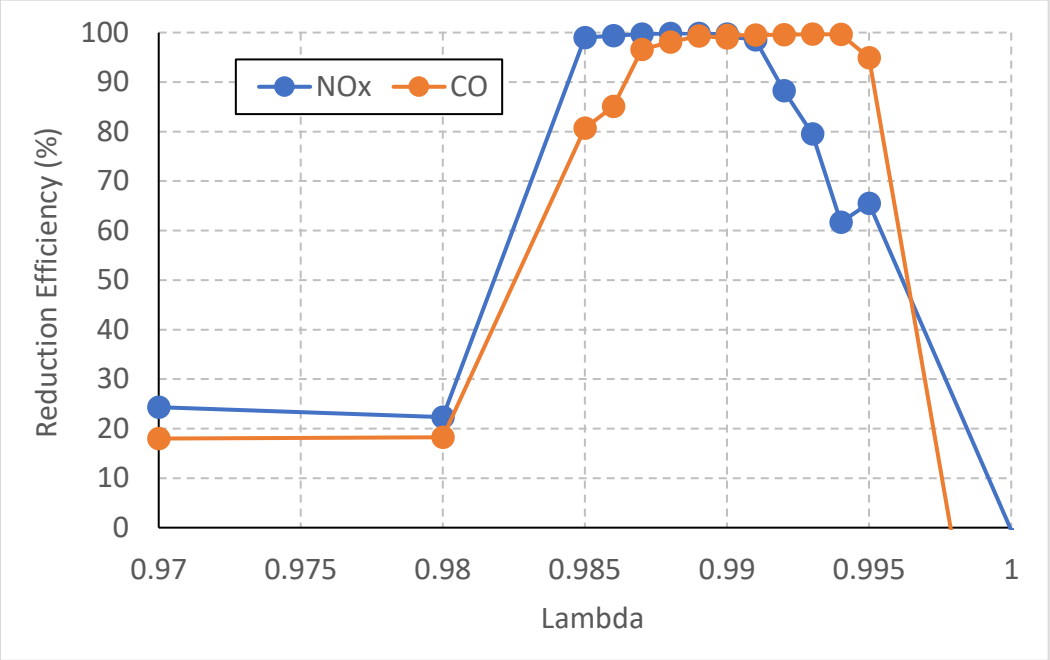

Figure 18: Reduction efficiency for the baseline lambda sweep with the standard catalyst. There is a small window between λ=0.987 and λ=0.992 where reduction efficiency is at a maximum for both NOx and CO.

CHAPTER 4: THREE-WAY CATALYST ADVANCED CONTROLS

4.1 DITHERING PARAMETER SWEEP

The first phase of dithering testing involved sweeping a range of frequencies and amplitudes in all combinations to observe which combination of dithering amplitude and frequency (if any) provided lower overall emissions than a steady state air-fuel ratio control. Based on prior experiments from other researchers, an amplitude range of 0.5 to 2.0% lambda was selected. Figure 19 shows the NOx emissions throughout the dithering sweep, and Figure 20 shows the CO emissions throughout the dithering sweep. The steady state emissions can be seen on the y-axis of each plot. The dithering NOx emissions are significantly higher than the steady state emissions at low frequencies (0.1 and 0.2 Hz) but are lower than the steady state emissions at higher frequencies (1 Hz). All dithering amplitudes (0-2%) follow the same trend, with higher emissions than steady state at low frequencies, and lower emissions than steady state at high frequencies.

The CO emission trends are similar, with the lower dithering frequencies giving higher CO emissions than steady state operation, but high frequency (1 Hz) dithering results in lower CO emissions than the steady state point. The 0.5% amplitude dithering test case did not lower CO emissions, and instead had the same emissions as the steady state point. However, the larger dithering amplitudes provided CO emissions reductions at higher frequencies. The optimal dithering parameter combination for minimum CO emissions is 2.0% amplitude and 1 Hz frequency, closely followed by 1.5% amplitude and 1 Hz frequency.

At dithering frequencies above 1 Hz, the engine system was not able to respond to the fueling changes quickly enough, and the pre-catalyst exhaust stream began to resemble that of steady state engine operation. This is likely due to spatial mixing of dithered fuel after the carburetor. The turbocharger and intake piping likely allows the rich and lean intake charges to mix, resulting in the midpoint air-fuel mixture entering the engine. For this reason, 1 Hz was the highest dithering frequency tested.

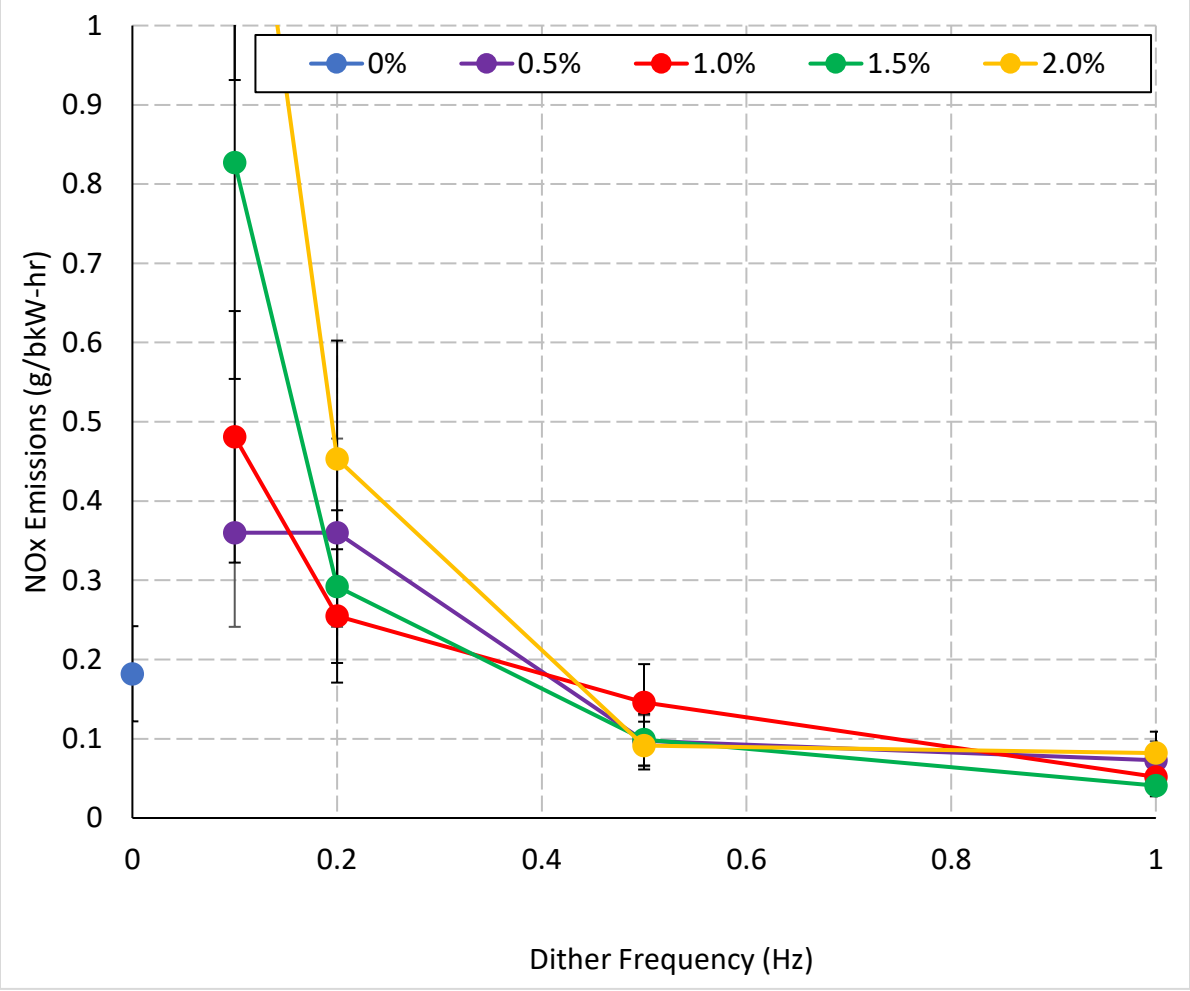

Figure 19: NOx emissions during the dithering parameter sweep. The parameters that provided the lowest NOx emissions were 1.5% lambda at 1 Hz.

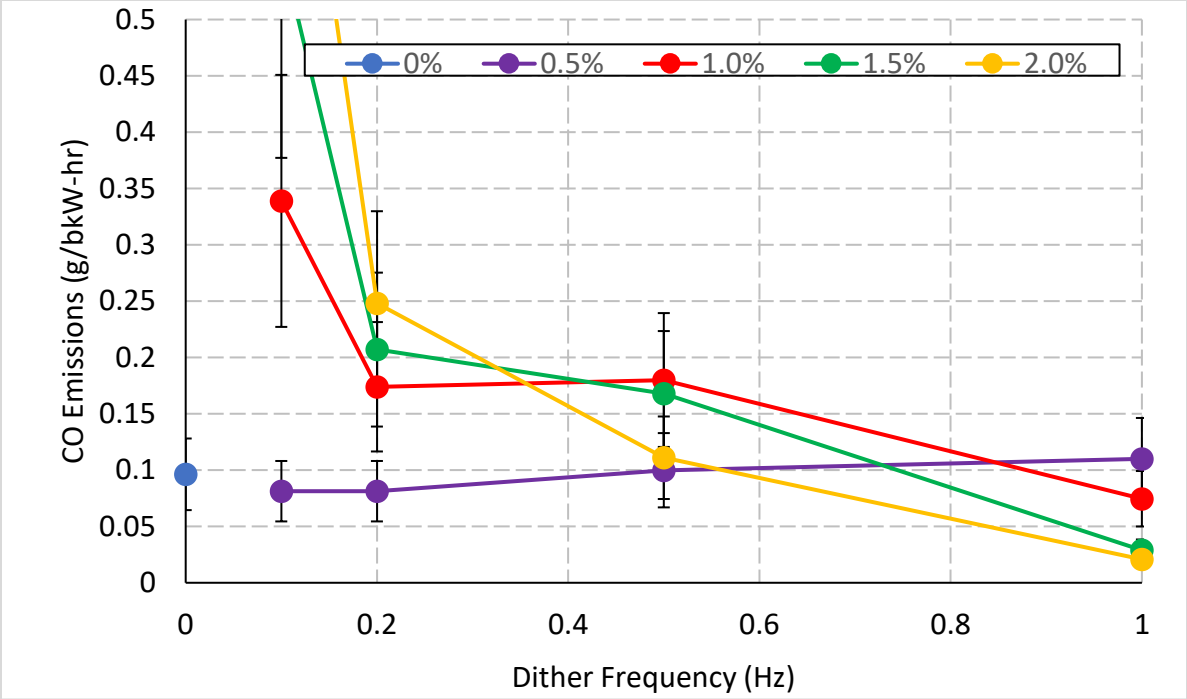

Figure 20: CO emissions during the dithering parameter sweep. The parameters that provided the lowest CO emissions were 2.0% lambda at 1 Hz, closely followed by 1.5% lambda at 1 Hz.

The slower dithering frequencies have significantly higher NOx and CO emissions because the catalyst is reaching oxygen saturation and depletion, meaning the extra emissions created by running the engine rich and lean are not reduced. At faster frequencies, the catalyst is not reaching saturation, so the reactions listed in

Table 3 are effective at reducing emissions.

During testing, it was noted that the 2.0% dithering introduced a waveform pattern into the engine speed. During rich shifts, the engine would speed up slightly, and during lean shifts, it would slow down. These fluctuations were audibly noticeable. Figure 21 shows the speed fluctuations recorded with the 2% lambda dithering case. Speed fluctuations were sometimes as large as +/-10 rpm from the setpoint of 1800 rpm. No significant changes in fuel consumption

were observed beyond the desired fuel fluctuations introducing dithering. This speed fluctuation is a result of adding and removing more fuel than the throttle control can compensate for.

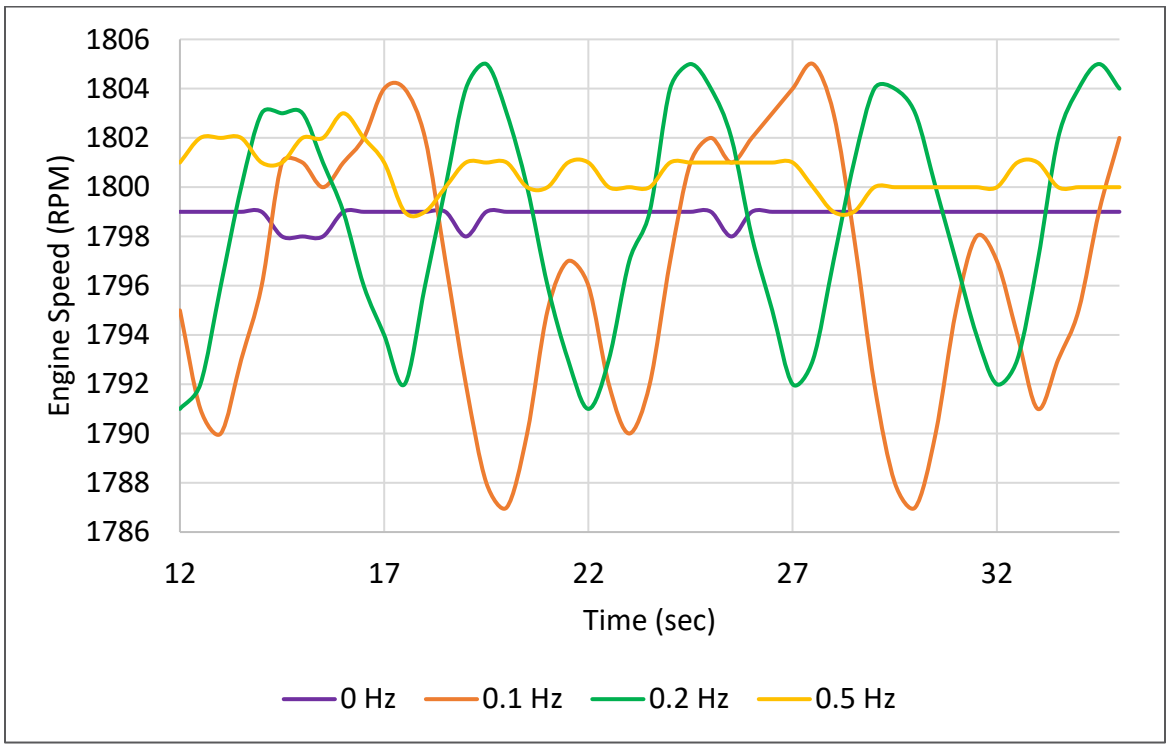

Figure 21: Speed fluctuations were noticeable for the 2% lambda dithering cases. This graph shows the speed fluctuations that a 2% lambda dither introduced to the engine speed.

Total hydrocarbons (THCs) were also measured during the dithering parameter sweep. Figure 22 shows the THC emissions across the dithering parameter sweep. At the 1.5% and 1 Hz dithering point (the best case for NOx and CO emissions), THC emissions were 0.651 g/bkW-hr, only slightly less than the steady state emissions of 0.715 g/bkW-hr. The 2% and 1 Hz point did provide slightly lower THC emissions, but this amplitude was determined to have too much effect on the engine speed to be used.

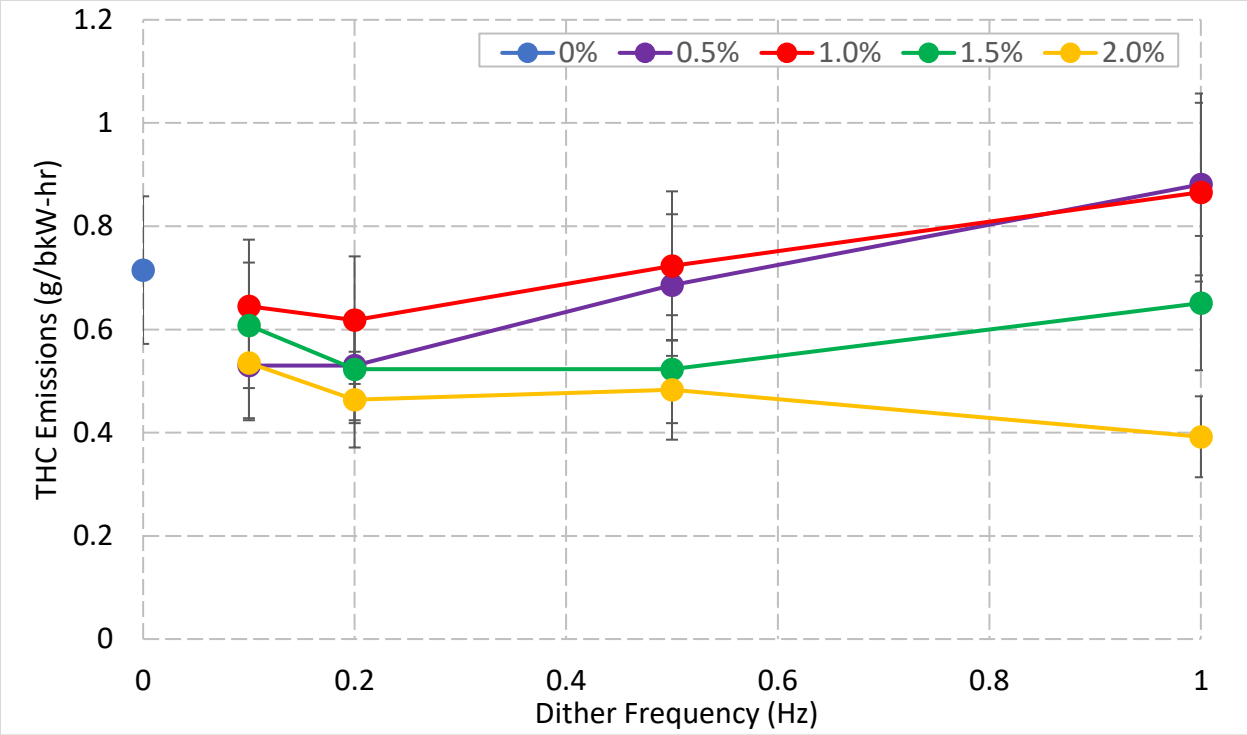

Figure 22: Total hydrocarbons (THC) emissions were not significantly impacted by dithering with the standard catalyst.

Total hydrocarbons are not regulated in most areas, but VOCs are regulated. VOCs are described as all non-methane and non-ethane hydrocarbon emissions, excluding formaldehyde. The EPA JJJJ emissions regulation for VOCs is 0.92 g/bkW-hr, as detailed in Chapter 1. Figure 23 shows the VOC emissions across the dithering parameter sweep. At the optimal dithering parameter combination for NOx and CO emissions (1.5%λ, 1Hz), VOC emissions are significantly reduced from the steady state point. The steady state emissions point is 0.059 g/bkW-hr, while the dithering emissions are 0.027 g/bkW-hr. This is a significant reduction in VOC emissions, although even the steady state point is significantly below the emissions limit. At the slower dithering frequencies, the larger dithering amplitudes (1.5% and 2%) result in higher VOC emissions, due to longer amounts of time spent in rich excursions.

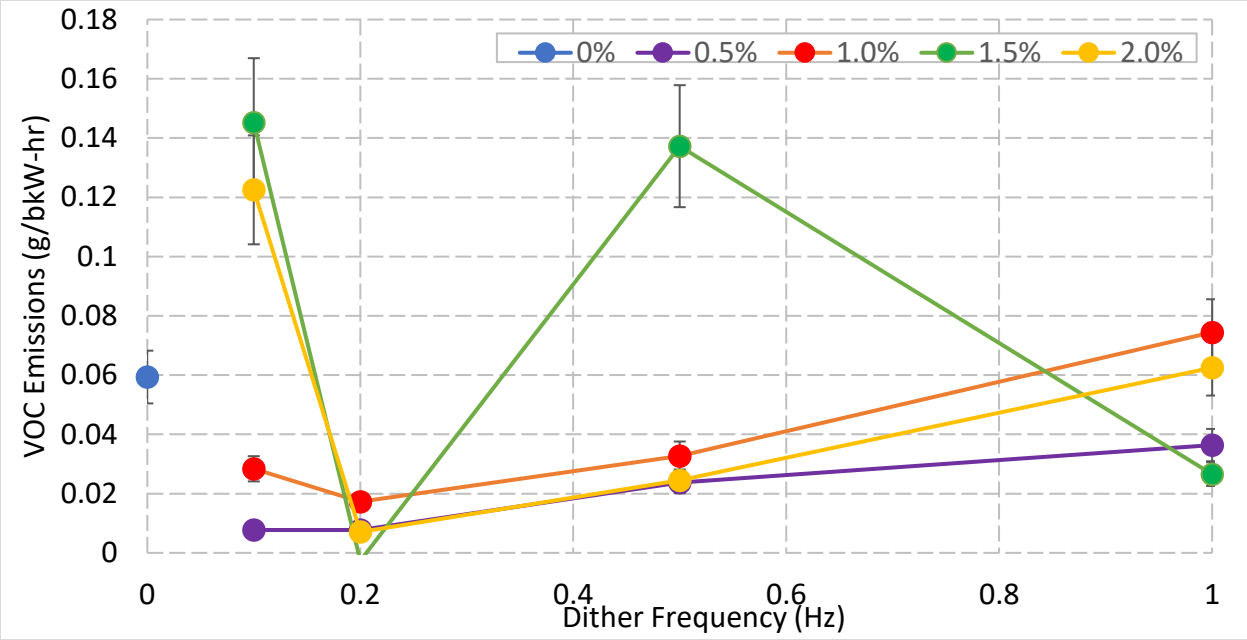

Figure 23: Non-methane and non-ethane hydrocarbon emissions. This includes all pollutants described in the EPA JJJJ regulations as "VOCs" or volatile organic compounds.

Ammonia (NH_3) is produced in the catalyst during rich engine operation. The more rich an engine runs, the more potential there is for ammonia production. Ammonia emissions are not currently regulated by the EPA for the CG137-8, but they are regulated in some local areas. Figure 24 shows the ammonia emissions across the dithering parameter sweep. Similar to other emissions, the slow dithering frequencies (0.1 and 0.2 Hz) increased emissions over the steady state emissions. This is due to longer rich excursions not being able to utilize oxygen release due to oxygen depletion in the catalyst. However, all dithering amplitudes saw significant reductions in ammonia production at high dithering frequencies (1 Hz). The steady state ammonia emissions were 13.69 ppm, while the dithering emissions for the 1.5% and 1 Hz case were 5.67 ppm.

Methane (CH_4) emissions are also currently unregulated in most areas but may be an area of concern in the future due to the greenhouse gas potential of methane. Figure 25 shows methane emissions throughout the dithering parameter sweep. Nearly every dithering parameter

combination provided lower methane emissions. The steady state methane emissions are 1.56 g/bkW-hr, while 1.5% and 1 Hz dithering can reduce the methane emissions to 0.11 g/bkW-hr.

A final emission of concern in some areas is formaldehyde (CH_2O). The CG137-8 at standard operating conditions with the standard catalyst already produces nearly no formaldehyde emissions, but dithering reduces formaldehyde to immeasurable amounts. Figure 26 shows the steady state formaldehyde emissions at 0.0016 ppm, while the dithering results are all nearly zero, below the range of measurement for the FTIR.

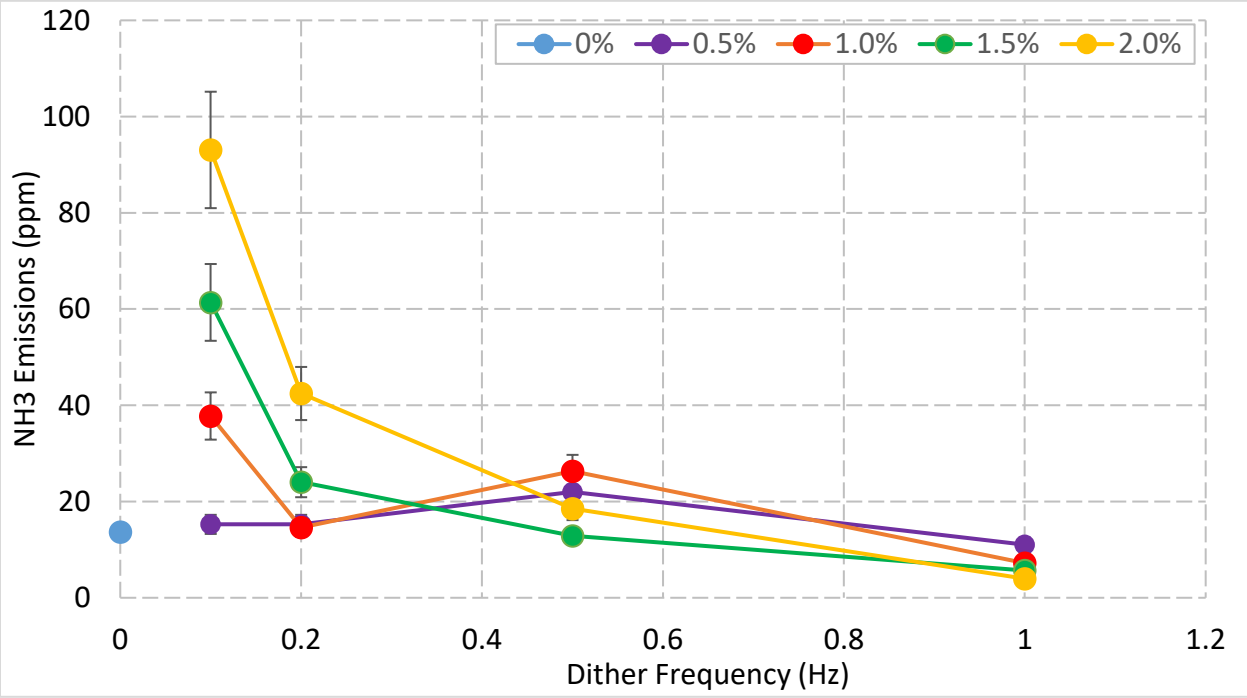

Figure 24: NH3 (ammonia) emissions during the dithering parameter sweep. Dithering does result in lower NH3 emissions. NH3 is not currently federally regulated for this engine class.

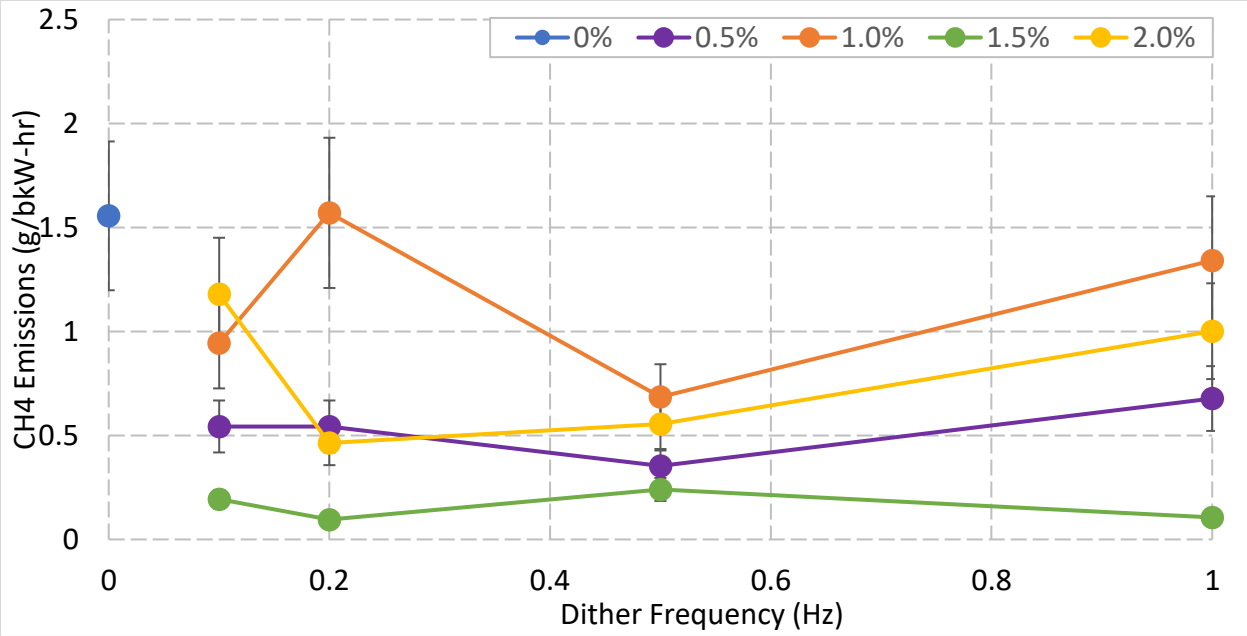

Figure 25: Methane emissions across the dithering parameter sweep. Nearly all dithering cases provided methane emissions reduction when compared to the steady (non-dithering) methane emissions. 1.5% and 1 Hz dithering results in the lowest methane emissions.

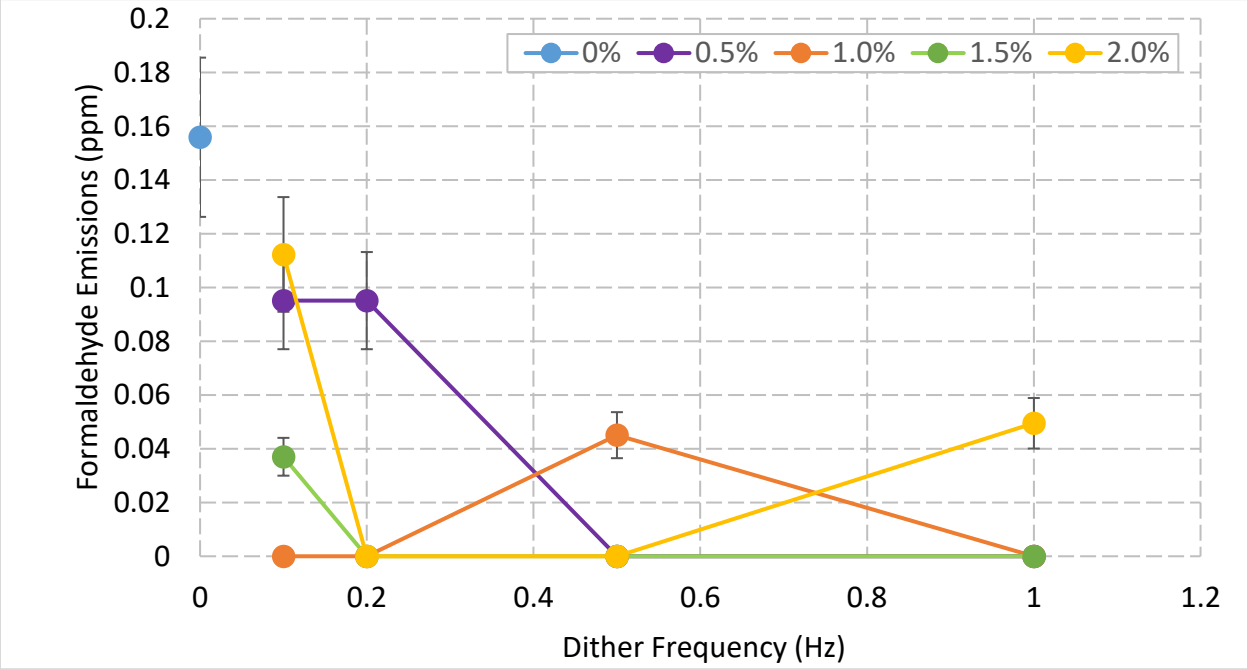

Figure 26: Formaldehyde emissions for the CG137-8 are already nearly zero, but dithering brings them down to an immeasurable amount. Emissions limits for the CG137-8 are 10.3 ppm (assuming an existing engine at a major source), so the measured emissions in all test cases are negligible.

Pre- and post-catalyst temperatures were recorded during the dithering parameter sweep. Dithering increased the average catalyst inlet temperatures in almost all cases, and increased catalyst outlet temperatures in every case. However, these temperature increases were still within the range of safe operation for the catalyst. Figure 27a shows pre-catalyst temperatures and Figure 27b shows post-catalyst temperatures.

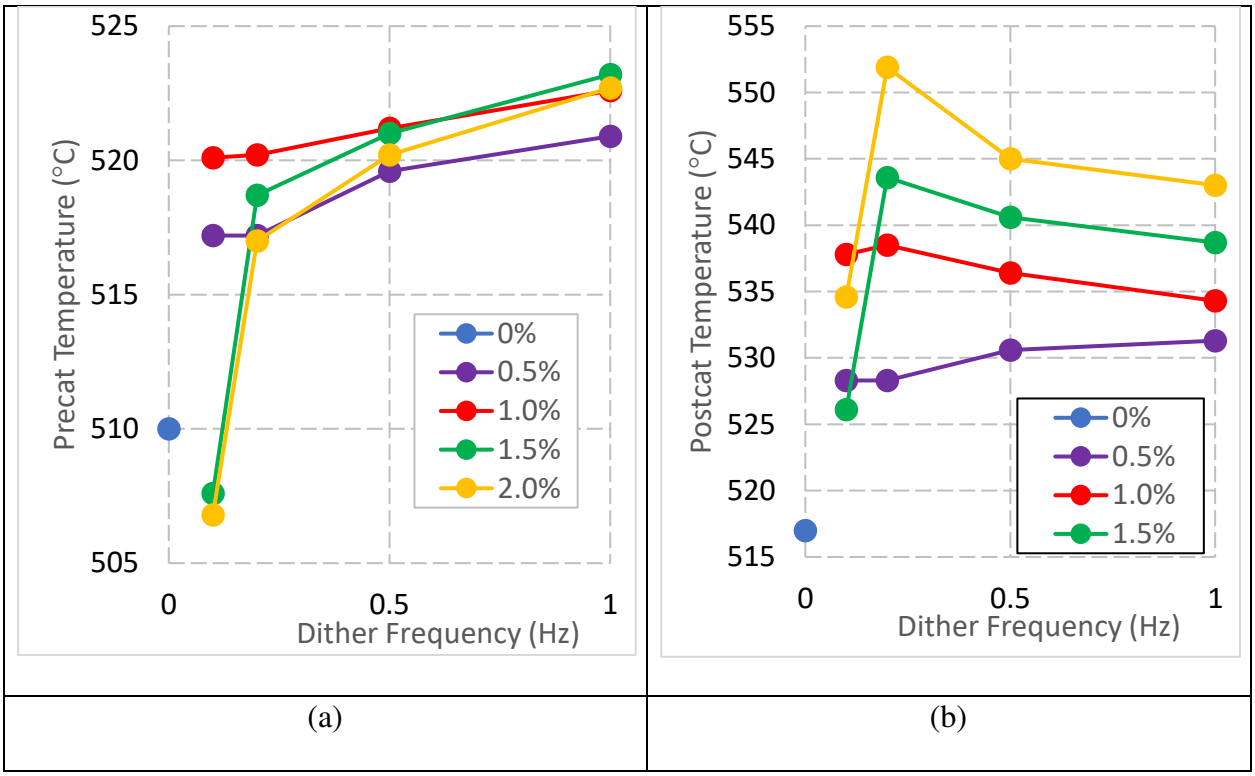

Figure 27: Catalyst temperatures with dithering. (a) shows pre-catalyst temperatures, and (b) shows post-catalyst temperatures. Dithering increased catalyst inlet and outlet temperatures.

4.2 LAMBDA SWEEP

A lambda sweep was performed, with and without dithering enabled. For the dithering test, 1.5% lambda and 1 Hz were used because those parameters showed the greatest emissions reduction when compared to steady state in previous testing. The steady state emissions followed

the same pattern seen in the baseline lambda sweep, with a region of low NOx and CO emissions between λ=0.987 and λ=0.992. The dithering emissions follow the same shape, but the low point is somewhat shifted towards the rich side from the steady state run. A large portion of this is due to the larger zone with low emissions. On the right side, dithering NOx emissions are slightly higher than the steady state emissions, but on the left side, dithering CO emissions stay low for much longer than the steady state emissions. This is because oxygen is being stored effectively during lean excursions and released during the rich phase. The oxygen storage results in significant reduction in CO emissions in the rich section of the lambda sweep.

Air-fuel ratio dithering has the potential to significantly reduce pollutant emissions in the typical air-fuel ratio operation window for stoichiometric natural gas engines. Total hydrocarbons are not regulated, but dithering has the potential to reduce total hydrocarbon emissions across a wide range of lambda. Figure 29 shows the THC emissions across the lambda sweep. From λ=0.98 to λ=1.01, THC emissions are lower for the dithering case than for the steady state case.

Non-methane and non-methane hydrocarbons, or VOCs as defined by EPA regulations, are not significantly affected by dithering. The dithering and steady emissions are within the uncertainty margin for most of the VOC emissions points, suggesting that dithering does not have a large effect on VOC emissions across a wide range of lambda values.

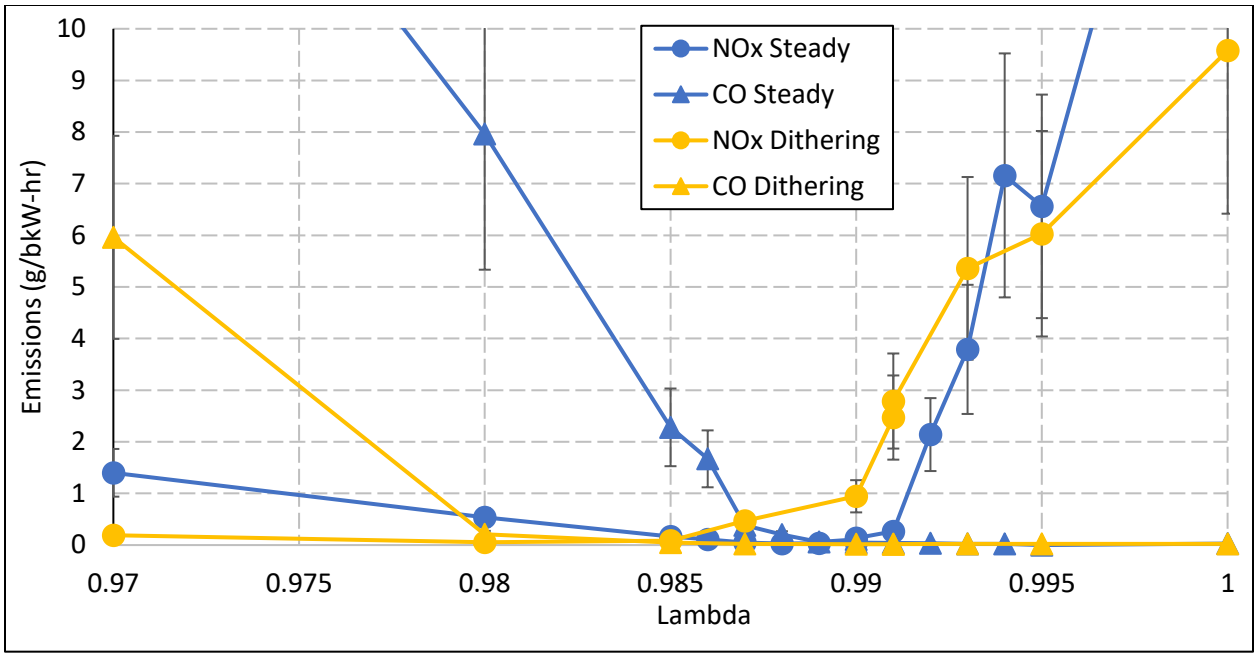

Figure 28: NOx and CO emissions across the lambda sweep, with and without dithering. The dithering points were all run with 1.5% lambda and 1Hz dithering.

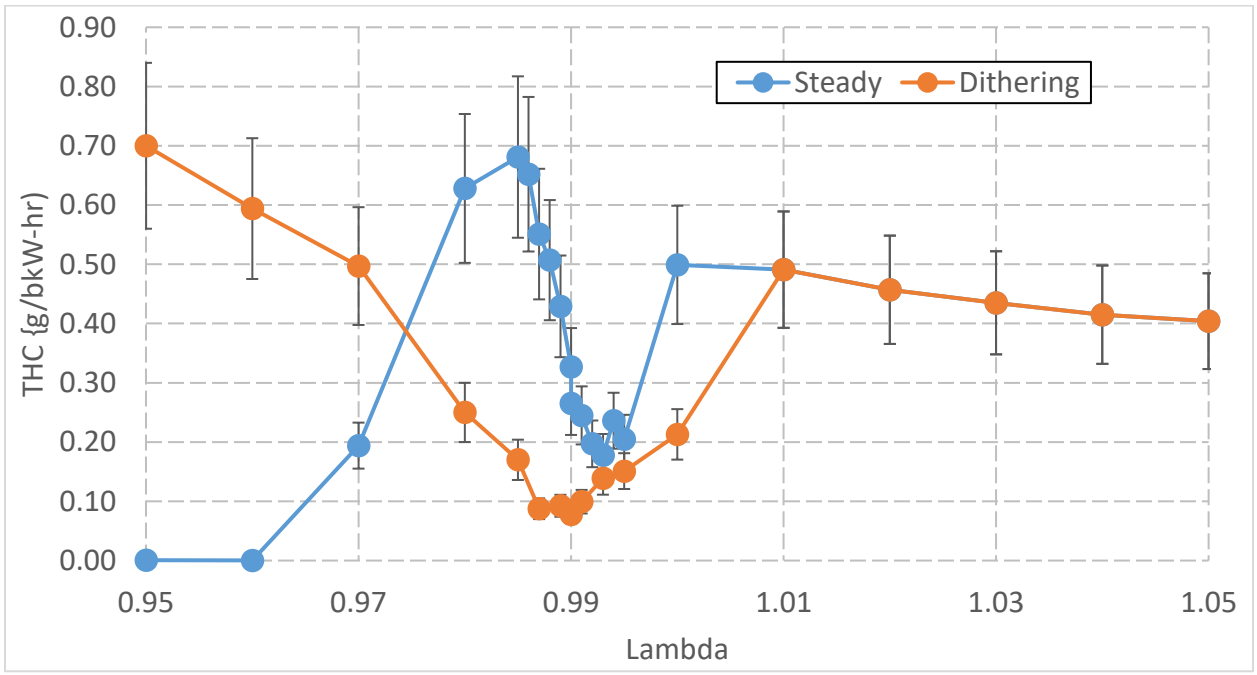

Figure 29: THC emissions during the lambda sweep. Dithering emissions are significantly lower than steady state emissions for most operation cases.

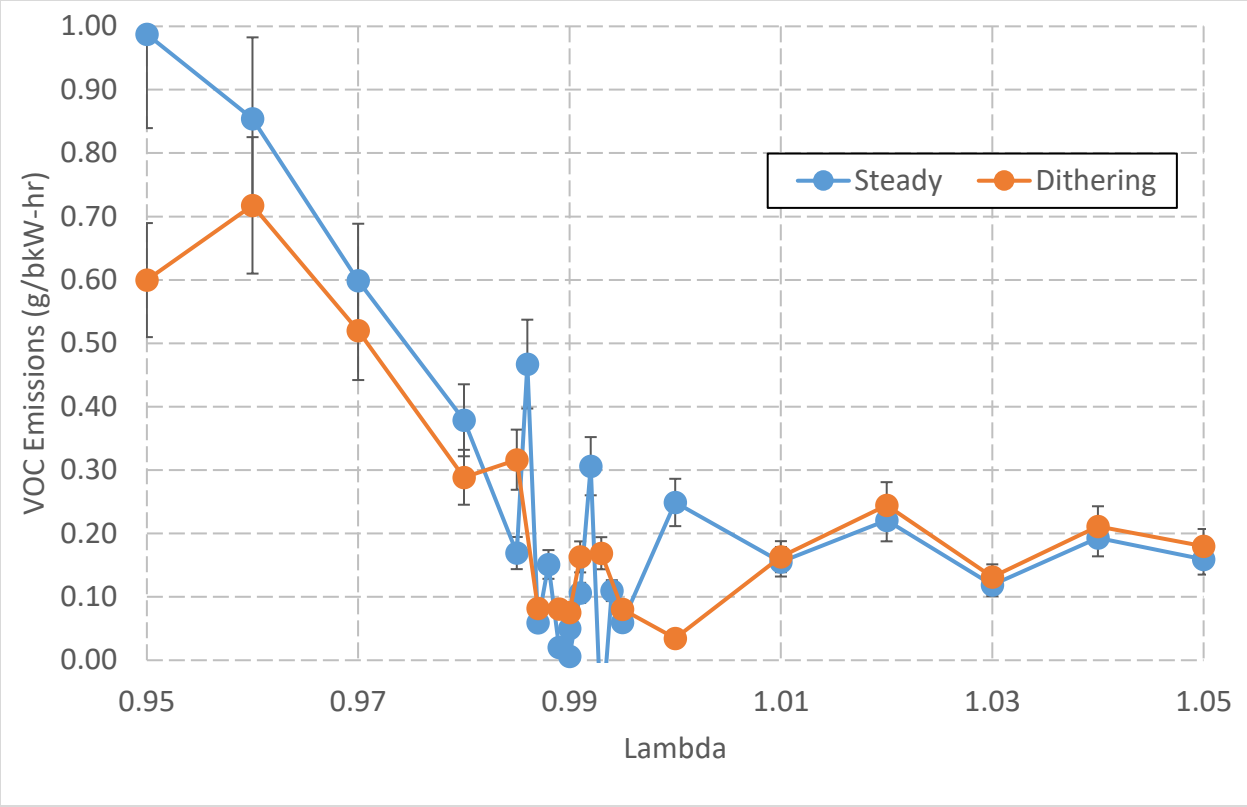

Figure 30: VOC emissions across the lambda sweep. Dithering emissions are slightly lower than steady state emissions, but not outside the error margin for the emissions measurement. Dithering does not have a large effect.

As previously mentioned, methane (CH_4) emissions are not currently regulated by the EPA, but are likely to come into greater focus in the future as concerns about greenhouse gasses increase. Figure 31 shows methane emissions for the dithering and steady state lambda sweeps. Near the stoichiometric point between λ=0.98 and λ=1.01, methane emissions for the dithering sweep are significantly lower than the steady (non-dithering) emissions. At lambdas richer than λ=0.98, methane emissions are higher due to the depth of rich excursions during dithering. At lambdas leaner than λ=1.01, the dithering and non-dithering emissions are nearly identical.

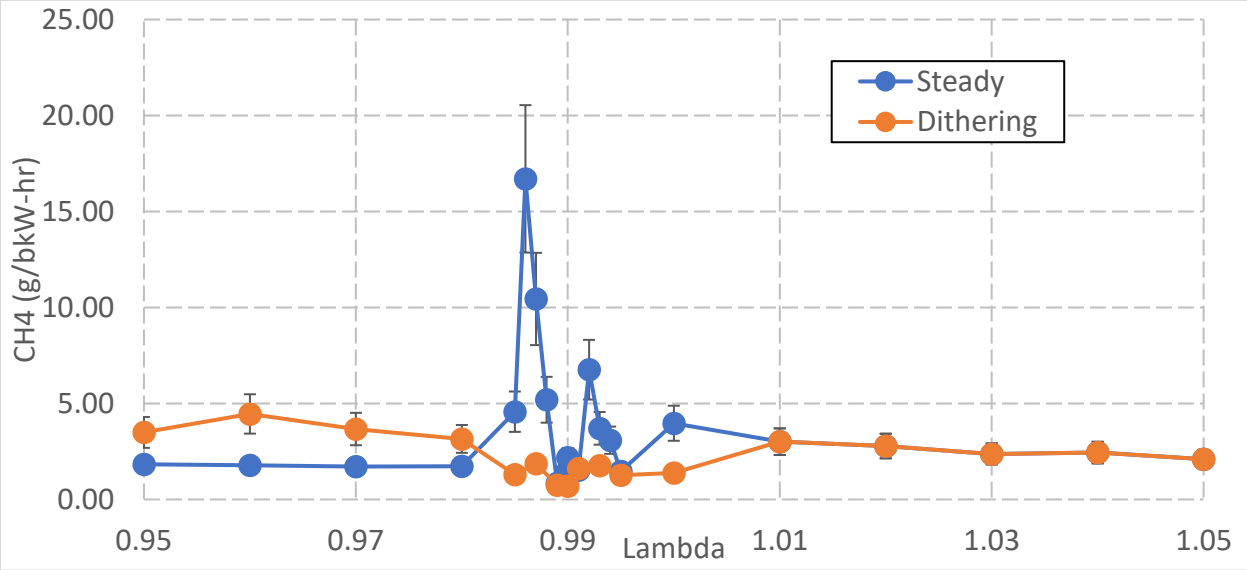

Figure 31: Methane emissions are significantly reduced by dithering from λ=0.98 to λ=1.01.

Ammonia emissions can be reduced by dithering if the dithering midpoint is not too rich. Figure 32 shows ammonia emissions during the lambda sweep. At lambdas richer than λ=1, dithering results in lower ammonia emissions than the steady state case. In the lean region where λ>1, ammonia production is nearly zero for both dithering and non-dithering cases.

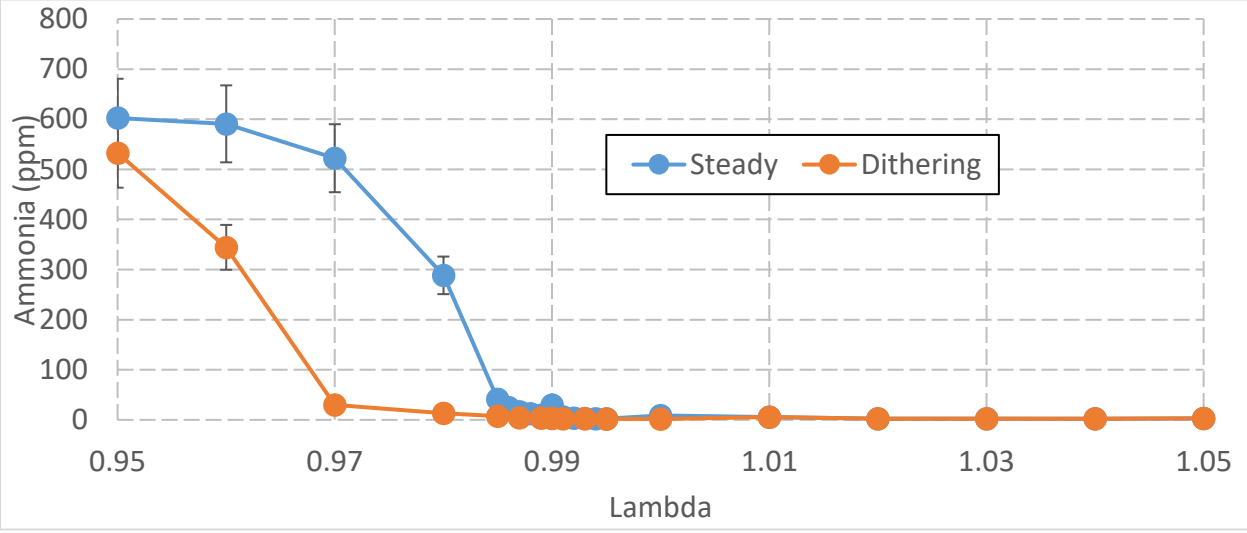

Figure 32: Ammonia emissions are reduced by dithering.

Formaldehyde emissions for the steady and dithering lambda sweeps are shown in Figure 33. In all cases, the formaldehyde emissions for the dithering test cases are lower than the steady

state test case emissions. There is a spike in steady state formaldehyde emissions around λ=0.987, but this spike is eliminated by dithering.

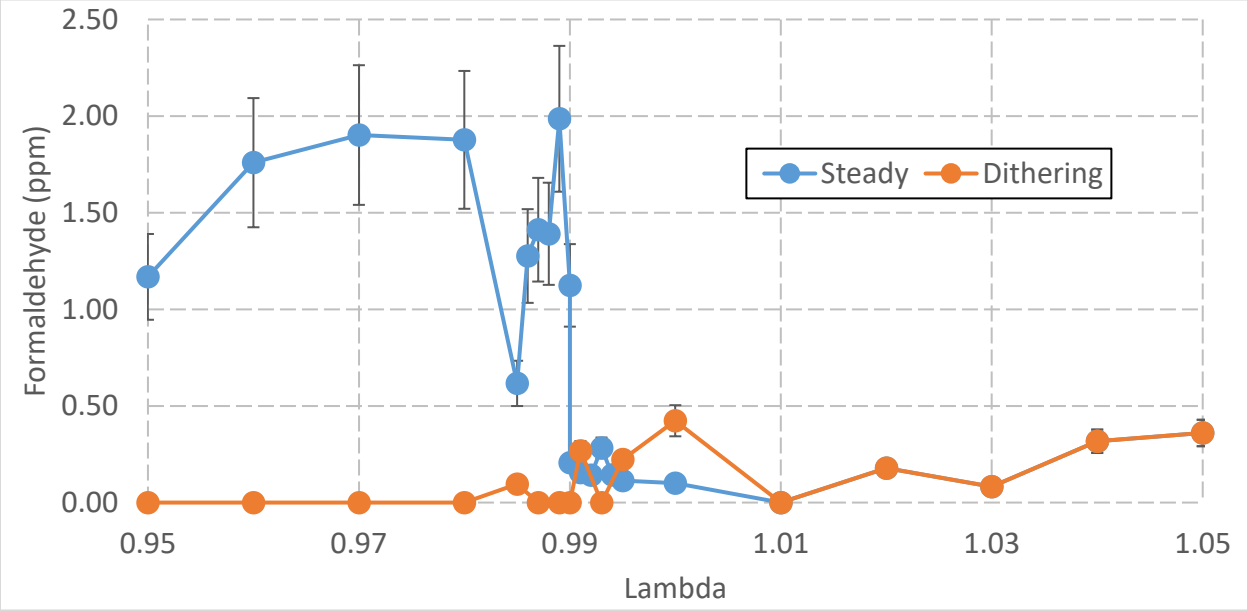

Figure 33: Formaldehyde emissions across the lambda sweep. Dithering reduces formaldehyde emissions across the whole range of lambdas, however all formaldehyde emissions are extremely low, compared to the EPA limit of 10.3 ppm.

Pre- and post-catalyst temperatures were recorded during the steady and dithering lambda sweeps to observe if dithering at different lambda values has a significant impact on catalyst temperatures. Figure 34 shows the pre-catalyst temperatures, and Figure 35 shows the post catalyst temperatures. Dithering did not have a significant impact on pre-catalyst temperatures. However, catalyst outlet temperatures were around 35°C higher in the lean region where λ>1, due to rich excursions.

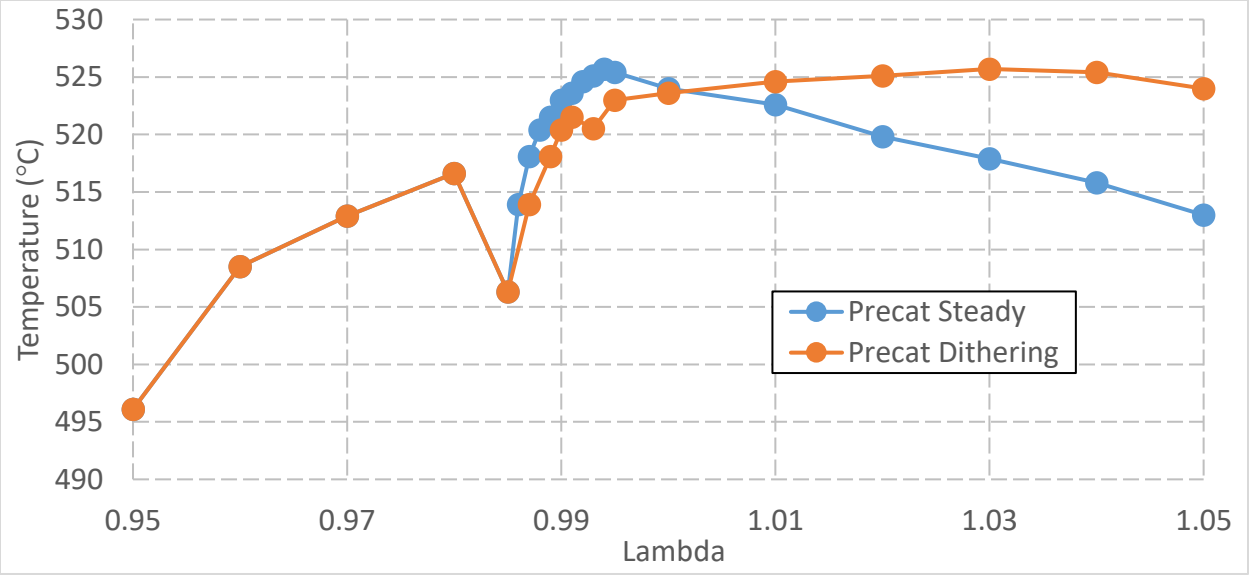

Figure 34: Pre-catalyst temperatures across the lambda sweep. Dithering did not have a significant impact on catalyst inlet temperature, with the biggest temperature difference between steady and dithering being 11°C.

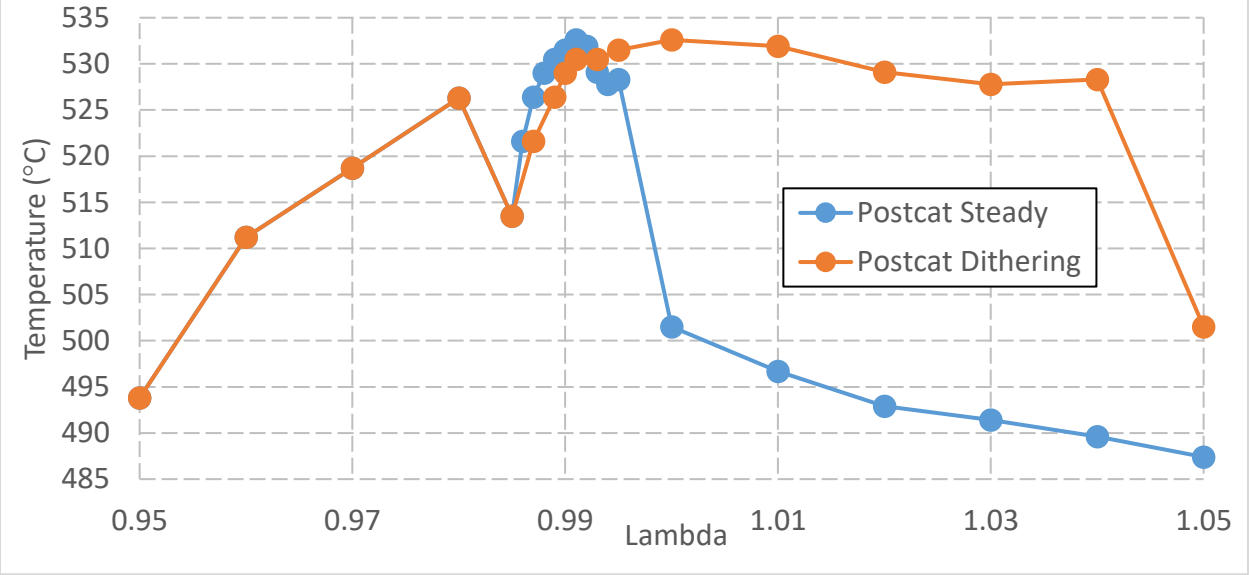

Figure 35: Post-catalyst temperatures. Dithering did not have a significant effect on catalyst outlet temperature other than from 1.00<λ<1.05. In this region, the catalyst outlet was approximately 35° hotter.

4.3 WINDOW OF COMPLIANCE

The window of compliance for stoichiometric natural gas engines has been previously discussed by Defoort and will be further investigated in this study [19]. Air-fuel ratio dithering has the potential to significantly reduce emissions across a wide range of air fuel ratios by utilizing the oxygen storage and release properties of the ceria in the washcoat in the catalyst. The equations in Table 3 detail how ceria can switch between CeO_2 and Ce_2O_3 during slight lean and rich excursions, storing and releasing oxygen in active sites. During lean excursions, excess oxygen from O_2, NO, and NO_2 is stored. This stored oxygen is then released during rich excursions when there is a lack of oxygen and oxidizes CO and H_2. These reactions supplement the steady state reactions listed in Table 2, providing greater emissions reductions.

Figure 36 shows the air-fuel ratio window of emissions compliance for the CAT CG137-8 with the standard production catalyst. The steady state window of compliance for the engine is 0.007λ, while the dithering window of compliance is 0.015λ. This is a significant improvement and would allow the engine to better remain in emissions compliance through unknown load and fuel transients. More of the widening of the window of compliance is on the rich side, with the CO emissions rising more slowly during the dithering lambda sweep than during the steady state lambda sweep. Lean excursions during rich operation can supply the catalyst with NOx, providing oxygen for release during the rich excursion.

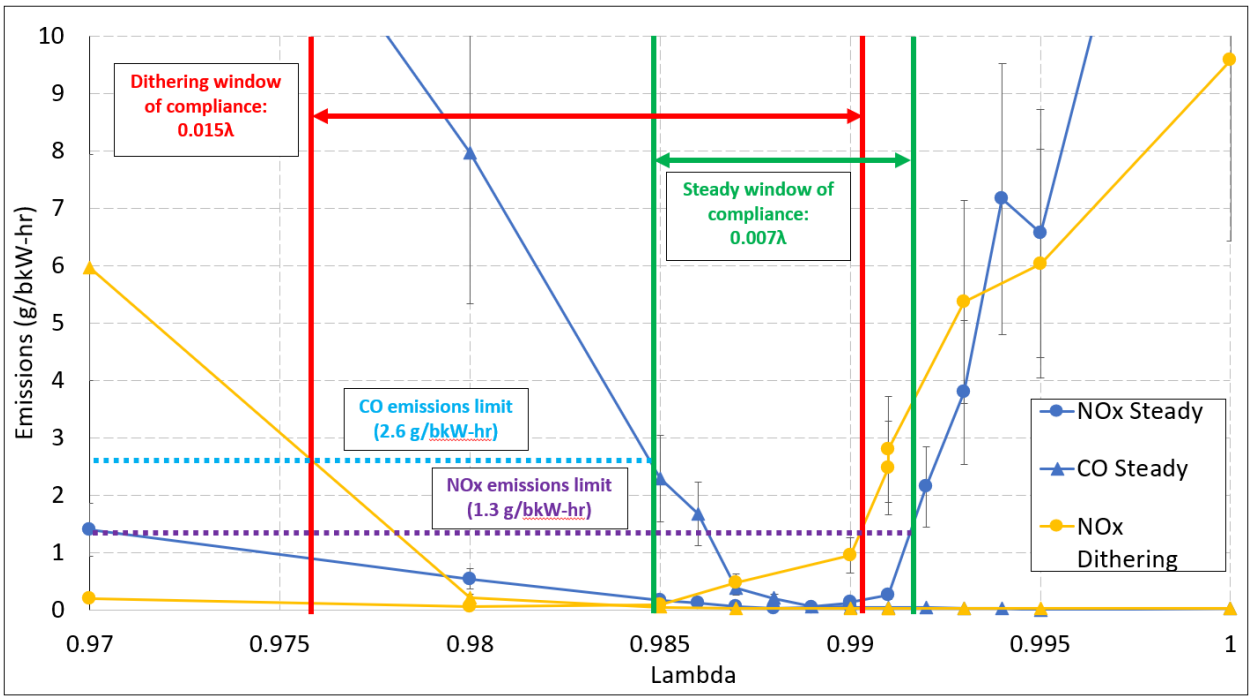

Figure 36: The window of emissions compliance through a dithering and non-dithering lambda sweep. Emissions are bound on the right side by the CO emissions limit and on the left by the NOx emissions limit. Dithering significantly expanded this window.

4.4 LONG TIME PERIOD DITHERING

To investigate the oxygen storage and release in the catalyst and how this can be tracked with the oxygen sensors, a long time period dither was tested. For this test, 1.5% amplitude was used, with a 15 second rich phase and a 15 second lean phase. This test allowed the catalyst to reach complete oxygen saturation and depletion. Figure 37 shows the sensor signals versus time. During rich excursions, the signal from the post catalyst oxygen sensor stays "leaner" than the pre-catalyst signal, signifying that the exhaust exiting the catalyst has a higher concentration of oxygen in it than the exhaust entering the catalyst. This is due to oxygen release from the ceria in the catalyst. During lean excursions, the post-catalyst sensor signal is "richer" than the pre-

catalyst signal, signifying oxygen storage. Oxygen from the exhaust stream entering the catalyst is being stored, so the post-catalyst exhaust has less oxygen. Each of these effects is seen for the first 7-8 seconds of the lean/rich excursion, but after that the pre- and post-catalyst signals follow each other closely. This is because after 7-8 seconds, the catalyst reaches oxygen saturation or depletion.

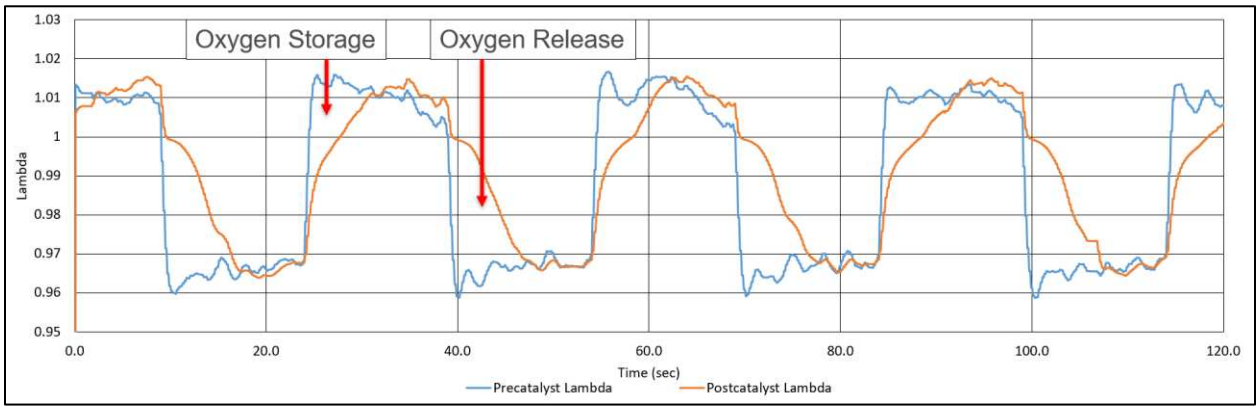

Figure 37: Pre- and post-catalyst lambda signals from the oxygen sensors. It takes about 8 seconds for the catalyst to saturate and deplete with oxygen.

4.5 NOx SENSOR MINIMIZATION POTENTIAL

The CG137-8 test cell was equipped with an ECM NOx sensor, which could potentially be used as an alternative to oxygen sensor control. While this is not the main focus of this experiment, it was noted that the ECM NOx sensor is indeed cross-sensitive to ammonia (NH¬3). If the engine is running lean, the ECM NOx sensor senses the NOx, outputting a value. If the engine is running rich, the ECM NOx sensor senses ammonia being produced and cannot distinguish it from NOx, and therefore outputs a value as if NOx were present. Figure 38 shows the NOx sensor output and compares it with the ammonia concentration in the exhaust. It is

evident that the NOx sensor is reacting to the ammonia in the exhaust in addition to the NOx in the exhaust stream. The window where the sensor output is low is between λ=0.985 and λ=0.991, the zone where NOx and CO emissions are also at a minimum. This is an ideal reaction from the NOx sensor, because if the air-fuel ratio is controlled to keep the NOx sensor signal at a minimum, it will also keep the NOx and CO emissions in their window of emissions compliance as measured in this study (Figure 36). The NOx sensor could offer a new strategy for engine control, where the engine control works to ensure the NOx sensor output is at a minimum.

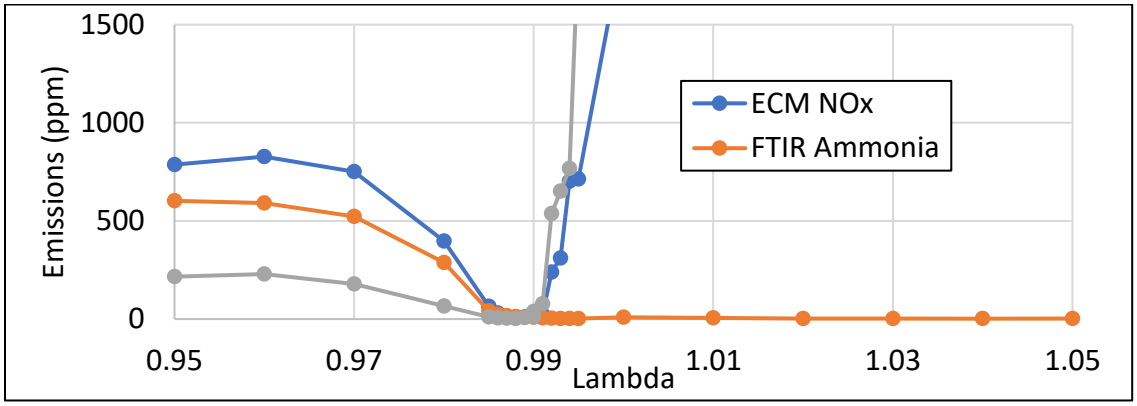

Figure 38: The ECM NOx sensor is cross-sensitive to ammonia. The NOx sensor output here is compared to ammonia as measured by lab equipment.

CHAPTER 5: ADVANCED CONTROL STRATEGIES AND THEIR EFFECTS ON DIFFERENT CATALYSTS

5.1 ½ OXYGEN STORAGE CAPACITY CATALYST

5.1.1 DITHERING PARAMETER SWEEP

The catalyst two was developed by BASF to have one half the oxygen storage capacity (OSC) of the standard catalyst. The OSC is primarily provided by ceria and the reactions listed in

Table 3. This catalyst was subjected to the same dithering parameter sweep as the standard catalyst. The first parameter of interest is NOx emissions across the dithering parameter sweep. The same trends that were seen with the standard catalyst can also be seen with the ½ OSC catalyst. The NOx steady state lambda emissions are 0.0412 g/bkW-hr (6.4 ppm) ,while the best-case dithering emissions are 0.002 g/bkW-hr (0.3 ppm) at 1.5% and 1 Hz. Emissions at low frequencies such as 0.1 Hz and 0.2 Hz are significantly higher than the steady state point. This is due to non-optimized oxygen storage.

The other primary emission of concern for this engine class is CO. Figure 40 shows the CO emissions during the dithering parameter sweep. Similar to the emissions from the standard catalyst, higher dithering frequencies at all amplitudes show an emissions reduction compared to the steady state, while slow frequencies result in higher emissions than steady state. At low frequencies, too much time is spent in the rich and lean zones, resulting in oxygen depletion and

oxygen storage in the catalyst. The steady state CO emissions are 0.44 g/bkW-hr, while the dithering emissions are 0.059 g/bkW-hr.

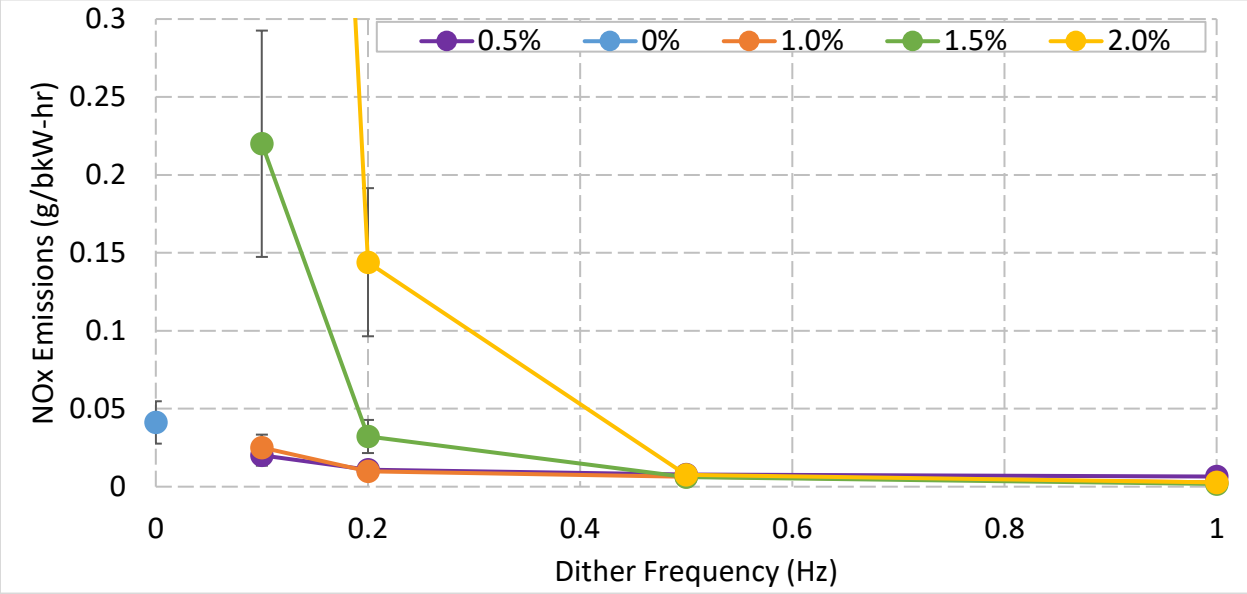

Figure 39: NOx emissions with the 1/2 OSC catalyst. NOx emissions are significantly reduced at high dithering frequencies, while low frequencies have significantly higher emissions than steady state.

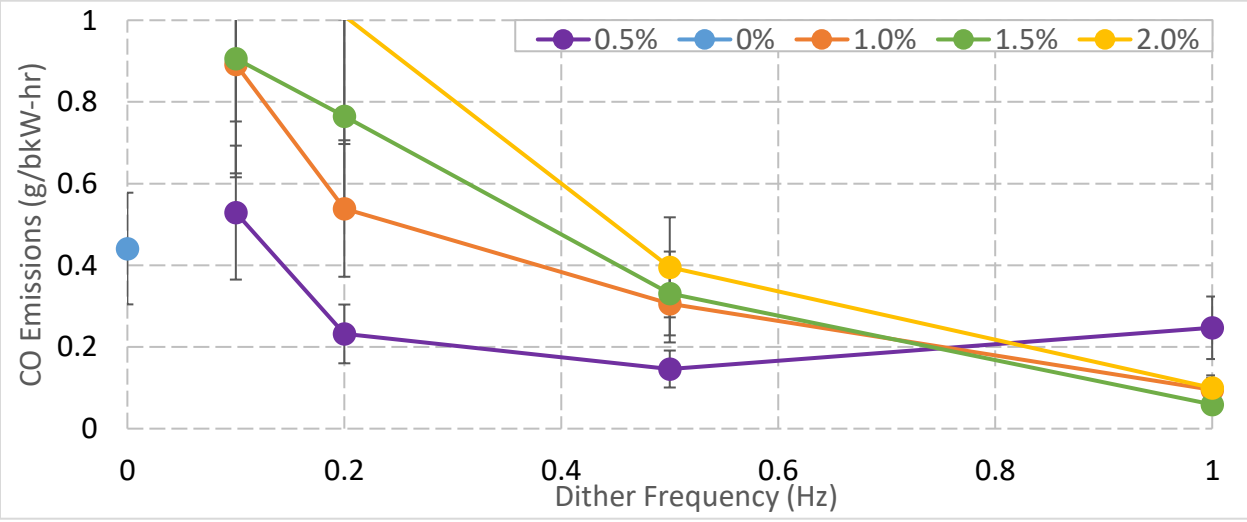

Figure 40: CO emissions during the dithering parameter sweep with the ½ OSC catalyst. CO emissions are reduced significantly at high frequencies and are significantly higher at low frequencies. 0.5% amplitude does not have as large of an effect on emissions as the larger dithering amplitudes.

NOx and CO emissions are the primary emissions concern for this engine class at this time, but other emissions such as total hydrocarbons are also of concern. Figure 41 shows the hydrocarbon emissions for the dithering sweep. With the ½ OSC catalyst, THC emissions are affected by dithering, unlike for the standard catalyst. THC emissions are the lowest at the lowest dithering frequency, 0.1 Hz. THC emissions increase with dithering frequencies. The best case for NOx and CO emissions is 1.5% dithering amplitude and 1 Hz dithering frequency. This is not the best case for THC emissions. Steady state THC emissions are 0.21 g/bkW-hr, while dithering THC emissions for the best NOx and CO point (1 Hz and 1.5%) is 0.23 g/bkW-hr. This means that dithering at the optimal frequency and amplitude for NOx and CO emission reduction results in slightly higher THC emissions with the ½ OSC catalyst. However, the increase is not significant and is within the error margin for both datapoints.

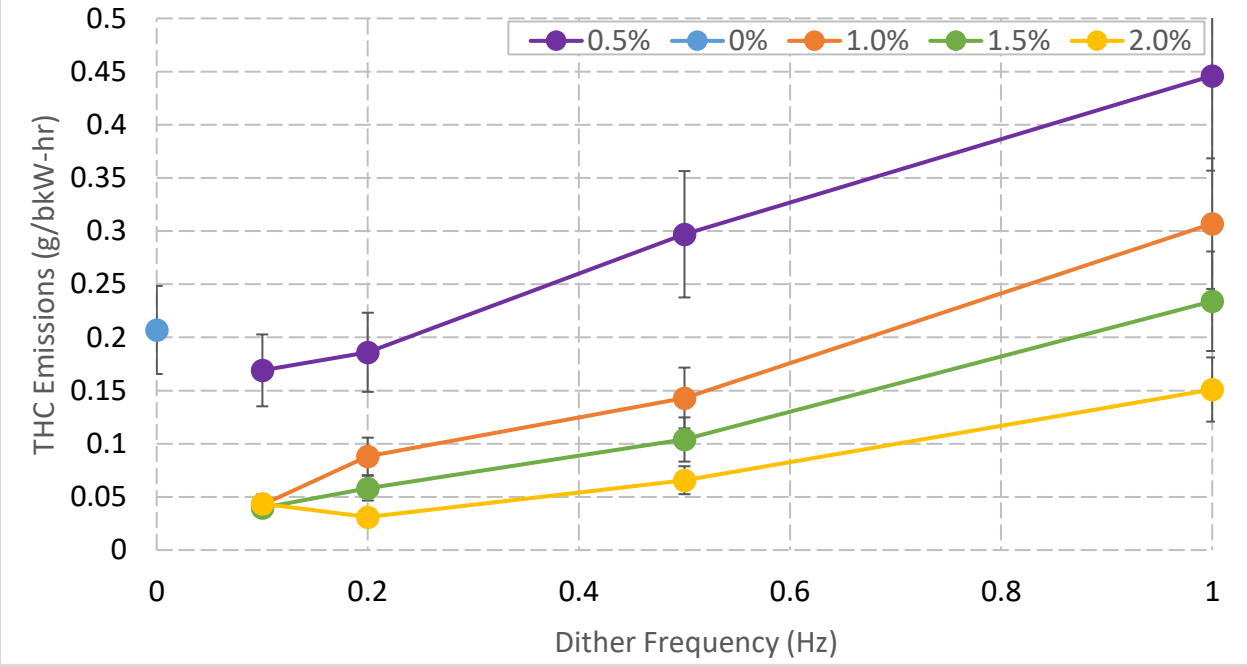

Figure 41: 1/2 OSC catalyst THC emissions across the dithering sweep. THC emissions are lowest at low dithering frequencies with high amplitudes. Higher frequencies increase emissions.

THC emissions are not regulated, but the non-methane and non-ethane hydrocarbon (VOCs) emissions are regulated by the EPA. Figure 42 shows the VOC emissions. 0.2Hz dithering has the highest VOC emissions at all dithering amplitudes, with emissions being nearly the same or higher. Steady state emissions are 0.071 g/bkW-hr, and the lowest dithering emissions are at the 1 Hz and 1.5% dithering case. This is also the case that provides the lowest NOx and CO emissions.

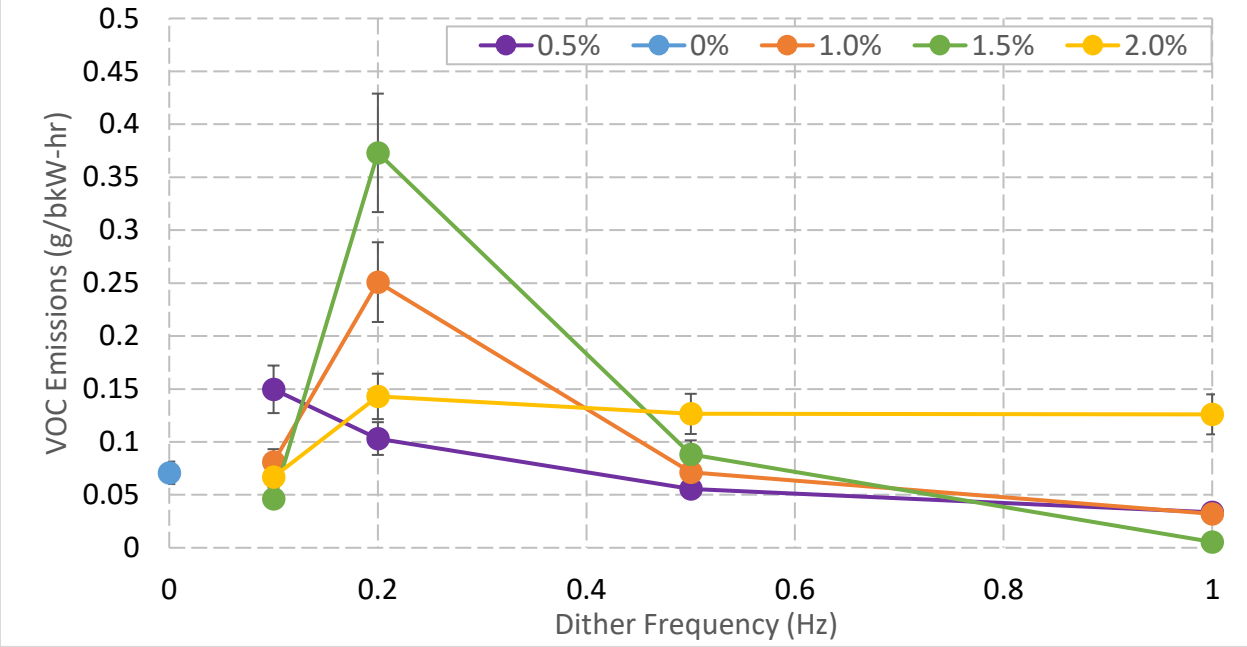

Figure 42: VOC emissions during the dithering sweep with the 1/2 OSC catalyst. 0.2Hz dithering has the highest emissions at all amplitudes, with 1Hz having the lowest emissions for nearly all dithering cases.

Another portion of the THC emissions are methane (CH_4) emissions. Figure 43 shows the methane emissions across the dithering sweep. For smaller amplitudes, dithering does not have much effect on the methane emissions. For larger amplitudes, emissions are significantly increased at 0.5 Hz, but at 1 Hz and 1.5% the CH_4 emissions reach a low point which is lower than the steady state point. Steady state methane emissions are 0.391 g/bkW-hr, while the dithering emissions at 1.5% and 1 Hz are 0.011 g/bkW-hr, a significant reduction. This is also

the optimal dithering point for NOx and CO emissions. Steady state CH_4 emissions are 0.391 g/bkW-hr, while optimal CH_4 emissions with dithering are 0.011 g/bkW-hr, a significant reduction.

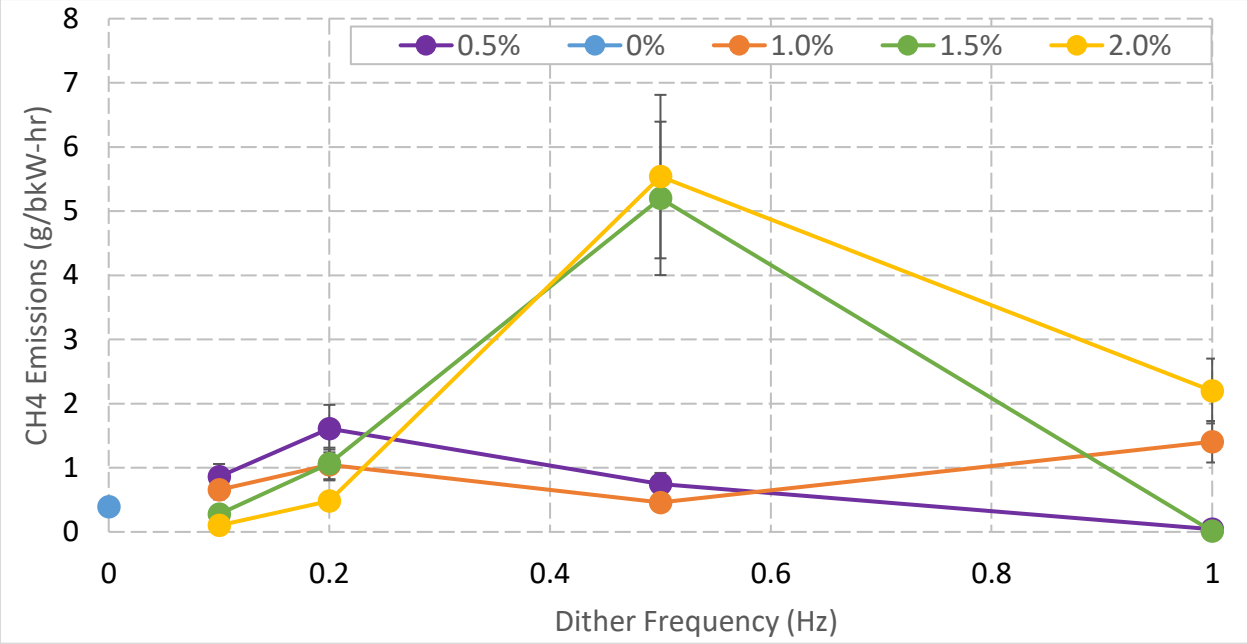

Figure 43: Methane emissions during the dithering sweep with the 1/2 OSC catalyst. methane emissions are slightly increased with dithering at lower frequencies but are minimized at 1 Hz and 1.5% dithering amplitude.

Ammonia (NH_3) production in the catalyst is another concern when applying dithering strategies. Figure 44 shows ammonia emissions across the dithering parameter sweep with the ½ OSC catalyst. At 0.1 Hz, emissions are slightly higher than the steady state point, and at 0.2 Hz emissions are significantly higher than the steady state point. At 0.5 Hz, emissions are comparable to the steady state point. At 1 Hz, 1% and 2% amplitude dithering have the lowest emissions, significantly lower than the steady state emissions. Steady state ammonia emissions are 143 ppm, while the best-case ammonia emissions (1.5% and 1 Hz) are 80 ppm. The optimal dithering point for low ammonia emissions is the same point as the optimal for NOx and CO.

Ammonia emissions are higher than expected for all cases likely because the engine was running slightly richer than λ=0.99 as a midpoint due to oxygen sensor calibration.

A final emission of concern is formaldehyde, CH_2O. Steady state formaldehyde emissions were already incredibly low, at 0.062 ppm. During the dithering tests, the emissions analyzer read nearly zero formaldehyde concentration for most tests, signaling that emissions were so close to zero they were non-readable. Therefore, the effect of dithering on formaldehyde emissions is minimal. The EPA NESHAP regulations for formaldehyde for this engine class are 10.3 ppm (assuming an existing engine at a major source), far above any measured formaldehyde emissions.

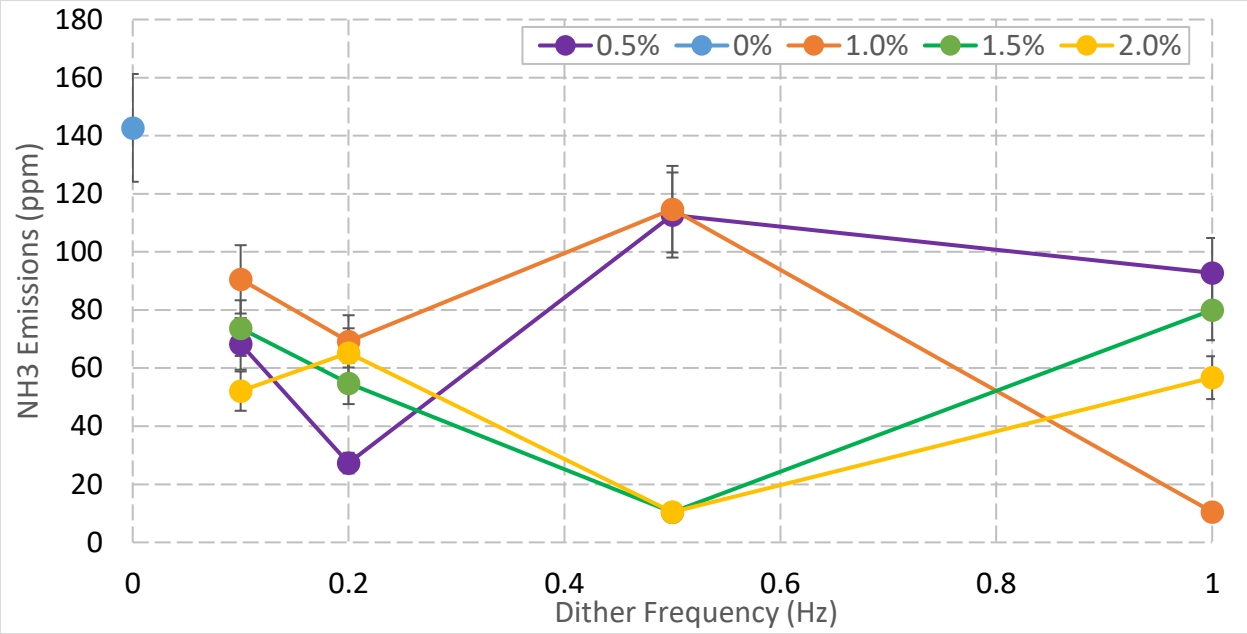

Figure 44: Ammonia emissions across the dithering sweep with the 1/2 OSC catalyst. Dithering at 0.2 Hz increases ammonia emissions for almost all amplitudes. Dithering at 1 Hz decreases emissions for all frequencies other than 2%.

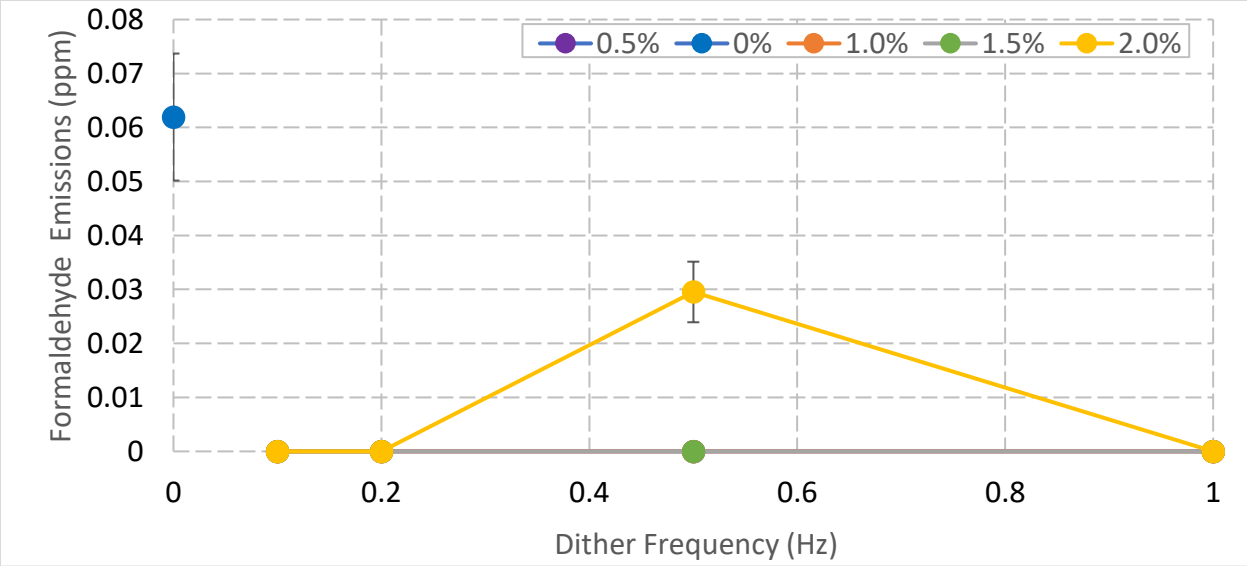

Figure 45: Formaldehyde emissions across the dithering sweep with the 1/2 OSC catalyst. Nearly all emissions read as zero on the emissions analyzer, signaling that formaldehyde emissions are nearly zero in all cases and unaffected by dithering. These emissions are significantly lower than the EPA emissions limit of 10.3 ppm (assuming an existing engine at a major source).

5.1.2 LAMBDA SWEEP WITH ½ OSC CATALYST\

The same lambda sweep that was performed on the standard catalyst was also performed on the ½ oxygen storage content catalyst to investigate the effects of dithering on rich and lean air fuel ratios, as well as on the window of compliance. On the steady state lambda sweep, a DAQ error resulted in the emissions data from datapoints λ=0.95 through λ=0.97 to not be recorded. This was not the main area of interest for the study, so a narrower look at lambda-based emissions data is acceptable for this study. Figure 46 shows the NOx and CO emissions

from the full lambda sweep, while Figure 47 shows a zoomed in version, highlighting the rich CO emissions reductions accomplished by dithering.

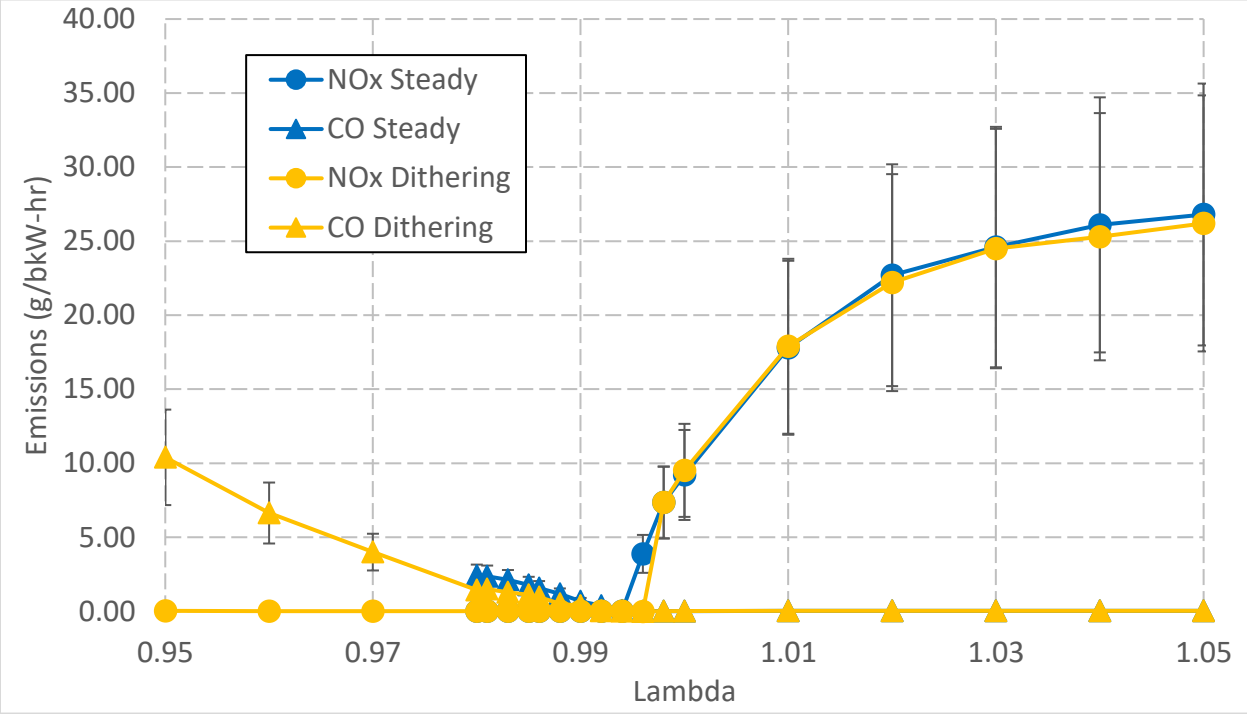

Figure 46: NOx and CO emissions during a lambda sweep with the 1/2 OSC catalyst. Dithering is more effective at reducing CO emissions in the rich region than it is at reducing NOx emissions in the lean region.

Both NOx and CO emissions are reduced in the region from λ=0.98 to λ=1.00, but a more consistent reduction is seen in the CO emissions. However, total hydrocarbon emissions are affected differently by dithering. Figure 48 shows THC emissions during a lambda sweep. During the lambda sweep, rich THC dithering emissions are much higher than the steady state case. This is due to rich excursions and non-optimal oxygen storage and release in the catalyst. For the lambda sweep, 1.5% amplitude and 1 Hz dithering were used. As can be seen in Figure 41, the THC emissions at this amplitude are higher than the steady state case. The effects of non-optimized dithering with this catalyst are amplified as the midpoint dithering amplitude shifts rich, and more hydrocarbons can slip through the catalyst.

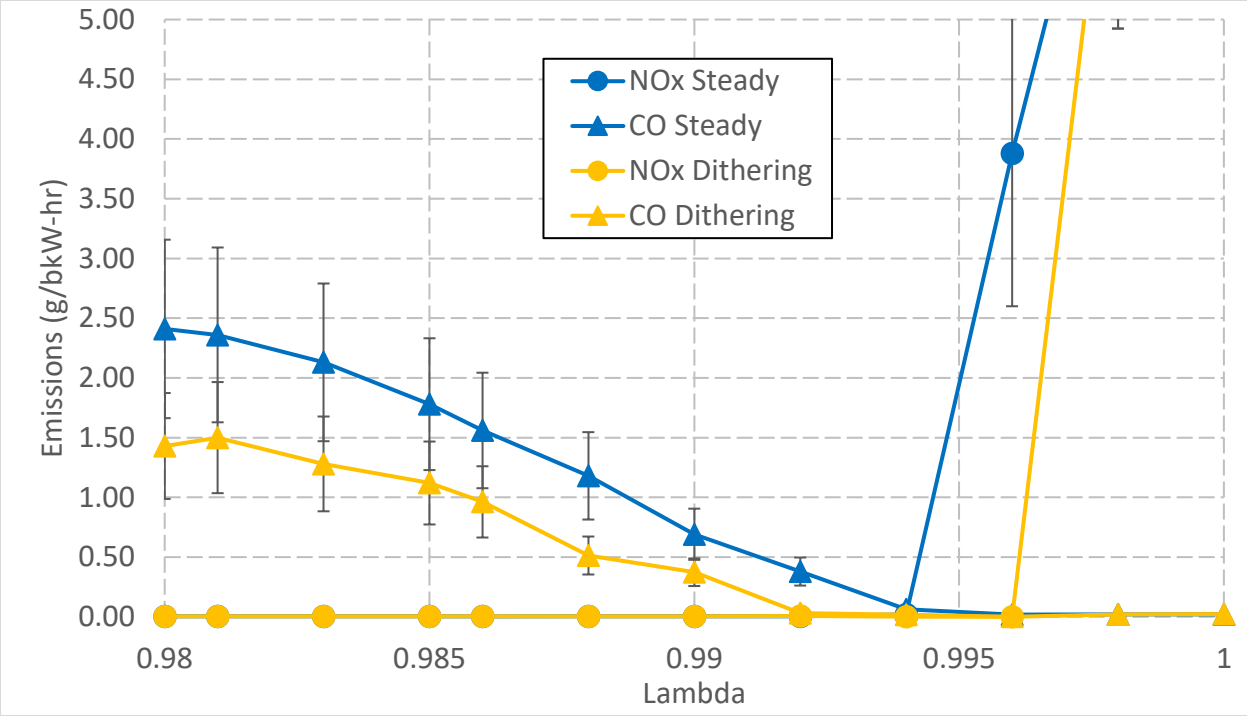

Figure 47: NOx and CO emissions over a narrow lambda range from the lambda sweep with the 1/2 OSC catalyst. Dithering is effective at reducing CO in the rich region.

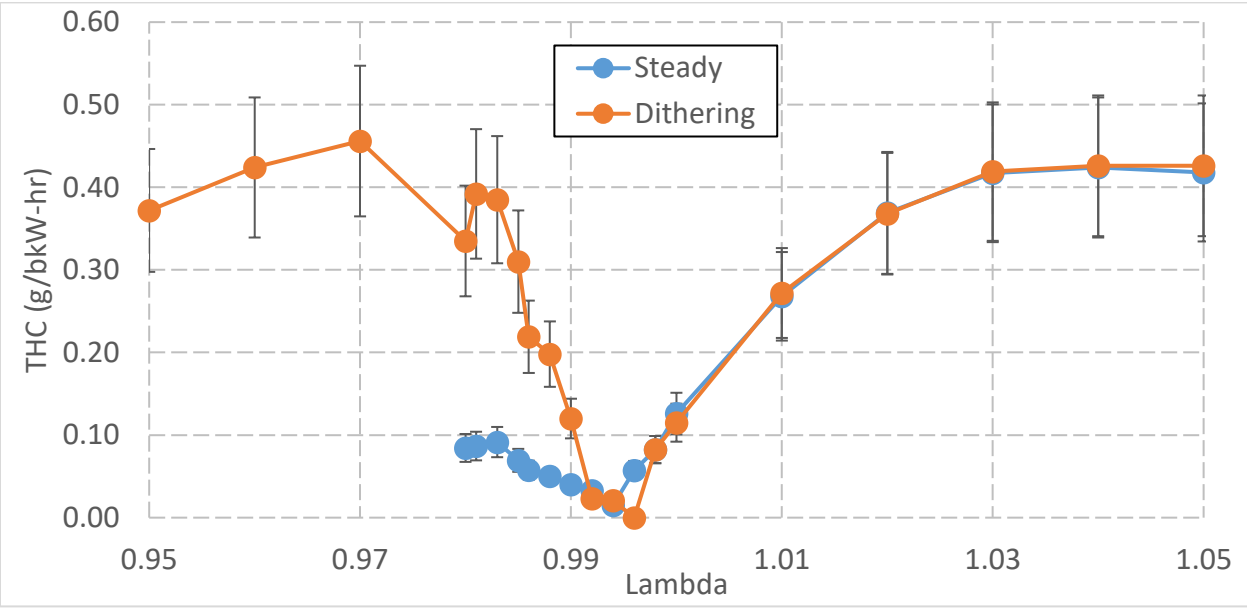

Figure 48: Steady vs. dithering THC emissions with the ½ OSC catalyst. The dithering THC emissions rise much more quickly with rich engine operation than the steady state THC emissions. Lean THC emissions are very similar for the dithering and non-dithering cases.

Non-methane and non-ethane hydrocarbons have a similar reaction to dithering. Figure 49 shows the VOC emissions during the dithering and steady state lambda sweeps. There is a spike in emissions for both the dithering and non-dithering case around λ=0.993. When comparing the dithering and steady state cases, it can be seen that in most test cases, the VOC emissions are higher for the dithering case than for the non-dithering case. The spike in VOC emissions is unexpected near λ=0.992 because during the dithering parameter sweep, the 1 Hz and 1.5% dithering case resulted in extremely low emissions (Figure 42). This spike was seen in both the dithering and non-dithering cases, so it is not caused by the dithering control modification.

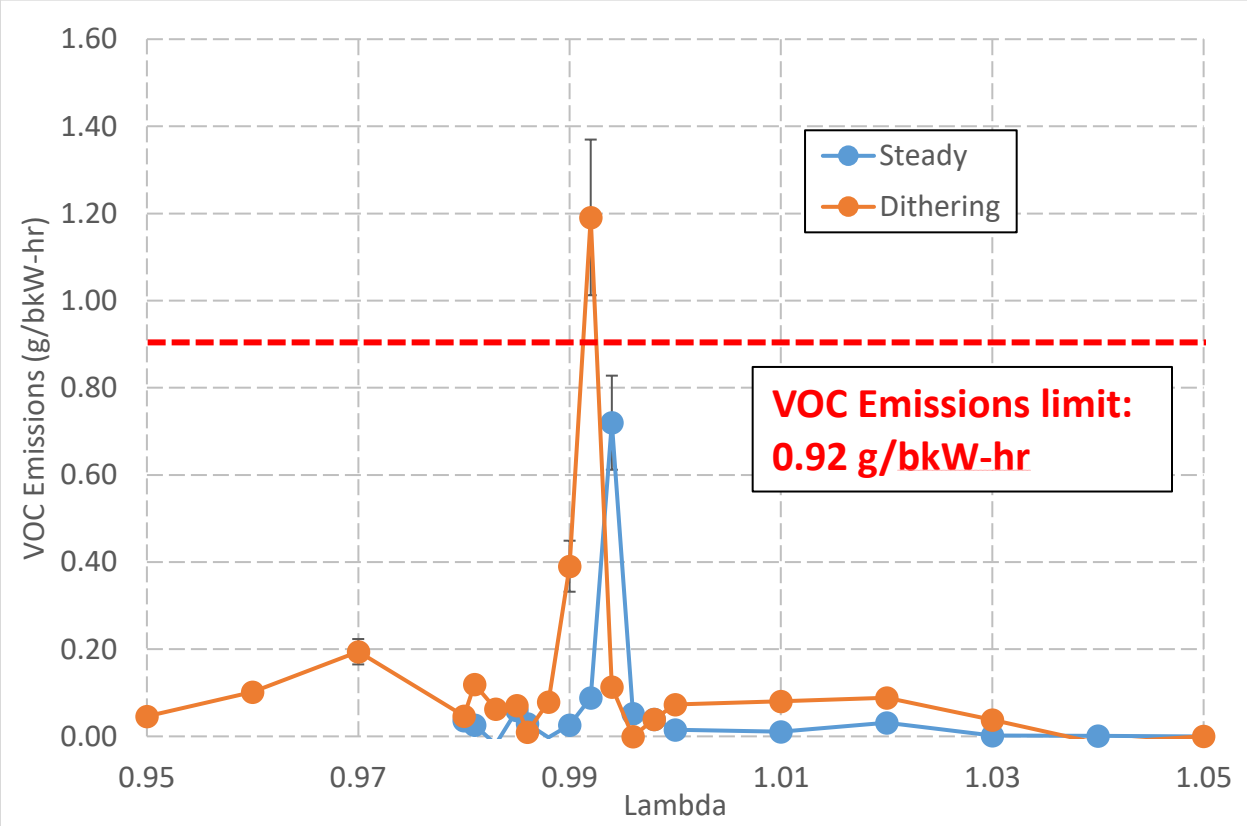

Figure 49: VOC emissions during the dithering sweep with the 1/2 OSC catalyst. There is a spike in VOC emissions around λ=0.992. Dithering emissions are slightly higher than the steady state emissions, but not significantly so.

Methane emissions with the ½ OSC catalyst during the lambda sweep are shown in Figure 50. The spike observed with VOC emissions is present in the steady state methane emissions at λ=0.992, but not in the dithering case. However, for every other lambda point, the dithering emissions are higher than the steady state emissions. This is again due to non-optimized dithering on the catalyst with less oxygen storage capability.

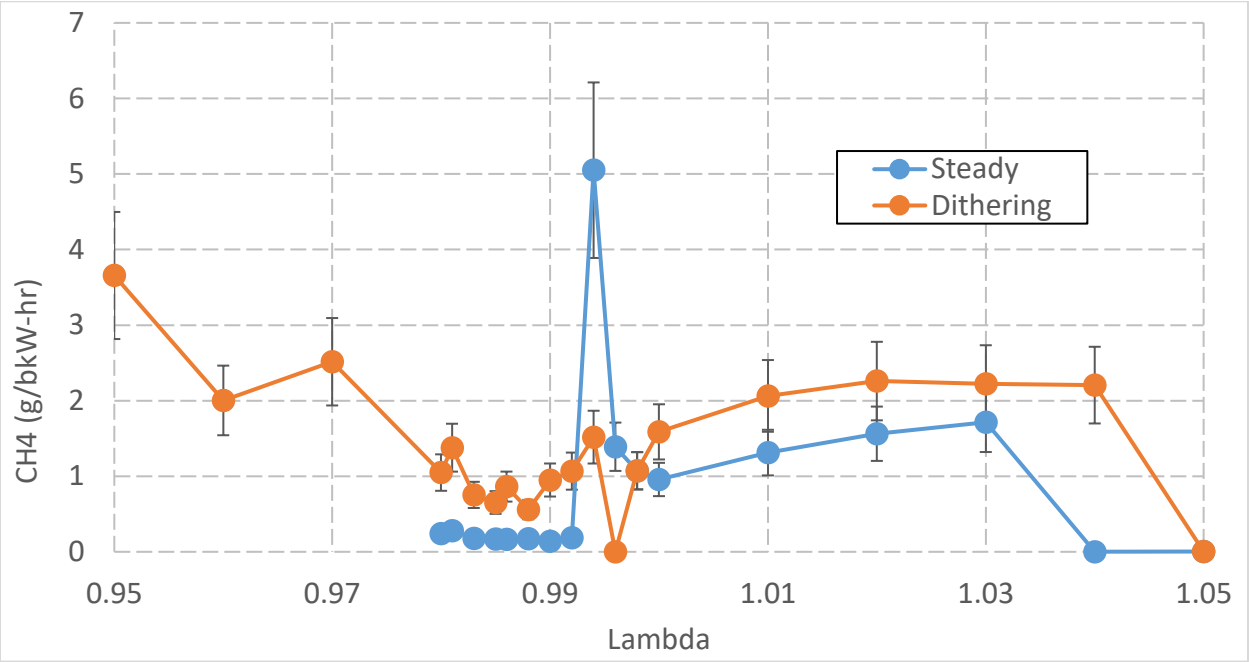

Figure 50:Methane emissions during the lambda sweep with the 1/2 OSC catalyst. Dithering emissions are higher than non-dithering emissions in almost all cases.

Ammonia emissions are not significantly affected in the lambda sweep. Figure 51 shows the ammonia emissions. In the rich region, dithering ammonia emissions are higher than the steady state emissions. In this region, significant rich excursions combined with dithering not optimized for the ½ OSC catalyst results in ammonia production. While leaner than λ=0.987, ammonia emissions are largely unaffected by dithering.

Figure 52 shows the formaldehyde emissions. The dithering and steady-state formaldehyde emission are both nearly zero, with the highest formaldehyde emissions recorded

being 0.47 ppm at the λ=0.981 dithering test case. The proximity of all the emissions values to zero signifies that dithering does not make a large change in formaldehyde emissions.

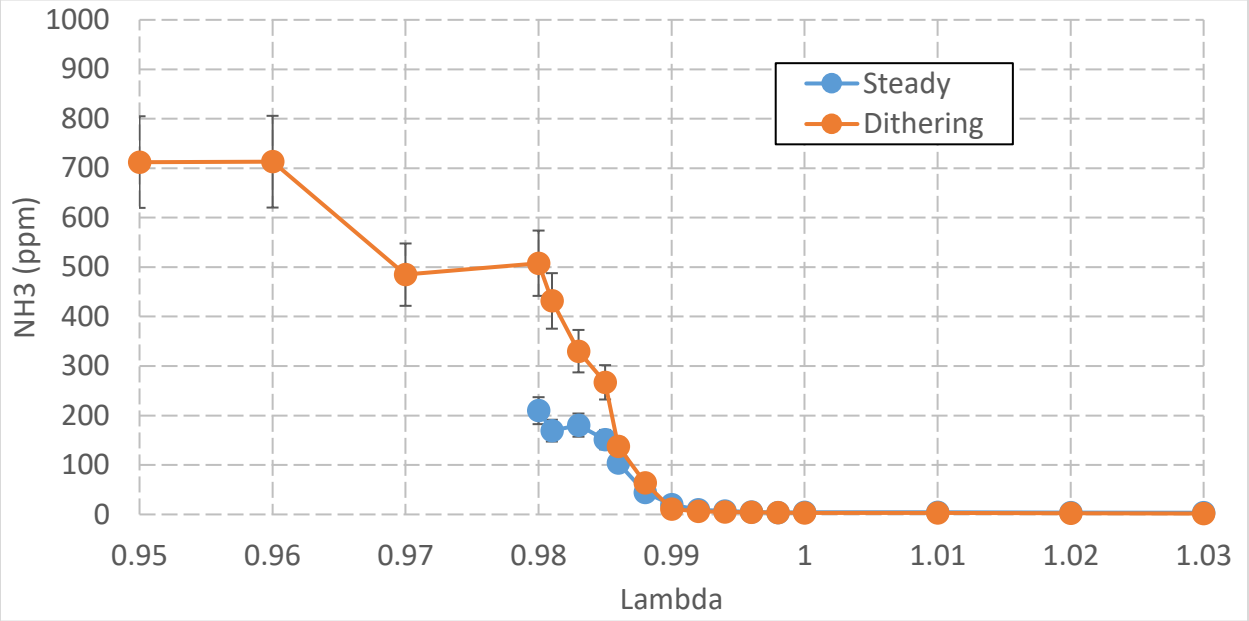

Figure 51: Ammonia emissions during the lambda sweep with the 1/2 OSC catalyst. Ammonia emissions are not significantly affected by dithering until lambda starts becoming rich.

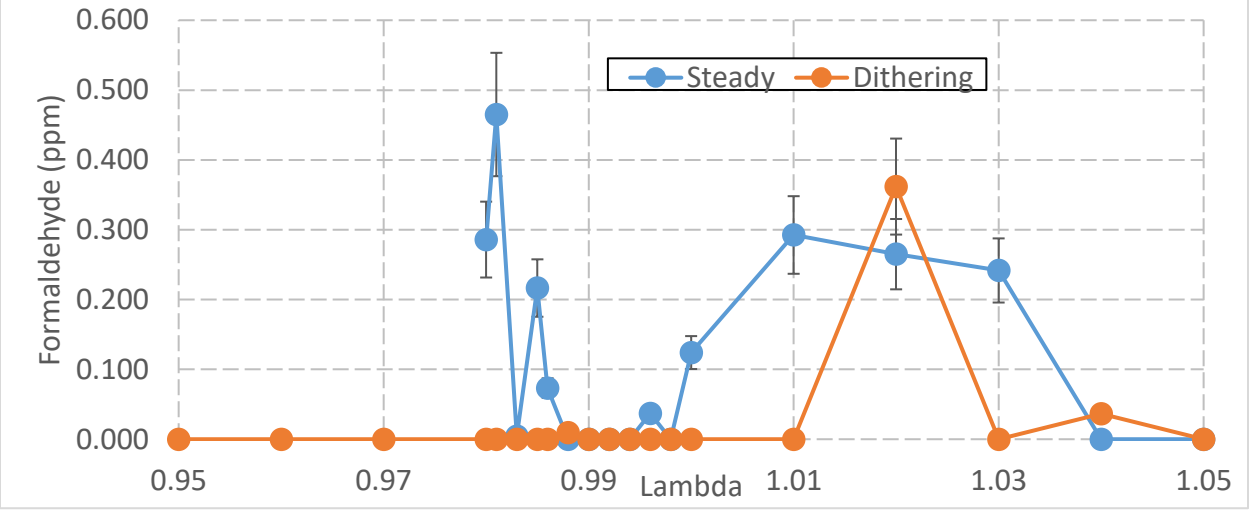

Figure 52: Formaldehyde emissions are nearly zero for every case, dithering and steady. The steady formaldehyde emissions are slightly higher, but both values are very close to zero. The EPA NESHAP emissions limit for formaldehyde is 10.3 ppm (assuming an existing engine at a major source).

5.1.3 WINDOW OF COMPLIANCE WITH ½ OSC CATALYST

It is important to investigate the window of emissions compliance for the new catalyst to determine if dithering is still able to improve it. Figure 53 shows the emissions window of compliance for dithering and steady test cases. The window of compliance was increased from 0.014 to 0.019λ with dithering control strategy applied. This shows that dithering is still effective even on a catalyst containing less oxygen storage material than the standard catalyst for the CAT CG137-8. As was seen in the window of compliance for the steady state case, the window is widened mainly on the rich side, because dithering is more effective at reducing CO emissions than NOx emissions.

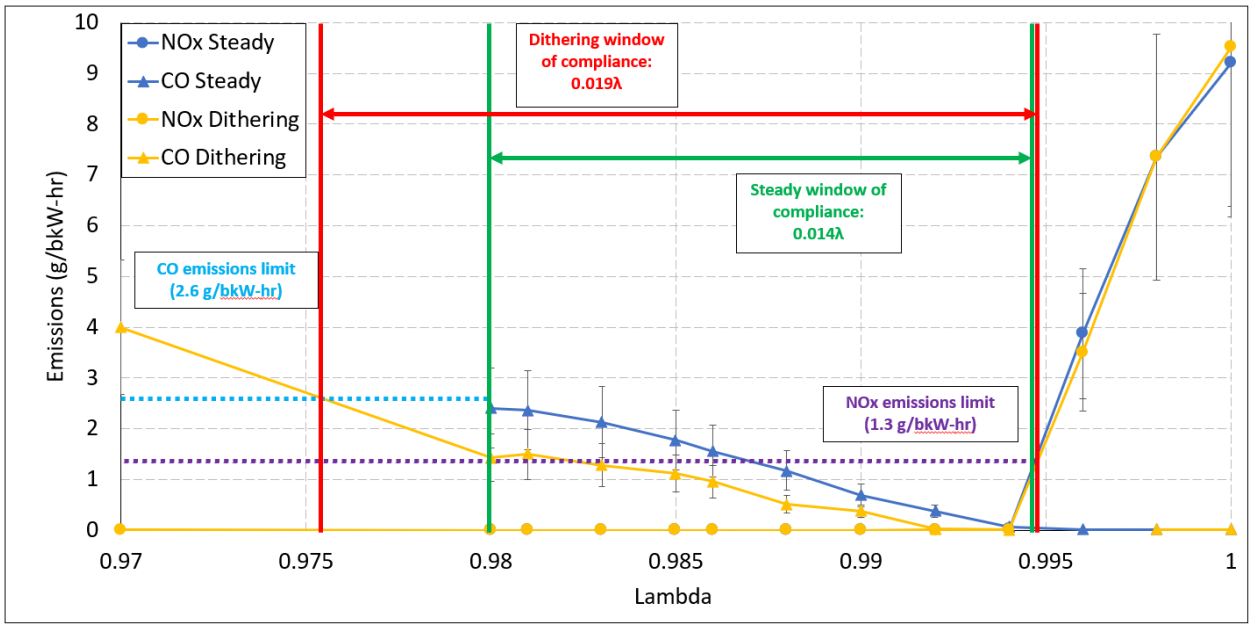

Figure 53: The window of emissions compliance for the 1/2 OSC catalyst. The window is expanded by dithering by 0.005λ.

5.2 AGED CATALYST

5.2.1 DITHERING PARAMETER SWEEP WITH AGED CATALYST

Catalyst three was artificially aged to 16,000 hours using methods described in Chapter 2. A dithering parameter sweep was run to investigate the effects of dithering on catalysts that are near end-of-life. NOx emissions are one of the primary regulated emissions of concern. Figure 54 shows the NOx emissions during the Dithering significantly increases NOx emissions at 0.1 and 0.2 Hz dithering frequencies, at all amplitudes. At 0.5 and 1.0 Hz dithering frequencies, NOx emissions are nearly equivalent to the steady state runs. The steady state NOx emissions with the aged catalyst are 0.086 g/bkW-hr, while the best-case dithering NOx emissions are 0.083 g/bkW-hr, at 1 Hz and 1% amplitude. This is not a significant decrease and suggests that dithering is no longer effective at decreasing NOx emissions in an aged catalyst. As the catalyst ages, active ceria sites can become permanently saturated with oxygen, reducing the oxygen storage capability of the catalyst.

A similar trend to the NOx emissions is seen in the CO emissions. Figure 55 shows the CO emissions during the dithering parameter sweep. Dithering CO emissions are much higher than the steady state case at low dithering frequencies (0.1 and 0.2 Hz) and are nearly equivalent at 0.5 Hz. At the 1 Hz dithering point, CO emissions are slightly reduced. Steady state CO emissions for the aged catalyst are 0.087 g/bkW-hr, while the best-case dithering CO emissions are 0.051 g/bkW-hr at 1% amplitude and 1 Hz. This is a good reduction in CO emissions, but not as significant of a reduction as was seen on the fresh catalyst in Figure 20.

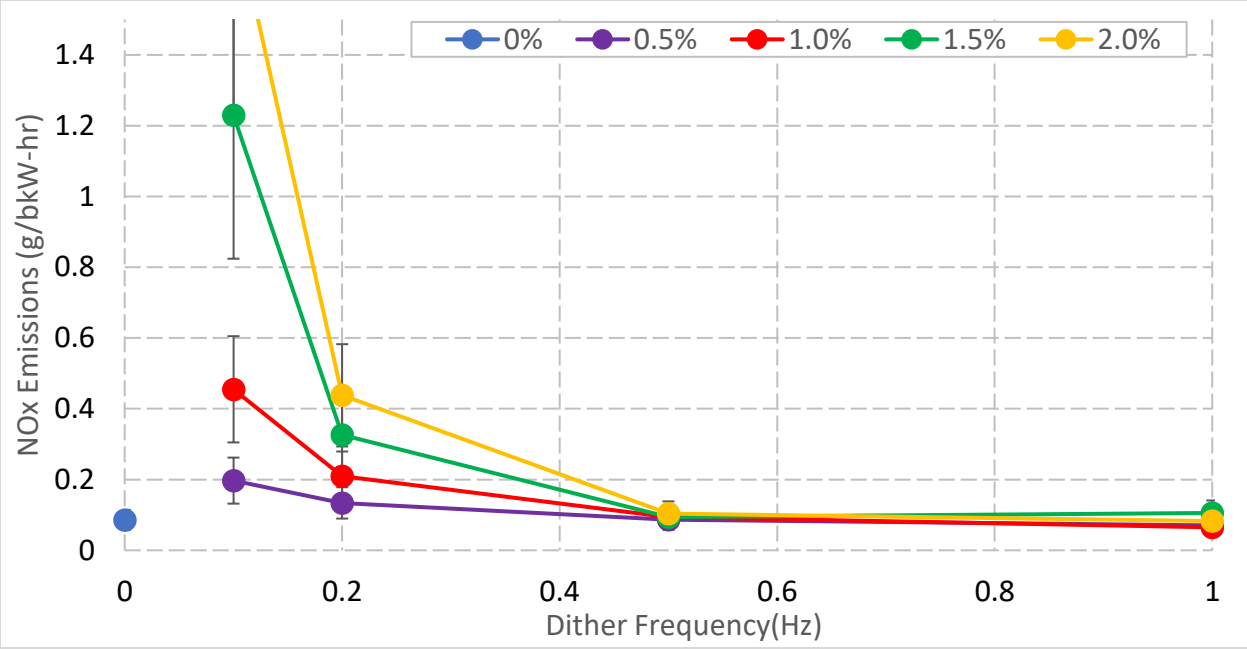

Figure 54: NOx emissions across the dithering parameter sweep with the aged catalyst. Dithering is not effective at reducing emissions in any test case, and at low frequencies dithering significantly increases NOx emissions.

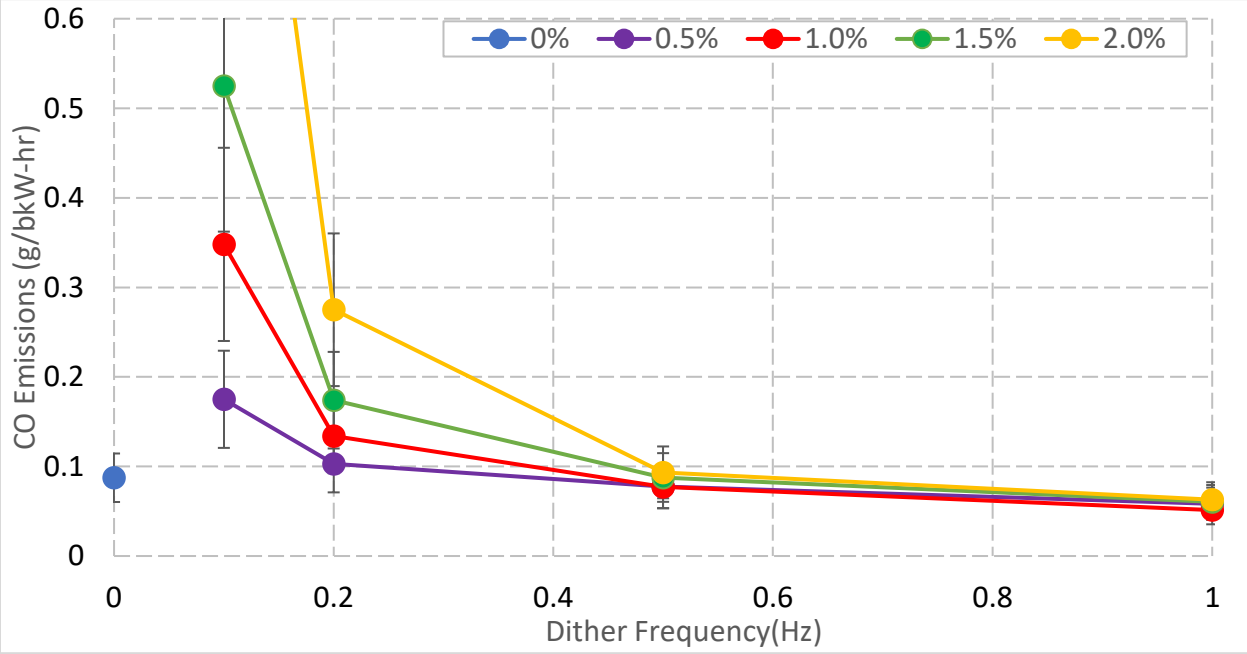

Figure 55: CO emissions across the dithering parameter sweep with the aged catalyst. At low frequencies, dithering significantly increases CO emissions. At high frequencies, CO emissions are slightly reduced by dithering.

As was seen with the fresh catalyst, THC emissions are not significantly affected by dithering frequency. Figure 56 shows the THC emissions across the dithering parameter sweep. Emissions do not change significantly with dithering frequency, but are somewhat dependent on dithering amplitude. 1.5% and 2% dithering amplitudes offer the lowest THC emissions. However, all dithering cases offer lower THC emissions than the steady state case. The steady state THC emissions with the aged catalyst are 0.654 g/bkW hr, while the best-case dithering THC emissions are 0.343 g/bkW-hr at 2% amplitude and 1 Hz dithering.

VOC emissions during the dithering parameter sweep with the aged catalyst are shown in Figure 57. For every case other than 2 % amplitude and 0.1 Hz frequency, dithering VOC emissions are equivalent or lower than the steady state emissions. Steady state VOC emissions are 0.085 g/bkW-hr, while the best-case dithering VOC emissions are 0.003 g/bkW-hr at 1% amplitude and 1 Hz dithering. This is a significant emissions reduction offered by dithering, even on the aged catalyst.

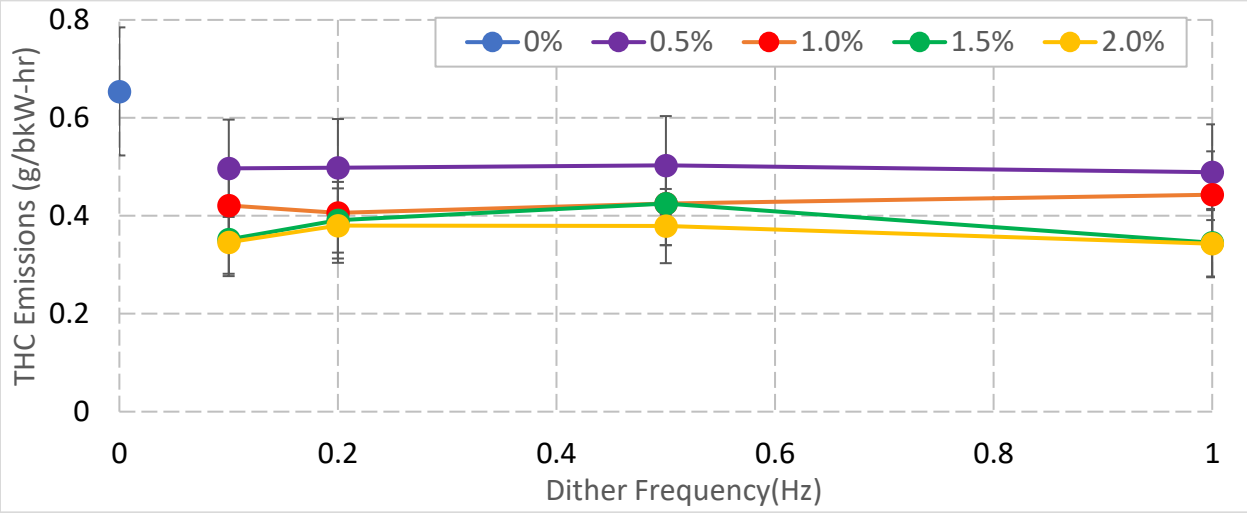

Figure 56: THC emissions with across the dithering parameter sweep with the aged catalyst. THC emission are not significantly affected by dithering. Emissions are reduced at all dithering frequencies, and emissions level is determined by amplitude. 1.5% and 2% amplitude have the lowest emissions.

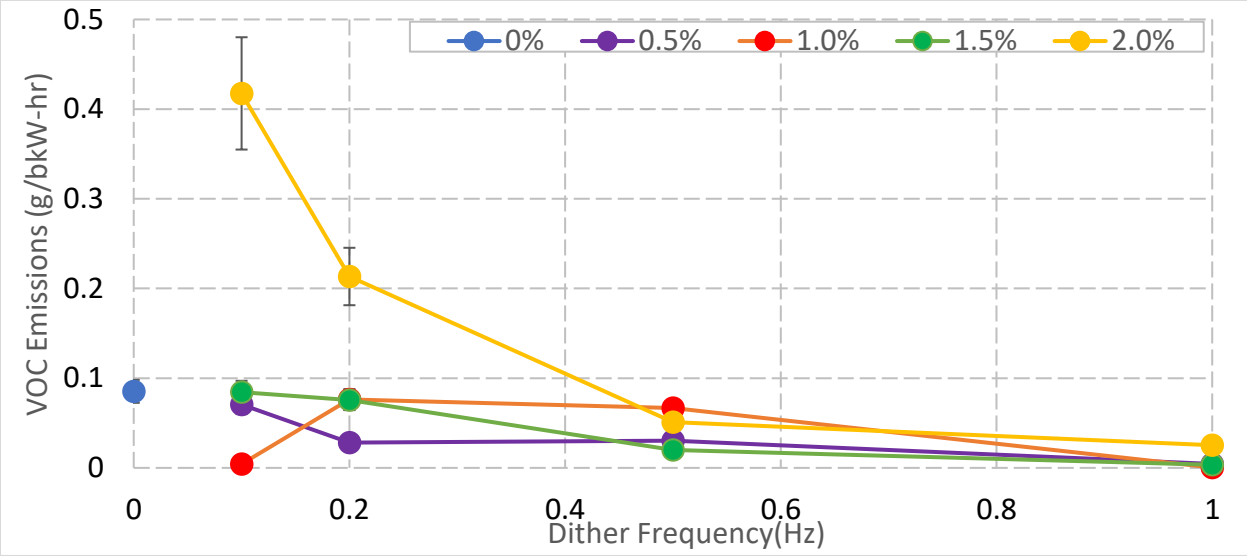

Figure 57: VOC emissions during the dithering parameter sweep with the aged catalyst. Emissions are somewhat reduced with higher dithering frequencies.

Methane emissions with the aged catalyst follow the same trend as the VOC emissions across the dithering parameter sweep. Figure 58 shows the methane emissions during the sweep. For all dithering amplitudes, 0.1 Hz dithering resulted in higher methane emissions than the steady state case. The 0.2 Hz and 0.5 Hz resulted in dithering emissions comparable to the steady state point. The lowest emissions at all dithering amplitudes occurred at 1 Hz dithering. Steady state methane emissions are 2.19 g/bkW-hr. Best-case dithering methane emissions are 0.08 g/bkW-hr, which occurs at 0.1% amplitude and 1 Hz dithering.

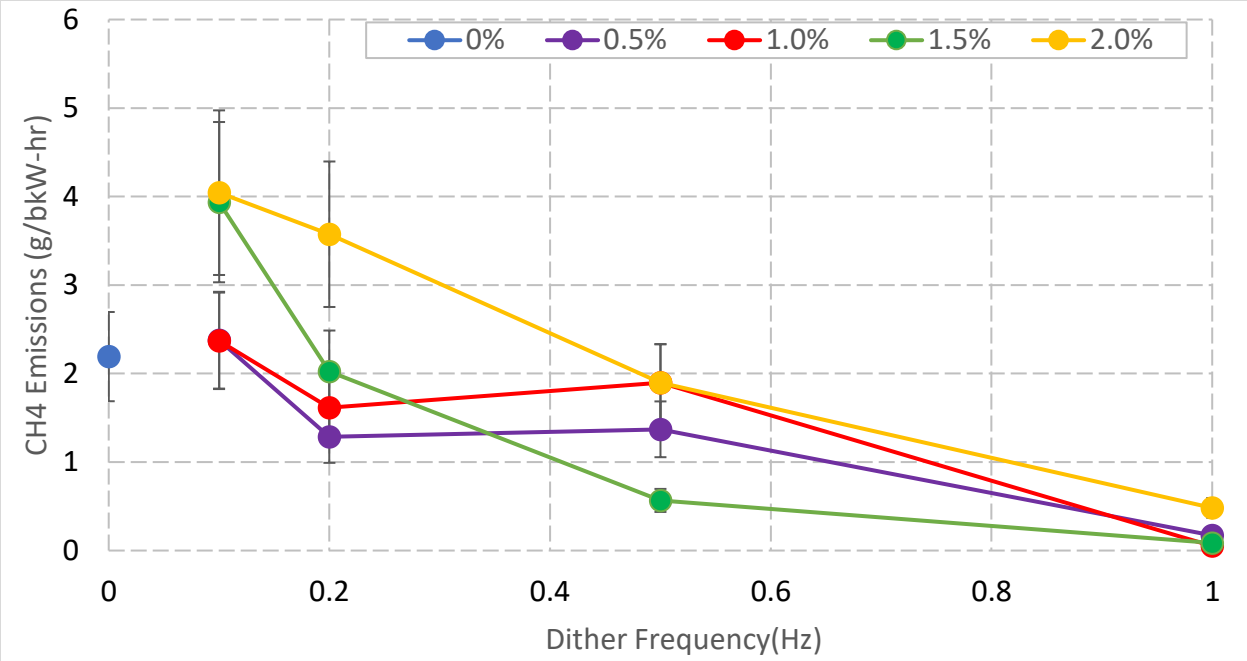

Figure 58: Methane emissions during the dithering parameter sweep with the aged catalyst. At low dithering frequencies, methane emissions are increased, but they are significantly reduced at lower frequencies.

Ammonia emissions during the dithering parameter sweep with the aged catalyst are shown in Figure 59. Steady state operation provides near the lowest ammonia emissions, while dithering at high frequencies resulted in the highest ammonia emissions. However, 1% dithering had the lowest emissions of all the 1 Hz amplitudes. It was observed in previous figures that 1% amplitude and 1 Hz dithering resulted in the lowest emissions of NOx, CO, and VOCs. Steady state ammonia emissions are 16.8 ppm, while the best-case dithering ammonia emissions are 8.58 ppm at 2% amplitude and 0.5 Hz dithering. Ammonia emissions at the 1 Hz and 1% amplitude point are 61.4 ppm, a significant increase from the steady state point.

Formaldehyde emissions for the lambda sweep with the aged catalyst are shown in Figure 60. The highest recorded formaldehyde emissions level was 0.0014 g/bkW-hr. All formaldehyde emissions levels were so close to zero that it can be concluded that dithering does not appreciably change emissions.

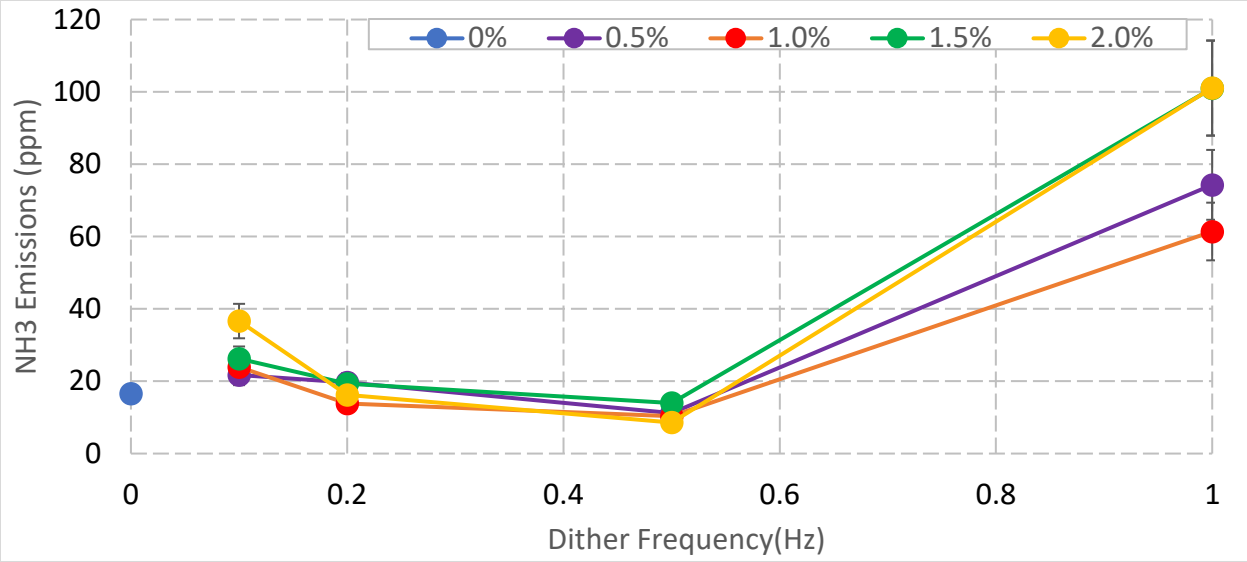

Figure 59: Ammonia emissions are generally significantly higher on the aged catalyst. Dithering at high frequency has an increased impact on ammonia emissions, increasing them to near 100 ppm in some cases.

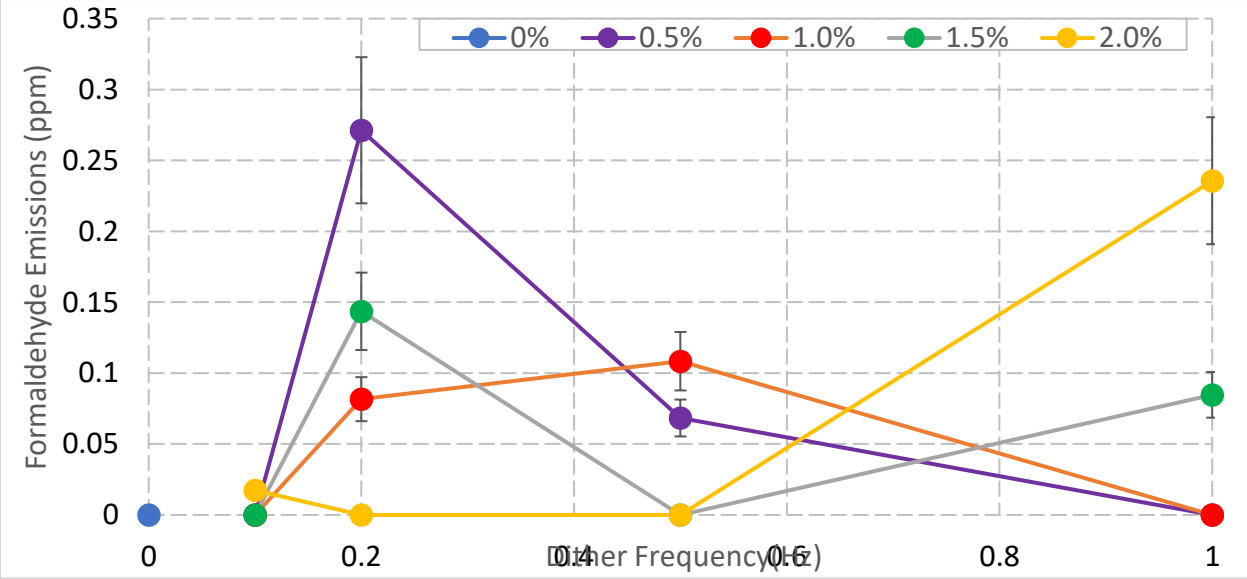

Figure 60: Formaldehyde emissions are all near zero. The largest measured formaldehyde emission level was 0.27 ppm. These emissions are insignificant when compared to the EPA NESHAP limit of 10.3 ppm (assuming an existing engine at a major source), and it can be assumed that dithering has little to no effect on formaldehyde emissions.

5.2.2 LAMBDA SWEEP WITH AGED CATALYST

A lambda sweep was performed on the aged catalyst to investigate the effects of dithering over a wide range of lambda values. Figure 61 shows the NOx and CO emissions across the lambda sweep with the aged catalyst for both dithering and non-dithering cases. Figure 62 shows the same data but displayed over a narrower data range for easier viewing. For most of the lambda sweep, dithering NOx and CO emissions are very slightly lower than the steady state emissions. From λ=1.00 to λ=1.03, dithering emissions are slightly higher than the steady state emissions. It is clear that dithering is not nearly as effective at reducing emissions across a wide range of lambda values when an aged catalyst is present.

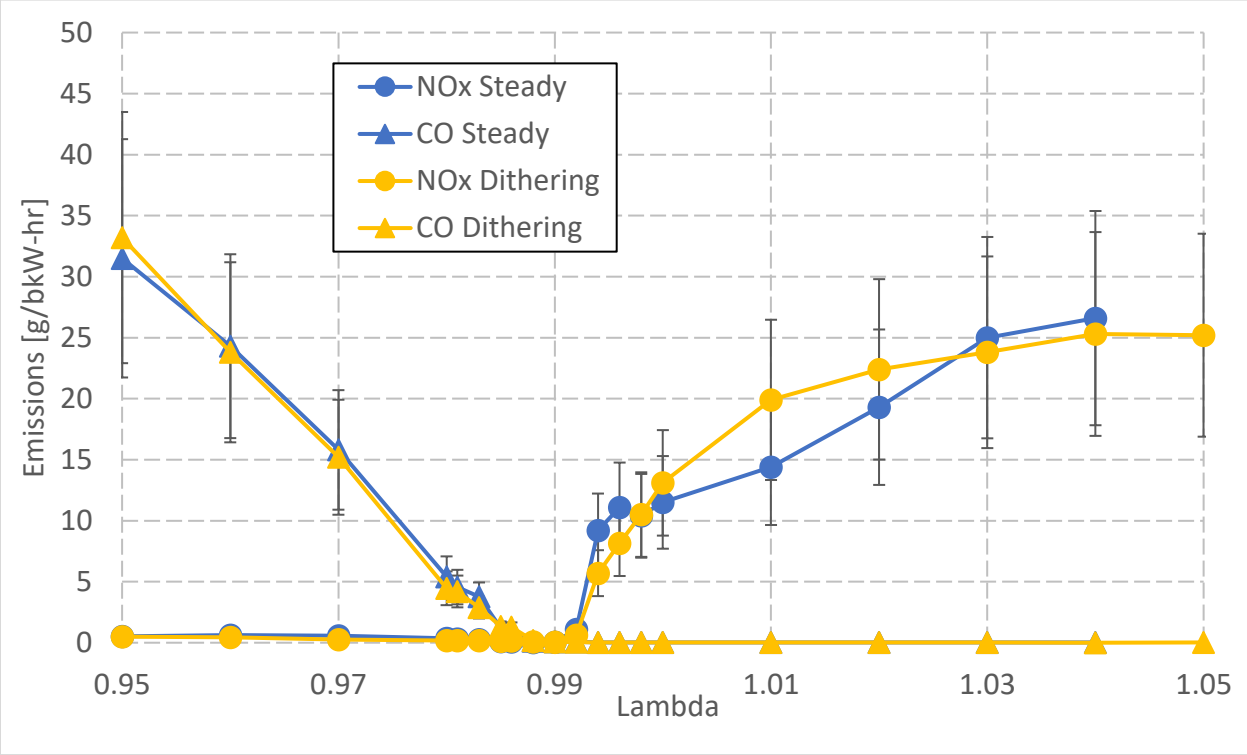

Figure 61: NOx and CO emissions across the lambda sweep with the aged catalyst. Emissions levels between steady state test points and dithering test points are not significant, signaling that dithering is not as effective at reducing NOx and CO emissions on an aged catalyst.

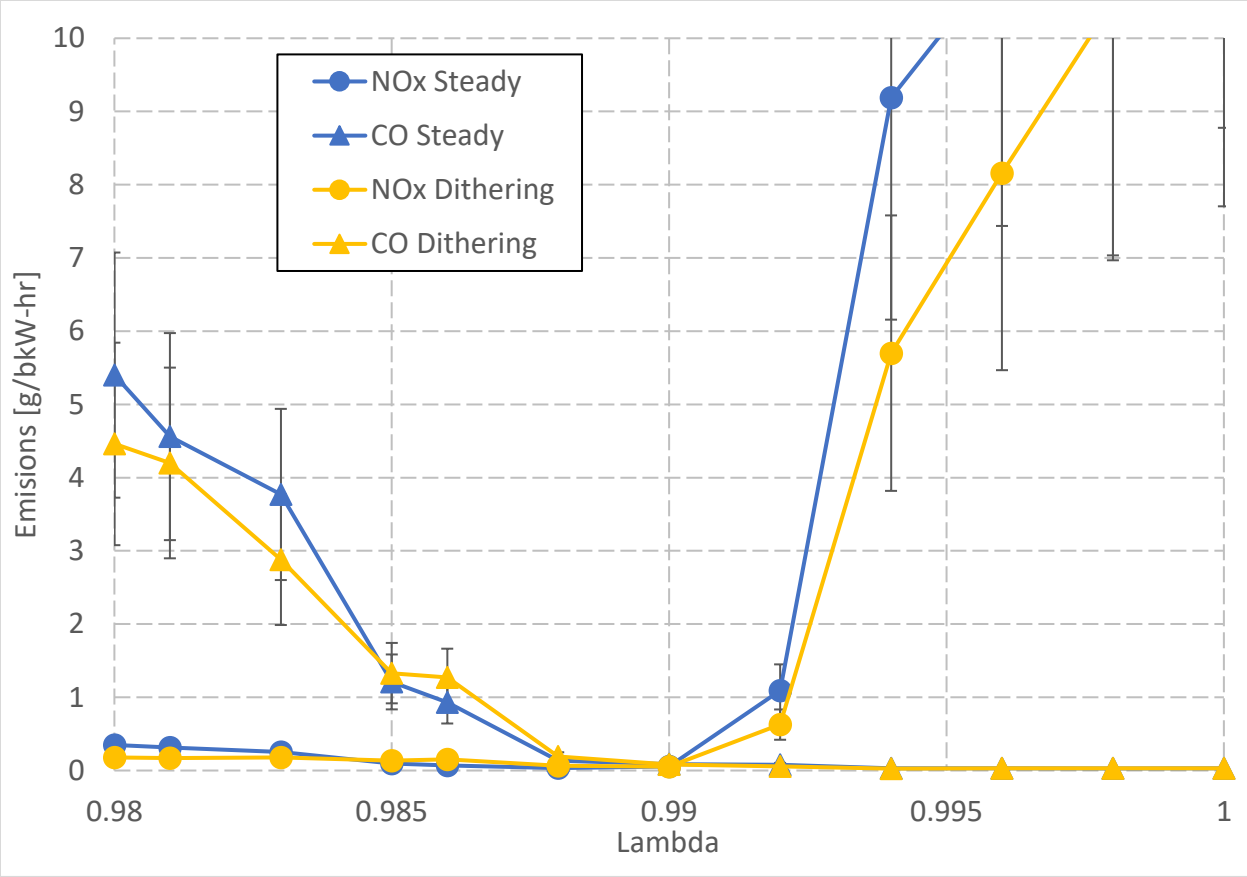

Figure 62: A zoomed in view of the NOx and CO emissions during the lambda sweep with the aged catalyst. Emissions are not significantly affected by dithering, and in some cases are slightly higher during dithering tests.

Figure 63 shows the THC emissions across the lambda sweep with the aged catalyst. For nearly every case, dithering THC emissions are lower than the steady state THC emissions. There is a region where $\lambda>1.00$ in which dithering THC emissions are slightly higher than the steady state emissions. Generally, dithering is still effective at reducing THC emissions on an aged catalyst in the typical area of engine operation from $\lambda=0.98$ to $\lambda=1.00$.

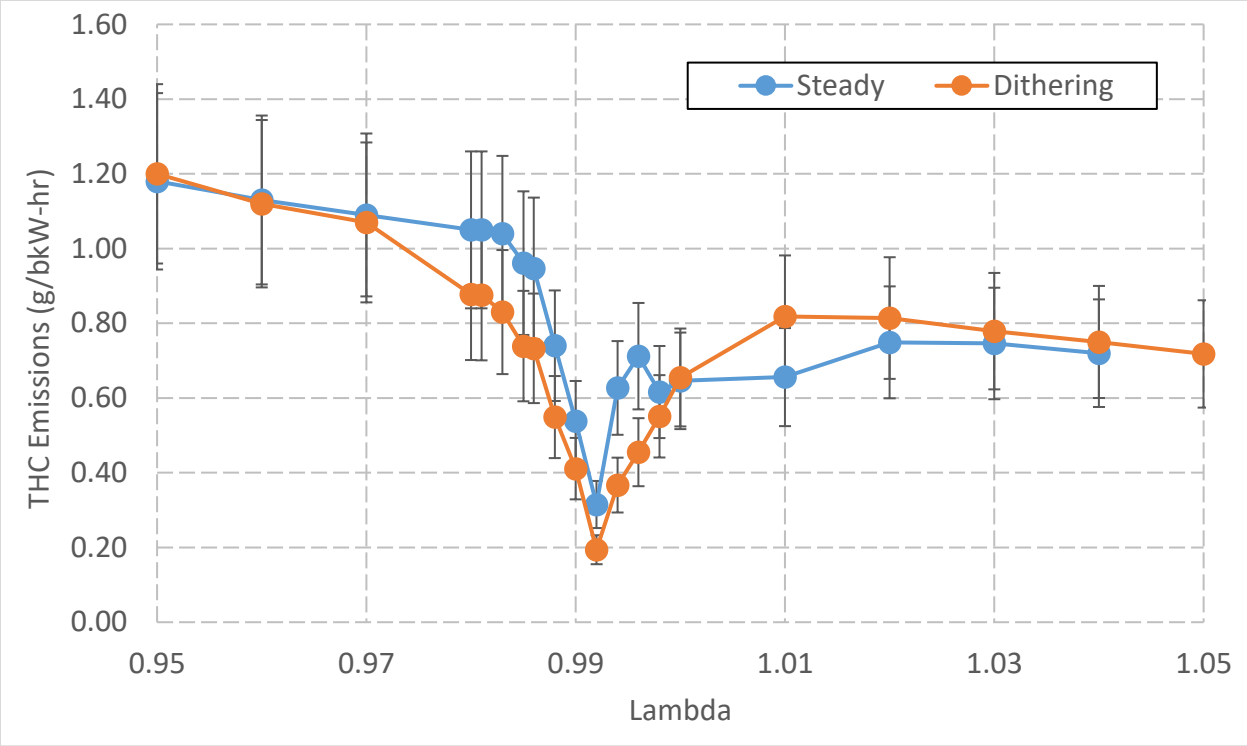

Figure 63: THC emissions across the lambda sweep with the aged catalyst. dithering emissions are slightly lower than the steady state emissions for most of the lambda sweep.

VOC emissions are shown in Figure 64 for the aged catalyst during the lambda sweep. It can be seen that dithering provides a small reduction in emissions during rich lambda values, and provides no emissions reduction during lean lambdas. There is an emissions spike at λ=0.992, but it is effectively reduced by dithering at the same lambda midpoint. Dithering is still effective at reducing VOC emissions on an aged catalyst, and does not put the engine out of emissions compliance.

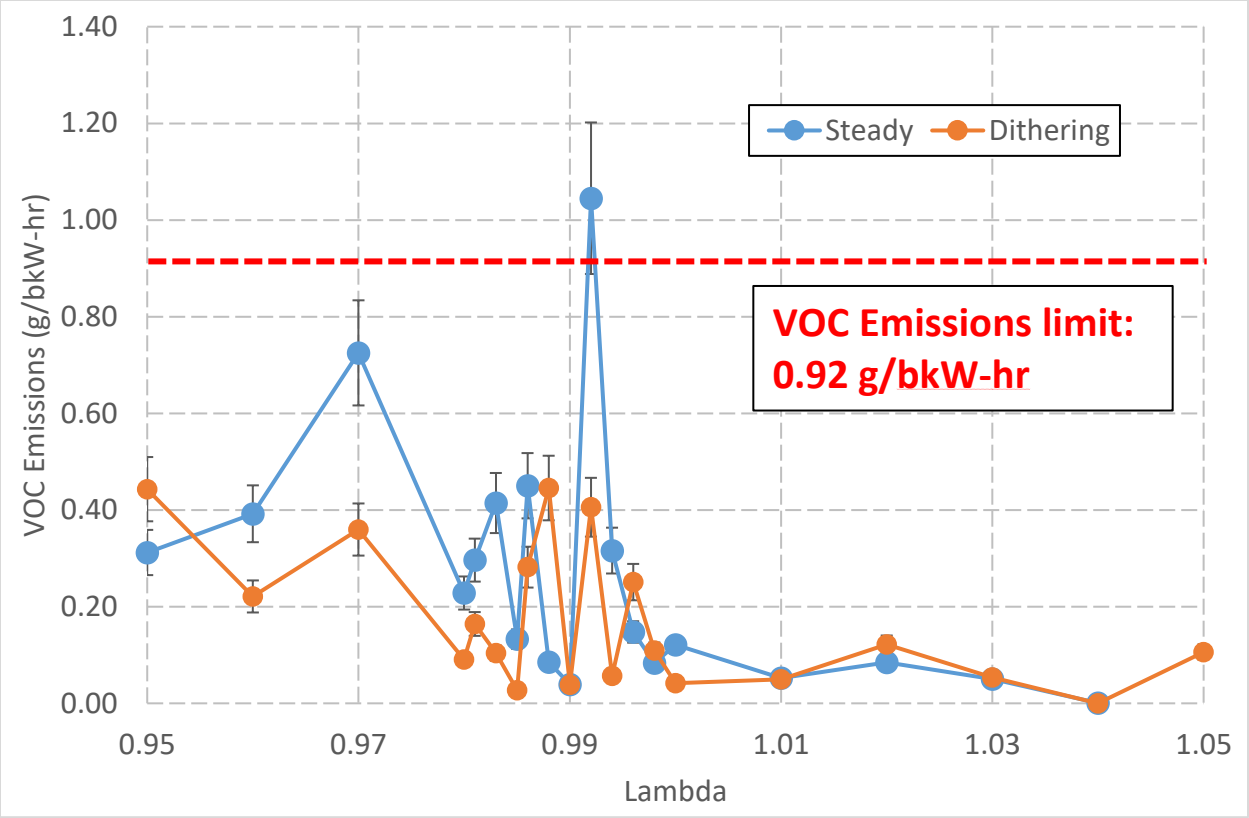

Figure 64: VOC emissions across the lambda sweep with the aged catalyst. Emissions are slightly decreased for many of the points.

Methane emissions during the lambda sweep with the aged catalyst follow the same trends as the VOC emissions and are shown in Figure 65. Methane emissions are not significantly affected by dithering across the lambda sweep other than from λ=0.985 to λ=1.00. In this region, methane emissions are reduced significantly from the spikes observed in the steady state lambda sweep.

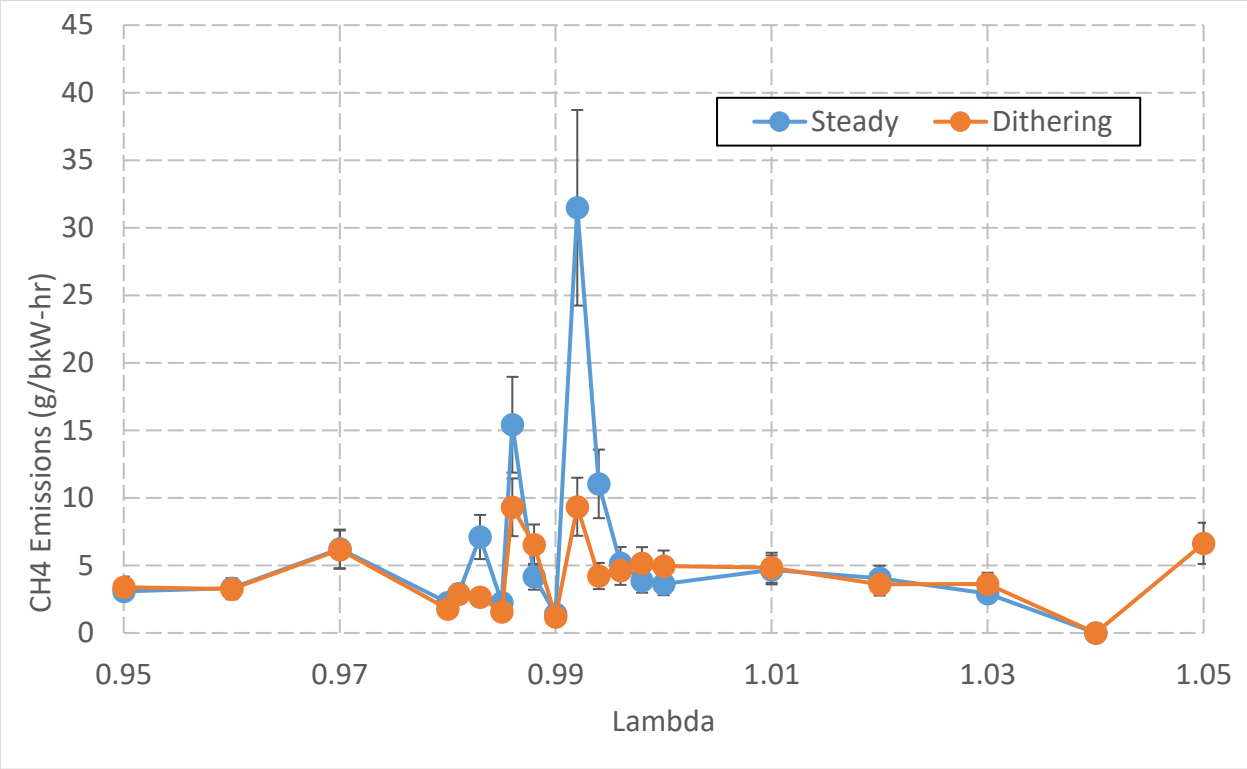

Figure 65: Methane emissions across the lambda sweep with the aged catalyst. for most test cases, methane emissions are unaffected by dithering. around λ=0.992, dithering reduces emissions.

Figure 66 shows ammonia emissions across the lambda sweep with the aged catalyst. In the region where 0.97<λ<0.98, dithering ammonia emissions are higher than the steady state emissions. However, for the rest of the lambda sweep, dithering ammonia emissions are equivalent or slightly less than the steady state ammonia emissions.

Figure 67 shows formaldehyde emissions during the lambda sweep with the aged catalyst. The maximum formaldehyde emissions observed are 1.6 ppm, observed at λ=0.97. In almost every case, dithering formaldehyde emissions are lower than the steady state formaldehyde emissions. All formaldehyde emissions levels are low enough that it can be concluded that dithering does not have a negative effect on formaldehyde emissions.

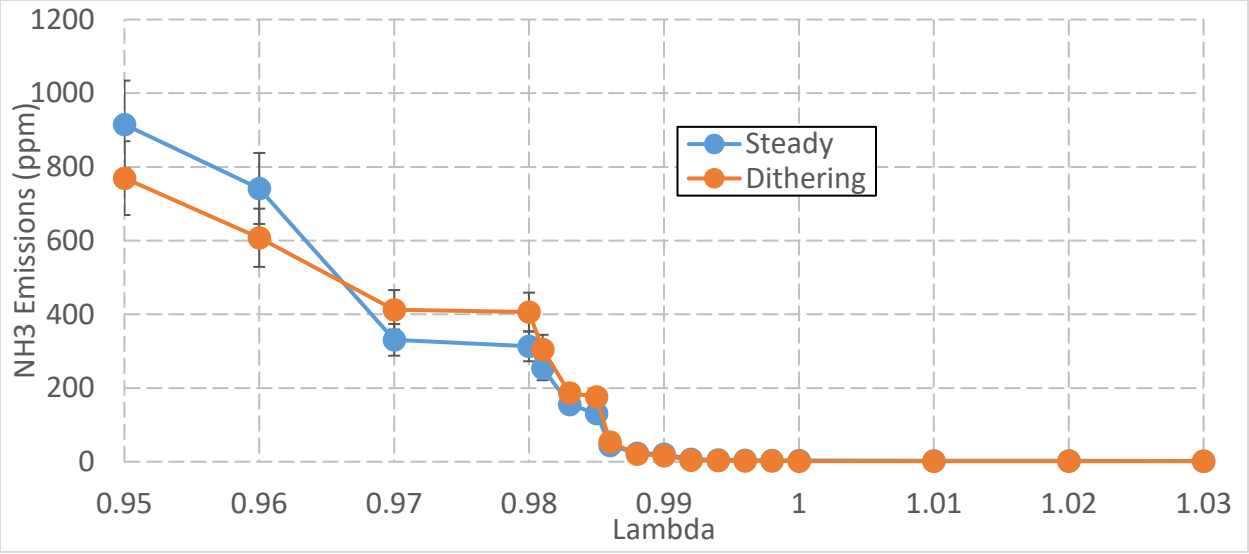

Figure 66: Ammonia emissions across the lambda sweep with the aged catalyst. There is a small area between λ=0.97 and λ=0.98 where ammonia emissions are higher while dithering, but in all other cases steady and dithering ammonia emissions are comparable.

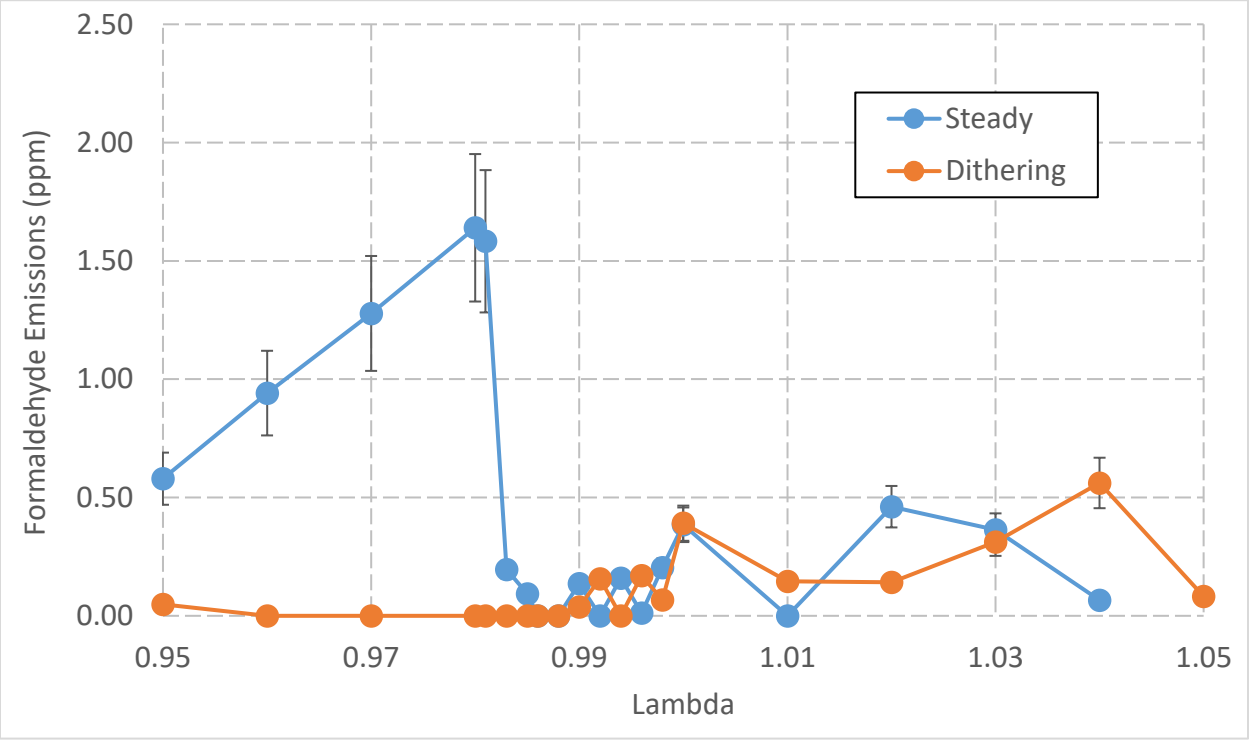

Figure 67: Formaldehyde emissions across the lambda sweep with the aged catalyst. At λ<0.98, steady state formaldehyde emissions are significantly higher than dithering formaldehyde emissions However, at λ>0.98, dithering and steady state formaldehyde emissions are comparable.

5.2.3 WINDOW OF COMPLIANCE WITH AGED CATALYST

The window of emissions compliance for the aged catalyst is show in Figure 68. The steady state window of emissions compliance is 0.007λ, similar to the steady window of compliance for the non-aged catalyst tested in Chapter 4. The dithering window of compliance is 0.009λ, just slightly wider than that of the steady state test. This is because dithering is not as effective at reducing emissions (both NOx and CO) on the aged catalyst. As the catalyst ages, the ceria becomes less active and is less effective at storing and releasing oxygen.

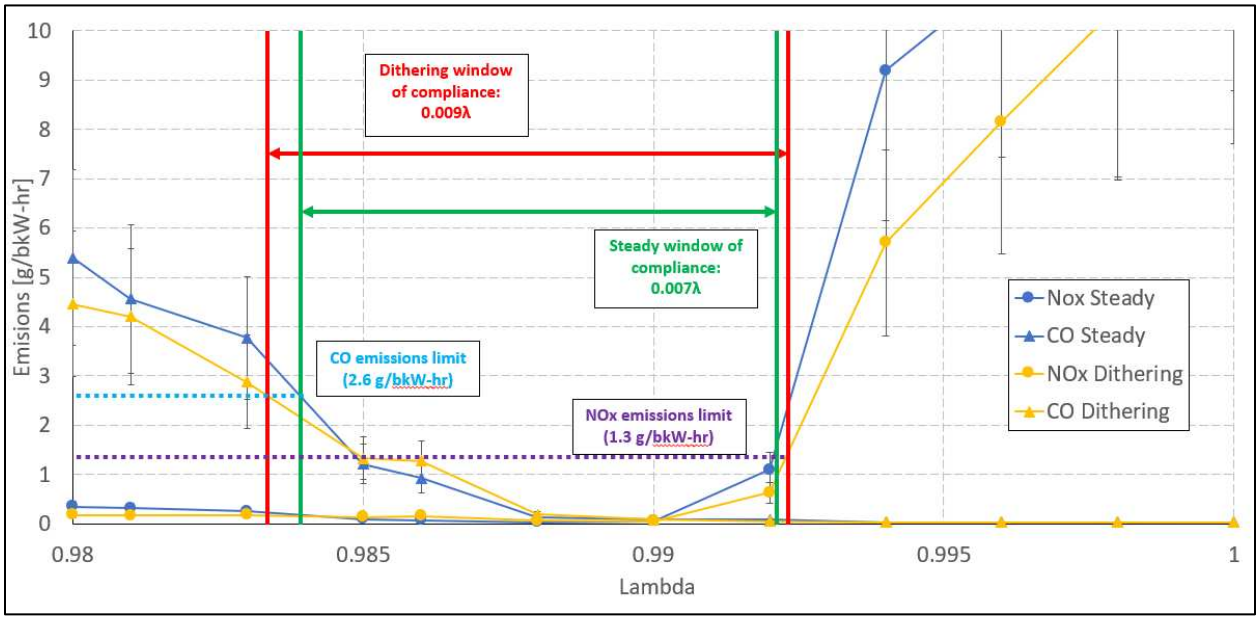

Figure 68: The window of emissions compliance for the aged catalyst. Dithering does not make a big change in the emissions window of compliance.

5.3 DITHERING CONTROLS AND CATALYST COMPARISON

Several key comments can be made on the dithering control strategies and how they affect three-way catalyst performance. The first observation is that NOx and CO emissions were always reduced at high dithering frequencies. In tests with each catalyst, the slow dithering frequency (0.1 and 0.2 Hz) test cases resulted in significantly higher NOx and CO emissions than the steady state test case. In these tests, it was noted that the best-case dithering emissions combination occurred at 1 Hz dithering frequency. For the fresh catalysts (standard and ½ OSC), the optimal dithering parameters for NOx and CO emission minimization were 1 Hz frequency with 1.5% amplitude. For the aged catalyst, the optimal dithering parameters for NOx and CO emission minimization were 1 Hz and 1% amplitude. This is because the aged catalyst is not as effective at storing and releasing oxygen, so smaller rich and lean excursions must be used. Figure 69 shows the best-case dithering NOx and CO emissions. Dithering is very effective at reducing emissions on the standard and ½ OSC catalysts, both of which were tested in the early phase of their usable lifetime. The aged catalyst was aged to 16,000 hours, and did not reduce emissions significantly with dithering as was seen with the other two catalysts. Table 9 shows the parameters that resulted in the lowest NOx and CO emissions for each catalyst.

Table 9: The dithering parameters resulting in the lowest NOx and CO emissions are listed in this table.

Catalyst	Optimal Frequency	Optimal Amplitude
Standard	1.0 Hz	1.5%
½ OSC	1.0 Hz	1.5%
Aged	1.0 Hz	1.0%

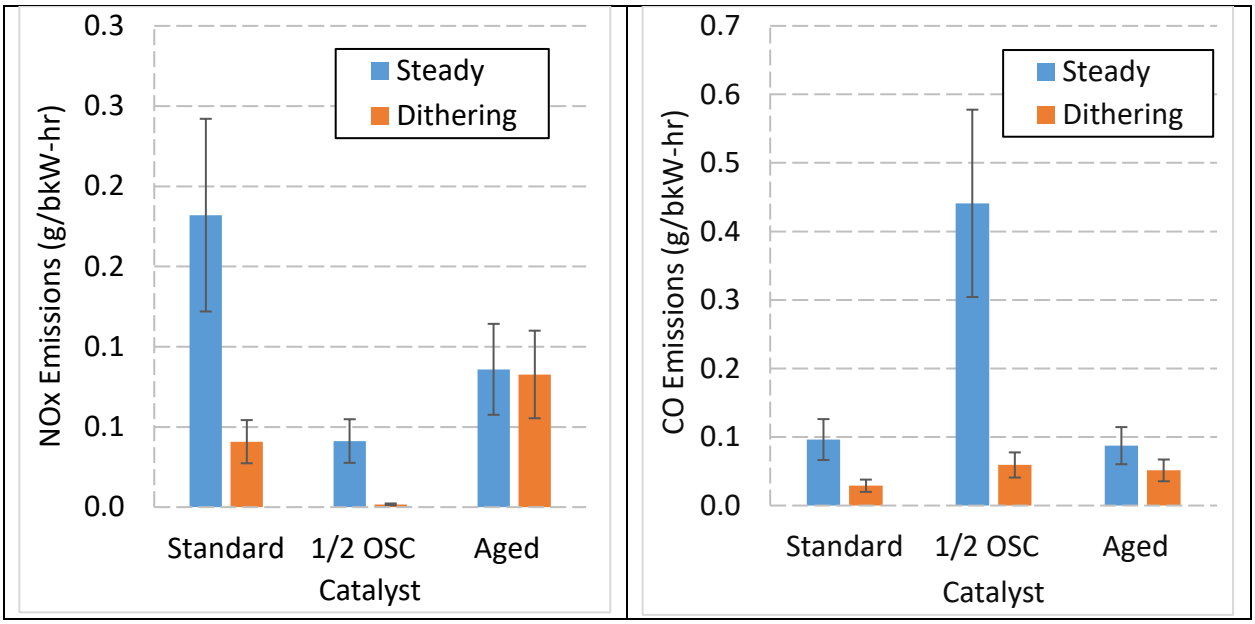

(a) (b)

Figure 69: NOx (a) and CO (b) emissions comparison with and without dithering on all three catalysts tested. Dithering significantly reduces emissions on the fresh catalysts but is less effective at reducing emissions on the aged catalyst.

It was observed that THC emissions with the standard catalyst (both fresh and aged) was not affected by dithering frequency and was only affected by dithering amplitude. For the ½ OSC catalyst, emissions were slightly worse than steady state for the best-case dithering NOx and CO emissions point. Figure 70 shows the THC emissions during dithering and steady testing with each catalyst. The emissions used in this figure for the dithering run were taken from the run with the dithering parameters with the lowest NOx and CO emissions which are shown in Table 9.

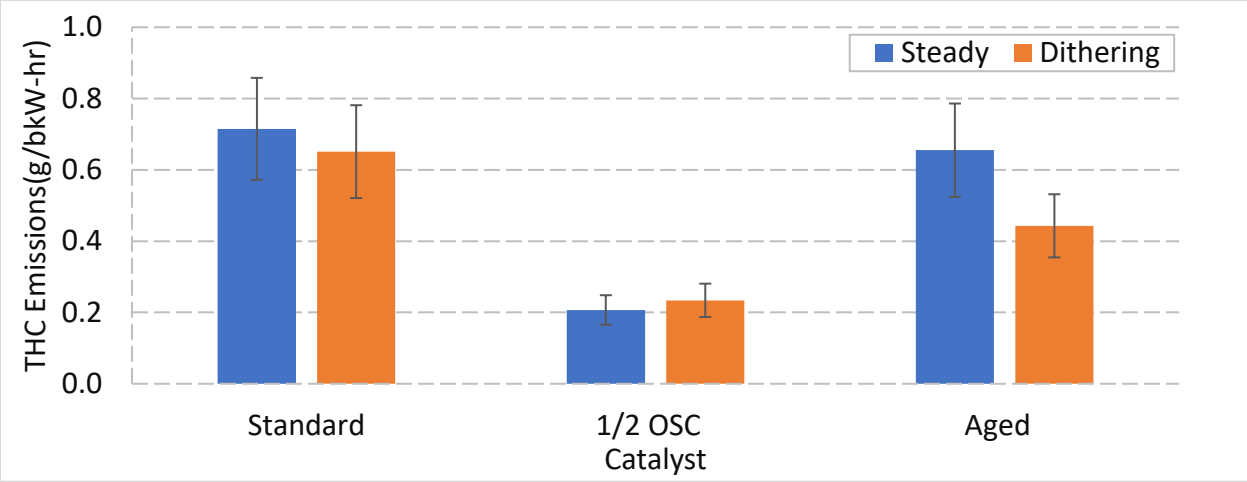

Figure 70: THC emissions comparison between catalysts, with and without dithering. The emissions data was taken from the dithering parameter combination with the best NOx and CO emissions.

Figure 71 shows the VOC and methane emissions for all catalysts tested. Dithering is extremely effective at reducing VOC emissions as well as methane emissions in all catalysts. This shows that the VOC and methane emissions reduction is not significantly affected by catalyst age or by the amount of oxygen storage content in a catalyst. Emissions levels shown in Figure 71 are the emissions with the optimal NOx and CO dithering parameters listed in Table 9.

Another observation is the ammonia emissions with the different catalysts. The standard catalyst does not produce nearly as much NOx as the ½ OSC catalyst during steady state operation. The ½ OSC catalyst produces a significant amount of ammonia, more than was expected. However, dithering for both the standard catalyst and the ½ OSC catalyst reduces the ammonia emissions significantly. The aged catalyst does not follow this trend, instead ammonia emissions are much higher with dithering than they are during steady state operation. The aged catalyst is not able to store oxygen as effectively, resulting in more ammonia slip during rich phases of dithering. One final note is that formaldehyde emissions were nearly zero for every test case, both dithering and steady state.

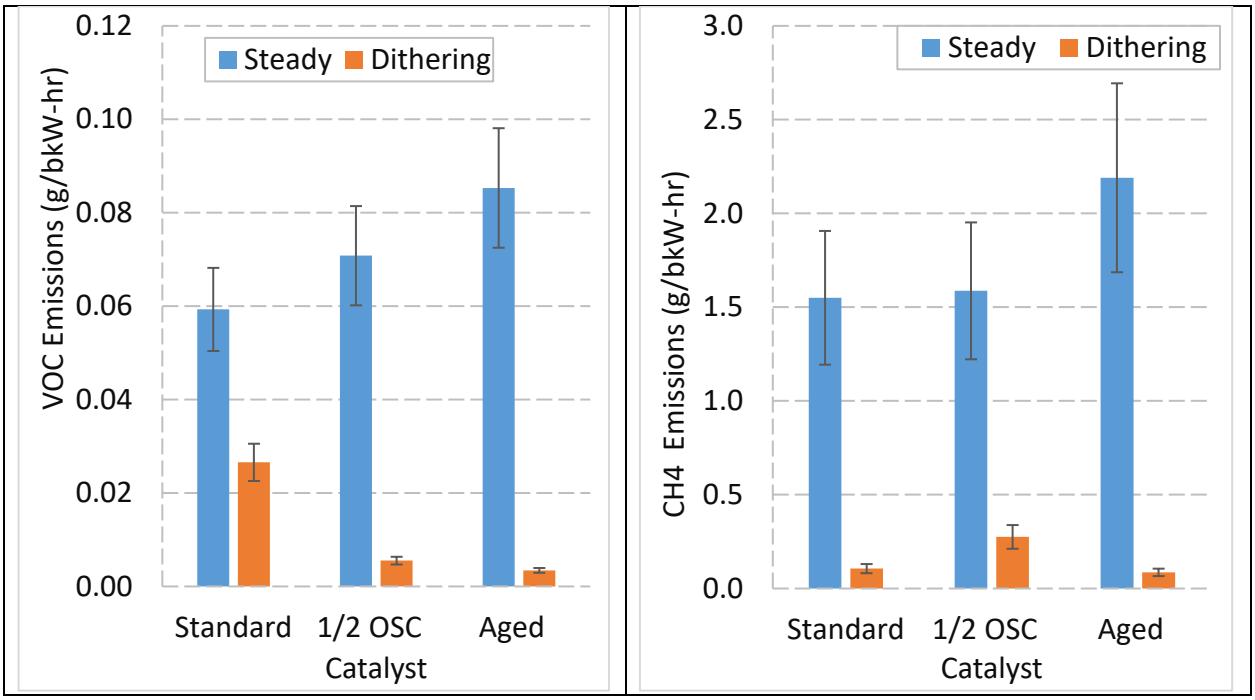

Figure 71: VOC emissions and methane emissions for dithering and steady state tests. Dithering is effective at reducing both VOC and methane emissions in all catalysts tested.

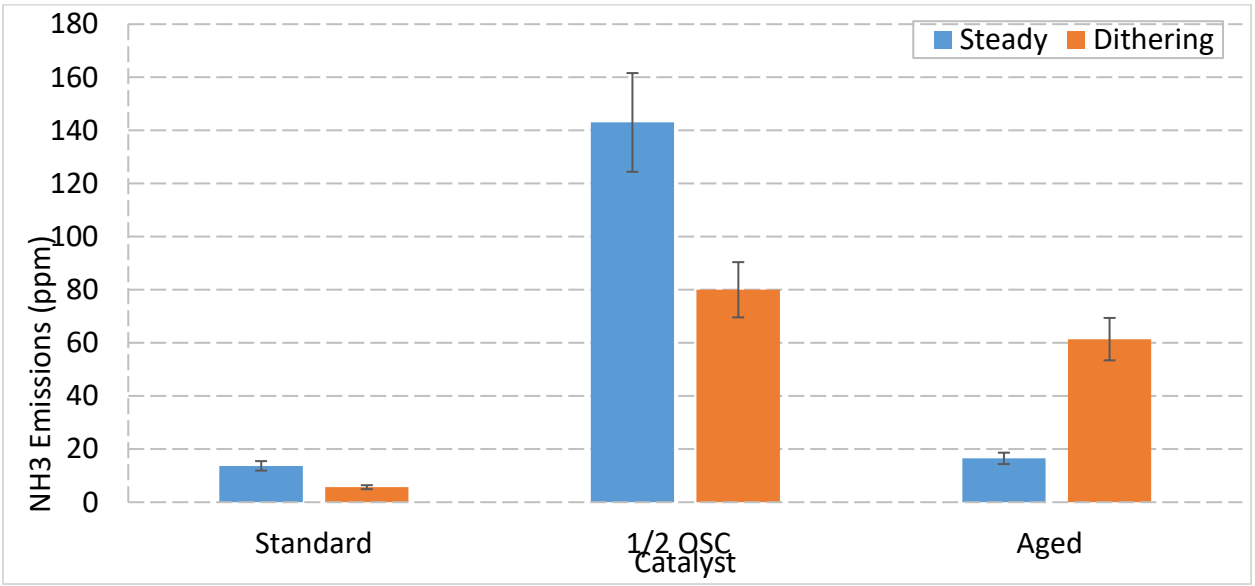

Figure 72: Ammonia emissions with and without dithering on each catalyst. Dithering reduces ammonia emissions on the standard and 1/2 OSC catalyst but increases ammonia emissions on the aged catalyst.

CHAPTER 6: CONCLUSION

The goal of this project was to investigate air-fuel ratio dithering and to expand on previous work done with dithering and its effects on three-way catalysts. Dithering utilizes oxygen storage capability of ceria in the catalyst washcoat. Oxygen can be stored during lean dithering excursions and released during rich excursions, resulting in lower overall emissions. For the experiments, a 2015 Caterpillar CG137-8 18L industrial 4-stroke natural gas engine (S/N: WWF00318) was installed in a test cell at the CSU Powerhouse with a Woodward LECM control system. This engine is an 8 cylinder, turbocharged, spark ignited natural gas engine with a 60 degree V8 head configuration. Three different catalysts were tested with a steady state and dithering tests, including a lambda sweep and a dithering parameter sweep. These tests helped find the optimal dithering parameters for different catalysts, as well as how the emissions window of compliance is affected by dithering.

These results definitively show that air-fuel ratio dithering can be used to significantly reduce pollutant emissions over a wide range of air-fuel ratios as well as on different catalysts. Dithering could be applied to any stoichiometric natural gas engine to increase its window of emissions compliance, regardless of the catalyst used. In testing, 1.5% amplitude with 1 Hz frequency dithering was shown to significantly reduce emissions on two different catalysts, so this amplitude and frequency should be used as a starting point for dithering tuning on similar engines. As the catalyst ages, the effectiveness of dithering is reduced, and near the end of its life, the catalyst is not nearly as effective at reducing NOx emissions as when it was fresh. This is important to consider when designing an engine system. Additionally, the aged catalyst had minimum NOx and CO dithering emissions at a smaller dithering amplitude than the fresh

catalysts. It may be beneficial to slowly decrease the dithering amplitude over the life of a catalyst to ensure that dithering remains optimized as the oxygen storage capability of the catalyst declines.

Dithering can also be investigated using pre- and post-catalyst oxygen sensors. For dithering to be optimized, the post-catalyst sensor should always be trailing the pre-catalyst sensor. During rich regions, oxygen release should always be occurring, meaning the post-catalyst oxygen sensor should be showing higher oxygen concentration or a leaner lambda than the pre-catalyst sensor. During lean regions, oxygen storage should be occurring, meaning the post-catalyst oxygen sensor should be showing lower oxygen concentration or a richer lambda than the pre-catalyst sensor. The catalyst becomes completely saturated with oxygen and depleted of oxygen in about 8 seconds. However, it was found that 0.5 second lean and rich phases (1 Hz) resulted in the lowest NOx and CO emissions. This suggests that it is best to keep the catalyst in the middle of saturation and depletion, with faster fluctuations between storage and release. The storage and release time both appear to be around 8 seconds, so it is likely not effective to investigate the effects of non-symmetric dithering.

The emissions reductions afforded by air-fuel ratio dithering have many benefits. The widened window of emissions compliance allows the engine to deal with fuel and load transients and remain in compliance more easily, as it is not pushed out of emissions compliance by small changes in the midpoint lambda. Additionally, emissions reductions were observed on the ½ OSC catalyst, meaning potentially less expensive catalysts could be used to meet the same emissions limits.

A future experiment that could help to better understand catalyst aging would be to artificially age a catalyst in 2000 hour increments and investigate how dithering performance

degrades over time. This would help fill in knowledge of how the oxygen storage ability of the catalyst degrades over time.

Another noted phenomenon in this experiment was the cross-sensitivity of the NOx sensor with ammonia, and how the minimum reading of the NOx sensor corresponded directly to the NOx and CO emissions minimum. Further studies could investigate using the NOx sensor signal to measure and adjust the midpoint air-fuel ratio. Currently, the engine was controlled by adjusting fueling to reach a desired lambda, as measured by the pre-catalyst oxygen sensor. It could be possible to adjust engine fueling based on minimizing the signal from the NOx sensor.

The main findings from this study were:

- Air-fuel ratio dithering around a set midpoint can drastically reduce NOx and CO emissions on a stoichiometric SI natural gas engine with a three-way catalyst. Optimal dithering parameters for optimizing oxygen storage on a standard catalyst were 1.5% amplitude with 1 Hz fluctuations.
- Air-fuel ratio dithering is effective on fresh catalysts (standard or ½ OSC) but largely ineffective on aged catalysts that are near end-of-life.
- Catalysts with less OSC can still perform oxygen storage and release, providing emission reductions. Aged catalysts are not as capable at oxygen storage release, resulting in emissions that are not significantly lower than steady state. Optimal dithering parameters for the catalyst with ½ OSC were 1.5% amplitude with 1 Hz fluctuations. On the aged catalyst, the optimal parameters were 1% amplitude with 1 Hz fluctuations.
- The window of emissions compliance can be expanded by 100% by dithering with a standard catalyst. The window of compliance can also be expanded on catalysts with less

oxygen storage capability, but to a lesser degree (40% increase). Dithering is ineffective at widening the window of compliance on aged catalysts.

In conclusion, applying air-fuel ratio dithering strategy to an air-fuel ratio controller can significantly reduce emissions of regulated pollutants such as NOx and CO. In addition to reducing emissions, air-fuel ratio dithering can widen the window of emissions compliance, even when applied to different three-way catalysts. These advantages will allow engine manufacturers and packagers to use catalysts with less ceria, and potentially smaller catalysts while meeting the same emissions regulations. In areas with stringent emissions regulations, dithering is a cost-effective way to meet lower emissions limits with no hardware changes.

REFERENCES

[1] Karavalakis, Georgios, Hajbabaei, Maryam, Jiang Yu, Kang, Jiacheng, Johnson, Kent, Cocker, David, and Durbin, Thomas. "Regulated greenhouse gas and particulate emissions from lean-burn and stoichiometric natural gas heavy-duty vehicles on different fuel compositions", *Fuel* 175 (2016), 146-156, https://doi.org/10.1016/j.fuel.2016.02.034

[2] Thiruvengadam, Arvind, Besch, Marc, Padmanaban, Vishnu, Pradhan, Saroj, and Demirgok, Berk. "Natural gas vehicles in heavy-duty transportation-a review", *Energy Policy* 122 (2018) 253–259, https://doi.org/10.1016/j.enpol.2018.07.052.

[3] Smith, I., Briggs, T., Sharp, C., and Webb, C., "Achieving 0.02 g/bhp-hr NOx Emissions from a Heavy-Duty Stoichiometric Natural Gas Engine Equipped with Three-Way Catalyst," *SAE Technical Paper* 2017-01-0957, 2017, https://doi.org/10.4271/2017-01-0957.

[4] Heywood J. B., “Internal Combustion Engine Fundamental”, McGraw-Hill Inc., 1988.

[5] Cho, Haeng Muk, and Bang-Quan He. “Spark Ignition Natural Gas Engines—A Review.” *Energy Conversion and Management*, vol. 48, no. 2, 2007, pp. 608–618., doi:10.1016/j.enconman.2006.05.023.

[6] Heywood J. B., “Internal Combustion Engine Fundamental”, McGraw-Hill Inc., 1988.

[7] James J., Jian Z., Chunshan S. Low Temperature Steam Reforming of Jet Fuel in the Absence and presence of Sulfur over Rh and Rh-Ni catalysts Fuel Cells, Journal of Catalysis (2005).

[8] Tsinoglou, Dimitrios N., et al. “Oxygen Storage Modeling in Three-Way Catalytic Converters.” *Industrial & Engineering Chemistry Research*, vol. 41, no. 5, 2002, pp. 1152–1165., doi:10.1021/ie010576c.

[9] Herz, Richard K., and Jeffrey A. Sell. “Dynamic Behavior of Automotive Catalysts.” Journal of Catalysis, vol. 94, no. 1, 1985, pp. 166–174., doi:10.1016/0021-9517(85)90092-2.

[10] Herz, Richard K., and Jeffrey A. Sell. “Dynamic Behavior of Automotive Catalysts.” Journal of Catalysis, vol. 94, no. 1, 1985, pp. 166–174., doi:10.1016/0021-9517(85)90092-2.

[11] Ivanova, A.s., et al. “Metal–Support Interactions in Pt/Al2O3 and Pd/Al2O3 Catalysts for CO Oxidation.” *Applied Catalysis B: Environmental*, vol. 97, no. 1-2, 2010, pp. 57–71., doi:10.1016/j.apcatb.2010.03.024.

[12] Nievergeld, A.j.l., et al. “The Performance of a Monolithic Catalytic Converter of Automobile Exhaust Gas with Oscillatory Feeding of Co, No, and O2: A Modelling Study.” *Catalysis and Automotive Pollution Control III, Proceedings of the Third International Symposium CAPoC 3 Studies in Surface Science and Catalysis*, vol. 96, 1995, pp. 909–918., doi:10.1016/s0167-2991(06)81484-9.

[13] Defoort, M, et al. “The Effect of Air-Fuel Ratio Control Strategies on Nitrogen Compound Formation in Three-Way Catalysts.” *International Journal of Engine Research*, vol. 5, no. 1, 6 Aug. 2003, pp. 115–122., doi:10.1243/146808704772914291.

[14] Shi, Xian, et al. “Fuel-Dithering Optimization of Efficiency of TWC on Natural Gas IC Engine.” *SAE International Journal of Engines*, vol. 8, no. 3, 2015, pp. 1246–1252., doi:10.4271/2015-02-1143.

[15] Shi, Xian, et al. “Fuel-Dithering Optimization of Efficiency of TWC on Natural Gas IC Engine.” *SAE International Journal of Engines*, vol. 8, no. 3, 2015, pp. 1246–1252., doi:10.4271/2015-02-1143.

[16] Finke, John and Olsen, Daniel, " Comparison of Dithering and Steady State NSCR Catalyst Control on a 7.5L Rich Burn Engine" *GMRC Gas Machinery Conference,* Denver, CO, October, 2016.

[17] Environmental Protection Agency Federal Register, “40 CFR Part 86 Emission Durability Procedures and Component Durability Procedures for New Light-Duty Vehicles, Light Duty Trucks and Heavy-Duty Vehicles; Final Rule and Proposed Rule, Part IV,” January 17, 2006

[18] K. Davis, “Oxidation Catalys Degredation in the Exhaust Stream of a Large Bore 2-Stroke Natural Gas Engine,” Colorado State University, Fort Collins, CO, 2015.

[19] Defoort, M, et al. “The Effect of Air-Fuel Ratio Control Strategies on Nitrogen Compound Formation in Three-Way Catalysts.” *International Journal of Engine Research*, vol. 5, no. 1, 6 Aug. 2003, pp. 115–122., doi:10.1243/146808704772914291.

APPENDIX

TEST PROCEDURE

At the beginning of each test day, valving in the Powerhouse basement was checked to ensure proper flow path for engine coolant was open. Then, coolant pumps were engaged, and cooling tower fans were activated. The basement was again checked to ensure that no coolant leaks were present. The engine was then cranked using the air starter and allowed to reach its idle speed of 900 rpm. After a minute of stable idle, the engine speed setpoint was increased to operation speed, 1800 rpm. After several minutes of no-load operation, load was ramped up to maximum load of 1580 N-m over a period of 350 seconds. The engine was then allowed to heat up to full operation temperature before data collection began. Lambda setpoint and dithering parameters could be selected using Woodward Toolkit.

The engine and plant system were primarily controlled and monitored using a LabVIEW VI with an HMI created by Kirk Evans. The engine was stopped and started through this HMI, and other temperatures and pressures were monitored and recorded. Other parameters including speed setpoint, engine load, exhaust back pressure, and inlet pressure and temperature were controlled as well. Data was also recorded through the LabVIEW VI, including data from the LECM transferred over a CAN connection. Figure A-1 shows the LabVIEW VI. Engine start and stop controls and data recording tools are on the right-most column. The second right-most column has inlet and exhaust settings. The second column from the left has emissions values in the bottom. The black box is where the engine dyno controls are displayed while the engine is running. The left column includes all key temperatures and pressures.

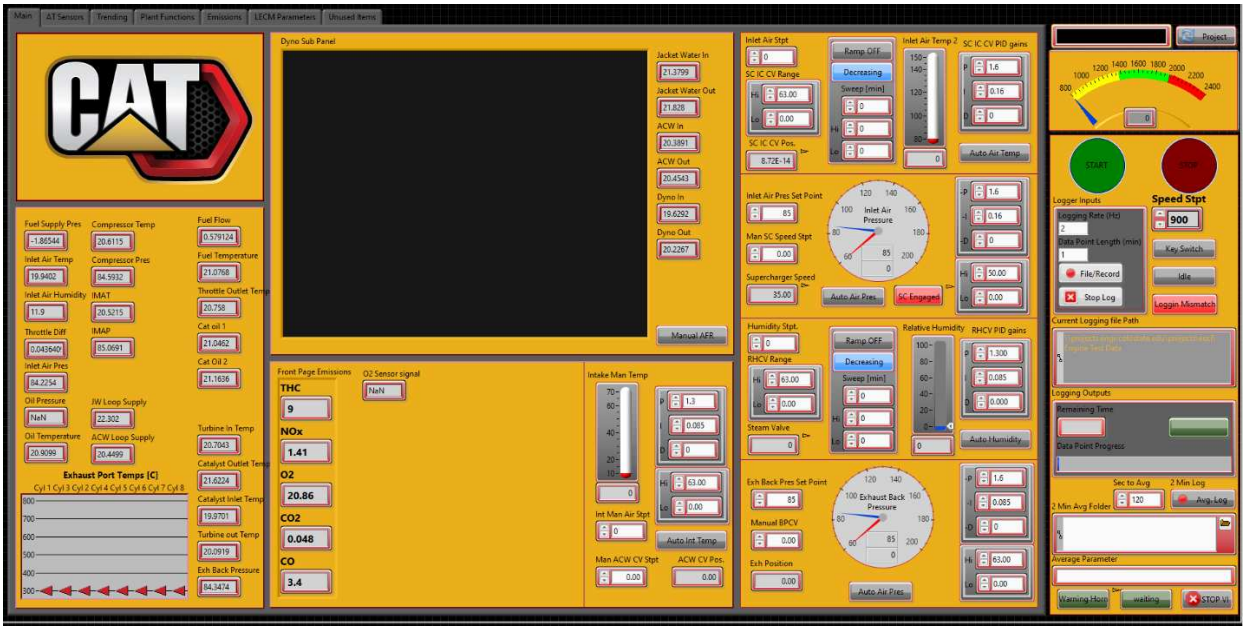

Figure 73: LabVIEW HMI created by Kirk Evans was used for general engine control, monitoring, and data recording.

Engine speed controller and fuel controller tuning were performed using an HMI created in Woodward Toolkit by Andrew Jones and Jeff Carlson. Figure A-2 shows the speed control PID tuning page, and Figure A-3 shows the AFR control PID tuning page. The left black box was used to monitor engine parameters useful for tuning, and the right black box plots the P, I, and D terms to monitor how the PID reacted to engine changes. The tables below them allowed for gain scheduling at different speeds and loads.

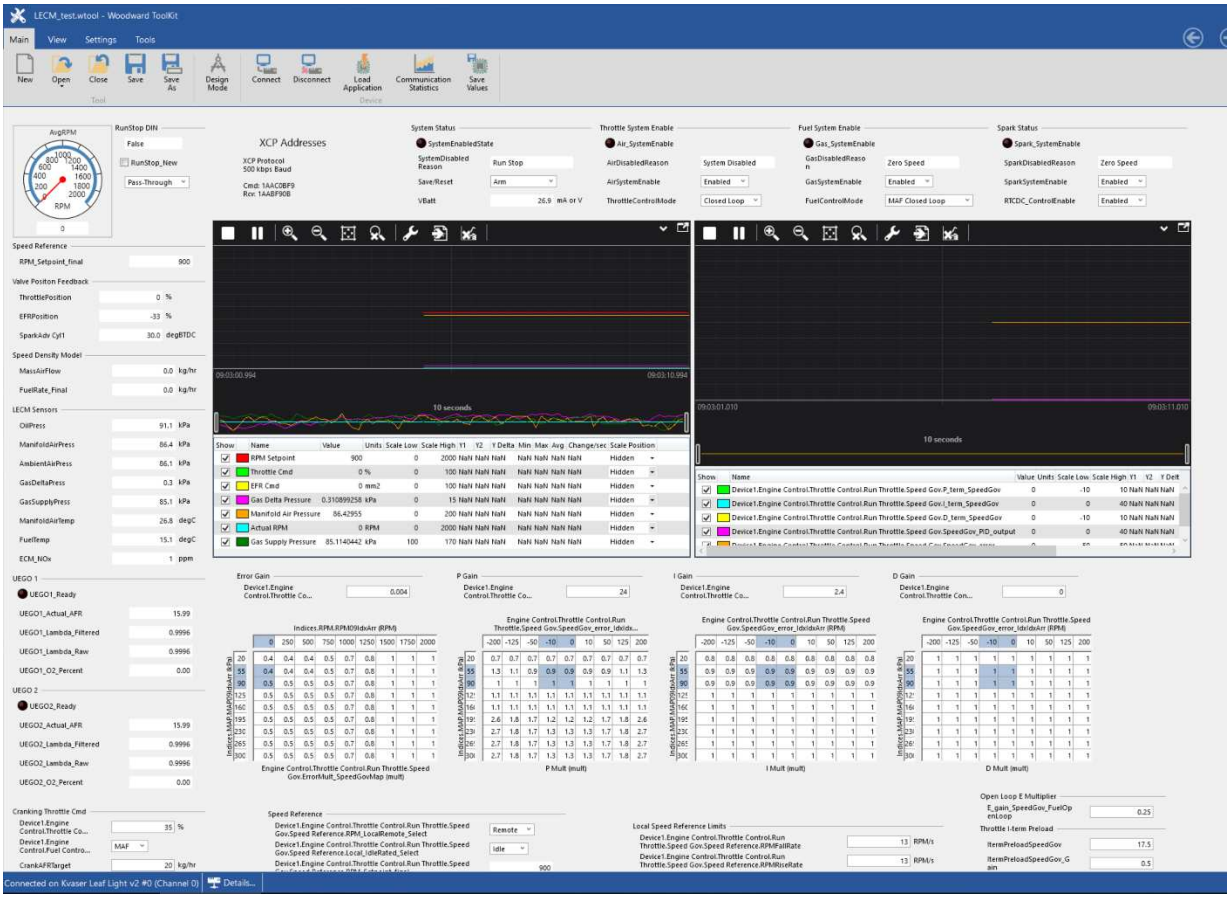

Figure 74: Woodward Toolkit speed control tuning page

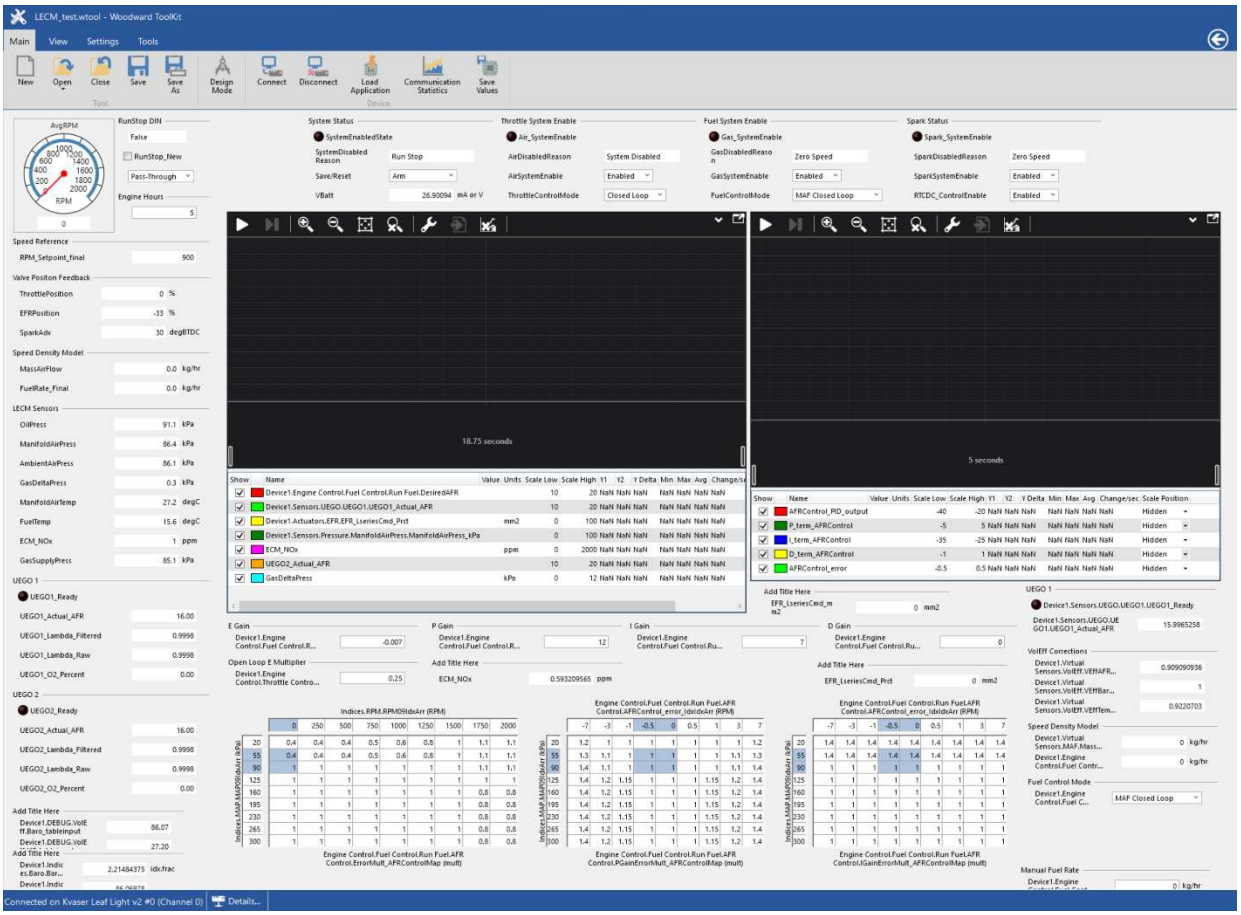

Figure 75: Woodward Toolkit air-fuel ratio control tuning page

Air-fuel ratio and dithering parameters were adjusted on the dithering Toolkit page, shown in **Error! Reference source not found.**A-4. Air-fuel ratio can be adjusted based on e ngine speed and load, but was constant for this project. The “custom waveform” section was used to add dithering. Rich and lean excursions could be adjusted in time and depth.

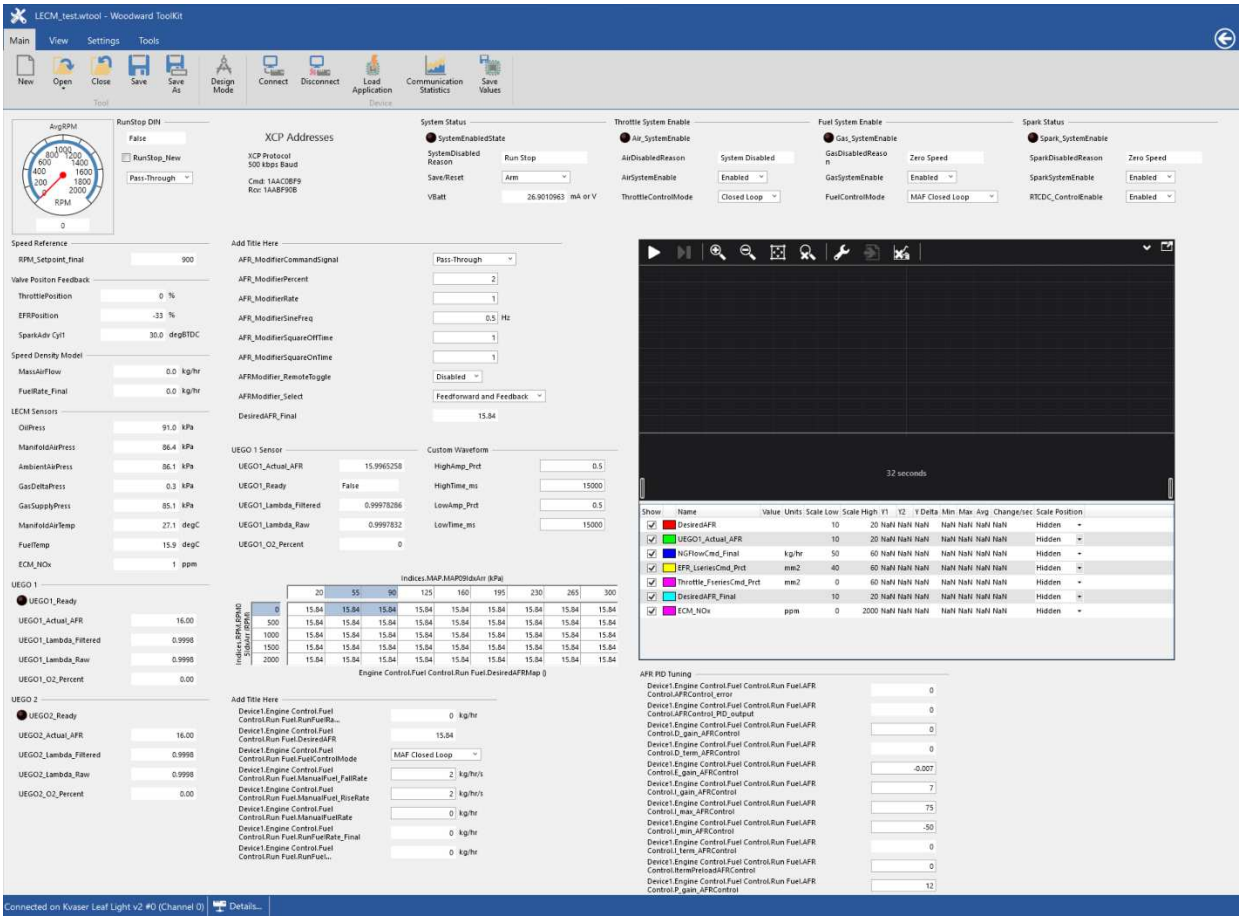

Figure 76: Woodward Toolkit air-fuel ratio adjustment and modification page. On this page, air-fuel ratio could be adjusted, and dithering could be applied.

DATA TABLES

Catalyst 1: Steady AFR Sweep

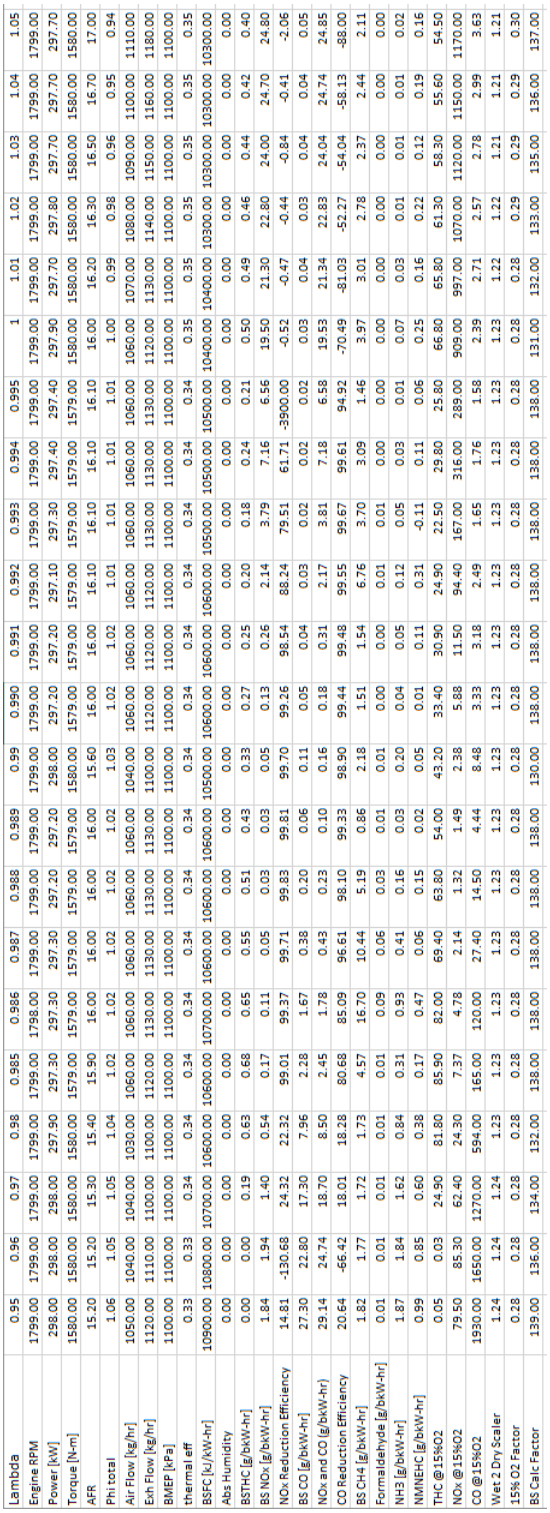

Lambda	0.95	0.96	0.97	0.98	0.985	0.986	0.987	0.988	0.989	0.99	0.990	0.991	0.992	0.993	0.994	0.995	1	1.01	1.02	1.03	1.04	1.05
Engine RPM	1799.00	1799.00	1799.00	1799.00	1799.00	1798.00	1799.00	1799.00	1799.00	1799.00	1799.00	1799.00	1799.00	1799.00	1799.00	1799.00	1799.00	1799.00	1798.00	1799.00	1799.00	1799.00
Power [kW]	298.00	298.00	298.00	297.90	297.30	297.30	297.30	297.20	297.20	298.00	297.20	297.20	297.10	297.30	297.40	297.40	297.90	297.70	297.80	297.70	297.70	297.70
Torque [N-m]	1580.00	1580.00	1580.00	1580.00	1579.00	1579.00	1579.00	1579.00	1580.00	1579.00	1579.00	1579.00	1579.00	1579.00	1579.00	1579.00	1580.00	1580.00	1580.00	1580.00	1580.00	1580.00
AFR	15.20	15.20	15.30	15.40	15.90	16.00	16.00	16.00	16.00	15.60	16.00	16.00	16.10	16.10	16.10	16.10	16.00	16.20	16.30	16.50	16.70	17.00
Phi total	1.06	1.05	1.05	1.04	1.02	1.02	1.02	1.02	1.02	1.03	1.02	1.02	1.01	1.01	1.01	1.01	1.00	0.99	0.98	0.96	0.95	0.94
Air Flow [kg/hr]	1050.00	1040.00	1040.00	1030.00	1060.00	1060.00	1060.00	1060.00	1060.00	1040.00	1060.00	1060.00	1060.00	1060.00	1060.00	1060.00	1060.00	1070.00	1080.00	1090.00	1100.00	1110.00
Exh Flow [kg/hr]	1120.00	1110.00	1100.00	1100.00	1120.00	1130.00	1130.00	1130.00	1130.00	1100.00	1120.00	1120.00	1120.00	1130.00	1130.00	1130.00	1120.00	1130.00	1140.00	1150.00	1160.00	1180.00
BMEP [kPa]	1100.00	1100.00	1100.00	1100.00	1100.00	1100.00	1100.00	1100.00	1100.00	1100.00	1100.00	1100.00	1100.00	1100.00	1100.00	1100.00	1100.00	1100.00	1100.00	1100.00	1100.00	1100.00
thermal eff	0.33	0.33	0.34	0.34	0.34	0.34	0.34	0.34	0.34	0.34	0.34	0.34	0.34	0.34	0.34	0.34	0.35	0.35	0.35	0.35	0.35	0.35
BSFC [kJ/kW-hr]	10900.00	10800.00	10700.00	10600.00	10600.00	10700.00	10600.00	10600.00	10600.00	10500.00	10600.00	10600.00	10600.00	10500.00	10500.00	10500.00	10400.00	10400.00	10300.00	10300.00	10300.00	10300.00
Abs Humidity	0.00	0.00	0.00	0.00	0.00	0.00	0.00	0.00	0.00	0.00	0.00	0.00	0.00	0.00	0.00	0.00	0.00	0.00	0.00	0.00	0.00	0.00
BSTHC [g/bkW-hr]	0.00	0.00	0.19	0.63	0.68	0.65	0.55	0.51	0.43	0.33	0.27	0.25	0.20	0.18	0.24	0.21	0.50	0.49	0.46	0.44	0.42	0.40
BS NOx [g/bkW-hr]	1.84	1.94	1.40	0.54	0.17	0.11	0.05	0.03	0.03	0.05	0.13	0.26	2.14	3.79	7.16	6.56	19.50	21.30	22.80	24.00	24.70	24.80
NOx Reduction Efficiency	14.81	-130.68	24.32	22.32	99.01	99.37	99.71	99.83	99.81	99.70	99.26	98.54	88.24	79.51	61.71	-3900.00	-0.52	-0.47	-0.44	-0.84	-0.41	-2.06
BS CO [g/bkW-hr]	27.30	22.80	17.30	7.96	2.28	1.67	0.38	0.20	0.06	0.11	0.05	0.04	0.03	0.02	0.02	0.02	0.03	0.04	0.03	0.04	0.04	0.05
NOx and CO [g/bkW-hr]	29.14	24.74	18.70	8.50	2.45	1.78	0.43	0.23	0.10	0.16	0.18	0.31	2.17	3.81	7.18	6.58	19.53	21.34	22.83	24.04	24.74	24.85
CO Reduction Efficiency	20.64	-66.42	18.01	18.28	80.68	85.09	96.61	98.10	99.33	98.90	99.44	99.48	99.55	99.67	99.61	94.92	-70.49	-81.03	-52.27	-54.04	-58.13	-88.00
BS CH4 [g/bkW-hr]	1.82	1.77	1.72	1.73	4.57	16.70	10.44	5.19	0.86	2.18	1.51	1.54	6.76	3.70	3.09	1.46	3.97	3.01	2.78	2.37	2.44	2.11
Formaldehyde [g/bkW-hr]	0.01	0.01	0.01	0.01	0.01	0.09	0.06	0.03	0.01	0.01	0.00	0.00	0.01	0.01	0.00	0.00	0.00	0.00	0.00	0.00	0.00	0.00
NH3 [g/bkW-hr]	1.87	1.84	1.62	0.84	0.31	0.93	0.41	0.16	0.03	0.20	0.04	0.05	0.12	0.05	0.03	0.01	0.07	0.03	0.01	0.01	0.01	0.02
NMNEHC [g/bkW-hr]	0.99	0.85	0.60	0.38	0.17	0.47	0.06	0.15	0.02	0.05	0.01	0.11	0.31	-0.11	0.11	0.06	0.25	0.16	0.22	0.12	0.19	0.16
THC @15%O2	0.05	0.03	24.90	81.80	85.90	82.00	69.40	63.80	54.00	43.20	33.40	30.90	24.90	22.50	29.80	25.80	66.80	65.80	61.30	58.30	55.60	54.50
NOx @15%O2	79.50	85.30	62.40	24.30	7.37	4.78	2.14	1.32	1.49	2.38	5.88	11.50	94.40	167.00	316.00	289.00	909.00	997.00	1070.00	1120.00	1150.00	1170.00
CO @15%O2	1930.00	1650.00	1270.00	594.00	165.00	120.00	27.40	14.50	4.44	8.48	3.33	3.18	2.49	1.65	1.76	1.58	2.39	2.71	2.57	2.78	2.99	3.63
Wet 2 Dry Scaler	1.24	1.24	1.24	1.23	1.23	1.23	1.23	1.23	1.23	1.23	1.23	1.23	1.23	1.23	1.23	1.23	1.23	1.22	1.22	1.21	1.21	1.21
15% O2 Factor	0.28	0.28	0.28	0.28	0.28	0.28	0.28	0.28	0.28	0.28	0.28	0.28	0.28	0.28	0.28	0.28	0.28	0.28	0.29	0.29	0.29	0.30
BS Calc Factor	139.00	136.00	134.00	132.00	138.00	138.00	138.00	138.00	138.00	130.00	138.00	138.00	138.00	138.00	138.00	138.00	131.00	132.00	133.00	135.00	136.00	137.00

Catalyst 1: Dithering AFR Sweep

Lambda	0.95	0.96	0.97	0.98	0.985	0.987	0.989	0.99	0.991	0.993	0.995	1	1.01	1.02	1.03	1.04	1.05
Engine RPM	1799.00	1799.00	1799.00	1799.00	1799.00	1799.00	1799.00	1799.00	1799.00	1799.00	1799.00	1799.00	1799.00	1799.00	1799.00	1799.00	1799.00
Power [kW]	298.00	298.00	298.00	297.90	297.80	297.80	297.90	297.80	297.80	297.90	297.80	297.80	297.70	297.80	297.70	297.70	297.70
Torque [N-m]	1581.00	1581.00	1581.00	1581.00	1581.00	1581.00	1581.00	1581.00	1581.00	1581.00	1581.00	1581.00	1580.00	1580.00	1580.00	1580.00	1580.00
AFR	15.40	15.60	15.70	15.80	15.80	15.80	15.90	15.90	15.90	16.00	16.10	16.20	16.20	16.30	16.50	16.70	17.00
Phi total	1.05	1.03	1.03	1.02	1.02	1.02	1.01	1.02	1.01	1.01	1.01	1.00	0.99	0.98	0.96	0.95	0.94
Air Flow [kg/hr]	1060.00	1060.00	1060.00	1050.00	1050.00	1050.00	1060.00	1060.00	1060.00	1060.00	1070.00	1070.00	1070.00	1080.00	1090.00	1100.00	1110.00
Exh Flow [kg/hr]	1130.00	1130.00	1120.00	1120.00	1120.00	1120.00	1120.00	1120.00	1120.00	1130.00	1130.00	1140.00	1130.00	1140.00	1150.00	1160.00	1180.00
BMEP [kPa]	1100.00	1100.00	1100.00	1100.00	1100.00	1100.00	1100.00	1100.00	1100.00	1100.00	1100.00	1100.00	1100.00	1100.00	1100.00	1100.00	1100.00
thermal eff	0.33	0.33	0.34	0.34	0.34	0.34	0.34	0.34	0.34	0.34	0.34	0.34	0.35	0.35	0.35	0.35	0.35
BSFC [kJ/kW-hr]	10900.00	10800.00	10600.00	10600.00	10600.00	10500.00	10500.00	10500.00	10500.00	10500.00	10500.00	10500.00	10400.00	10300.00	10300.00	10300.00	10300.00
Abs Humidity	0.00	0.00	0.00	0.00	0.00	0.00	0.00	0.00	0.00	0.00	0.00	0.00	0.00	0.00	0.00	0.00	0.00
BSTHC [g/bkW-hr]	0.70	0.59	0.50	0.25	0.17	0.09	0.09	0.08	0.10	0.14	0.15	0.21	0.49	0.46	0.44	0.42	0.40
BS NOx [g/bkW-hr]	0.31	0.25	0.19	0.05	0.09	0.47	2.47	0.95	2.79	5.36	6.03	9.58	21.30	22.80	24.00	24.70	24.80
NOx Reduction Efficiency	97.33	98.14	98.77	99.67	99.52	97.41	86.65	94.86	84.92	71.64	68.10	51.62	0.00	-1.79	-1.69	0.00	1.59
BS CO [g/bkW-hr]	25.80	14.20	5.96	0.21	0.05	0.02	0.02	0.02	0.02	0.02	0.02	0.02	0.04	0.03	0.04	0.04	0.05
CO Reduction Efficience	9.47	40.83	70.05	98.80	99.69	99.84	99.86	99.87	99.86	99.84	99.84	99.77	99.53	99.47	99.20	98.69	97.45
NOx and CO (g/bkW-hr)	26.11	14.45	6.15	0.26	0.13	0.49	2.49	0.96	2.81	5.38	6.05	9.60	21.34	22.83	24.04	24.74	24.85
BS CH4 [g/bkW-hr]	3.49	4.46	3.67	3.16	1.29	1.87	0.74	0.69	1.61	1.76	1.27	1.38	3.01	2.78	2.37	2.44	2.11
Acetaldehyde [g/bkW-hr	0.00	0.00	0.00	0.00	0.00	0.00	0.00	0.00	0.01	0.00	0.00	0.00	0.00	0.00	0.00	0.00	0.00
NH3 [g/bkW-hr]	3.39	3.21	1.52	0.20	0.13	0.07	0.03	0.02	0.03	0.02	0.01	0.01	0.03	0.01	0.01	0.01	0.02
NMNEHC [g/bkW-hr]	0.60	0.72	0.52	0.29	0.32	0.08	0.08	0.08	0.16	0.17	0.08	0.03	0.16	0.24	0.13	0.21	0.18
THC @15%O2	88.90	77.10	64.80	32.50	22.10	11.50	12.20	10.20	13.00	18.20	19.80	27.80	65.80	61.30	58.30	55.60	54.50
NOx @15%O2	13.80	11.40	8.54	2.47	3.90	21.60	113.00	43.10	127.00	244.00	276.00	437.00	997.00	1070.00	1120.00	1150.00	1170.00
CO @15%O2	1880.00	1060.00	444.00	15.40	3.52	1.77	1.47	1.47	1.41	1.55	1.58	1.86	2.71	2.57	2.78	2.99	3.63
Wet 2 Dry Scaler	1.24	1.24	1.23	1.23	1.23	1.23	1.23	1.23	1.23	1.23	1.23	1.23	1.22	1.22	1.21	1.21	1.21
15% O2 Factor	0.28	0.28	0.28	0.28	0.28	0.28	0.28	0.28	0.28	0.28	0.28	0.28	0.28	0.29	0.29	0.29	0.30
BS Calc Factor	136.00	134.00	133.00	134.00	133.00	132.00	132.00	133.00	133.00	133.00	133.00	134.00	132.00	133.00	135.00	136.00	137.00

Catalyst 1: Dithering Parameter Sweep

	00amp00hz	05amp01hz	05amp02hz	05amp05hz	05amp10hz	10amp01hz	10amp02hz	10amp05hz	10amp10hz	15amp01hz	15amp02hz	15amp05hz	15amp10hz	20amp01hz	20amp02hz	20amp05hz	20amp10hz
Engine RPM	1799	1799	1799	1799	1799	1799	1799	1799	1799	1798	1799	1799	1799	1799	1799	1799	1799
Power [kW]	297.6	297.5	297.5	297.5	297.4	297.5	297.5	297.4	297.4	297.4	297.5	297.6	297.5	297.7	297.8	298	298
Torque [N-m]	1580	1579	1579	1579	1579	1579	1579	1579	1579	1579	1580	1580	1579	1581	1580	1580	1580
AFR	15.6	15.6	15.6	15.5	15.4	15.5	15.5	15.5	15.4	15.8	15.8	15.8	15.8	15.9	15.9	15.9	15.9
Phi total	1.02	1.02	1.02	1.02	1.02	1.02	1.02	1.02	1.02	1.02	1.02	1.02	1.02	1.01	1.01	1.01	1.01
Air Flow [kg/hr]	1040	1050	1050	1050	1040	1050	1050	1040	1040	1050	1050	1050	1050	1060	1060	1050	1050
Exh Flow [kg/hr]	1110	1110	1110	1120	1110	1110	1110	1110	1110	1120	1120	1110	1110	1120	1120	1120	1110
BMEP [kPa]	1100	1100	1100	1100	1100	1100	1100	1100	1100	1100	1100	1100	1100	1100	1100	1100	1100
thermal eff	0.344	0.344	0.344	0.343	0.344	0.343	0.344	0.344	0.344	0.342	0.343	0.344	0.344	0.342	0.342	0.344	0.345
BSFC [kJ/kW-hr]	10500	10500	10500	10500	10500	10500	10500	10500	10500	10500	10500	10500	10500	10500	10500	10500	10400
Abs Humidity	0.00284	0.00286	0.00286	0.00267	0.00255	0.00246	0.00244	0.00247	0.00253	0.00276	0.00284	0.00279	0.00285	0.00294	0.00314	0.00323	0.00337
BSTHC [g/bkW-hr]	0.715	0.53	0.53	0.686	0.881	0.645	0.618	0.723	0.866	0.608	0.523	0.523	0.651	0.535	0.464	0.483	0.392
BS NOx [g/bkW-hr]	0.182	0.36	0.36	0.0975	0.0728	0.481	0.255	0.146	0.0519	0.827	0.292	0.0989	0.0408	1.39	0.453	0.0914	0.0819
BS CO [g/bkW-hr]	0.0963	0.0813	0.0813	0.0999	0.11	0.339	0.174	0.18	0.0746	0.563	0.207	0.168	0.0289	0.84	0.248	0.111	0.0208
NMNEHC [g/bkW-hr]	0.059343682	0.00771449	0.00771449	0.023693934	0.036375743	0.028372466	0.01727673	0.0326822	0.074430821	0.145177111	-0.002645789	0.137260417	0.026564082	0.12251288	0.007054899	0.024459798	0.062453095
Acetaldehyde [g/bkW-hr]	0.008383283	0.005871172	0.005871172	0.003980582	0.004157682	0.020700824	0.023104354	0.008486197	0.015633259	0.102181246	0.003874585	0.020968545	0.010480157	0.027462283	0.004809846	0.008820386	0.029401415
THC @15%O2	95.5	70.8	70.8	91.6	118	86.2	82.7	96.9	116	81.3	69.8	69.9	87.2	71.1	61.7	64.4	52.4
NOx @15%O2	8.46	16.8	16.8	4.54	3.39	22.4	11.9	6.85	2.43	38.5	13.6	4.61	1.9	64.6	21	4.25	3.82
CO @15%O2	7.36	6.21	6.21	7.64	8.45	26	13.3	13.8	5.73	43.1	15.8	12.8	2.22	63.9	18.9	8.48	1.59
Wet 2 Dry Scaler	1.23	1.23	1.23	1.23	1.23	1.23	1.23	1.23	1.23	1.23	1.23	1.23	1.23	1.23	1.23	1.23	1.23
15% O2 Factor	0.279	0.279	0.279	0.279	0.279	0.279	0.279	0.279	0.279	0.279	0.279	0.279	0.279	0.28	0.279	0.279	0.279
BS Calc Factor	130	130	130	130	130	130	130	129	129	130	130	130	130	131	131	131	130

Catalyst 2: Steady AFR Sweep

Lambda	0.98	0.981	0.983	0.985	0.986	0.988	0.99	0.992	0.994	0.996	0.998	1	1.01	1.02	1.03	1.04	1.05
Engine RPM	1799.00	1799.00	1799.00	1799.00	1799.00	1799.00	1799.00	1799.00	1799.00	1799.00	1799.00	1799.00	1799.00	1799.00	1799.00	1798.00	1798.00
Power [kW]	297.20	297.20	297.30	297.40	297.50	297.50	297.50	297.50	297.50	297.50	297.50	297.50	297.40	297.50	297.40	297.30	297.40
Torque [N-m]	1579.00	1579.00	1579.00	1579.00	1579.00	1579.00	1579.00	1579.00	1579.00	1579.00	1579.00	1579.00	1579.00	1579.00	1579.00	1579.00	1579.00
AFR	15.90	16.00	16.00	16.00	16.00	16.00	16.00	16.00	16.00	16.10	16.20	16.20	16.60	16.90	17.10	17.40	17.60
Phi total	1.03	1.02	1.02	1.02	1.02	1.02	1.02	1.02	1.02	1.02	1.01	1.01	0.99	0.97	0.96	0.94	0.93
Air Flow [kg/hr]	1060.00	1060.00	1050.00	1050.00	1050.00	1050.00	1050.00	1050.00	1050.00	1050.00	1060.00	1060.00	1070.00	1090.00	1100.00	1110.00	1130.00
Exh Flow [kg/hr]	1120.00	1120.00	1120.00	1120.00	1120.00	1120.00	1110.00	1110.00	1110.00	1110.00	1120.00	1120.00	1140.00	1150.00	1170.00	1180.00	1190.00
BMEP [kPa]	1100.00	1100.00	1100.00	1100.00	1100.00	1100.00	1100.00	1100.00	1100.00	1100.00	1100.00	1100.00	1100.00	1100.00	1100.00	1100.00	1100.00
thermal eff	0.34	0.34	0.34	0.34	0.34	0.34	0.34	0.34	0.34	0.34	0.34	0.34	0.35	0.35	0.35	0.35	0.35
BSFC [kJ/kW-hr]	10700.00	10600.00	10600.00	10600.00	10600.00	10600.00	10500.00	10500.00	10500.00	10500.00	10500.00	10500.00	10400.00	10400.00	10300.00	10300.00	10300.00
Abs Humidity	0.00	0.00	0.00	0.00	0.00	0.00	0.00	0.00	0.00	0.00	0.00	0.00	0.00	0.00	0.00	0.00	0.00
BSTHC [g/bkW-hr]	0.08	0.09	0.09	0.07	0.06	0.05	0.04	0.03	0.02	0.06	0.08	0.13	0.27	0.37	0.42	0.42	0.42
BS NOx [g/bkW-hr]	0.00	0.00	0.00	0.00	0.00	0.00	0.00	0.00	0.02	3.88	7.35	9.21	17.80	22.70	24.60	26.10	26.80
BS CO [g/bkW-hr]	2.41	2.36	2.13	1.78	1.56	1.18	0.69	0.38	0.06	0.02	0.02	0.02	0.03	0.04	0.04	0.04	0.04
NOx +CO [g/bkW-hr]	2.41	2.36	2.13	1.78	1.56	1.18	0.69	0.38	0.08	3.90	7.37	9.23	17.83	22.74	24.64	26.14	26.84
CH4 [g/bkW-hr]	0.24	0.28	0.18	0.17	0.16	0.17	0.14	0.19	5.05	1.39	1.07	0.96	1.31	1.56	1.72	0.00	0.00
NH3 [g/bkW-hr]	0.58	0.52	0.58	0.45	0.34	0.22	0.22	0.27	0.51	0.05	0.04	0.01	0.01	0.01	0.01	0.01	0.01
Formaldehyde [g/bkW-hr]	0.00	0.00	0.00	0.00	0.00	0.00	0.00	0.00	0.00	0.00	0.00	0.00	0.00	0.00	0.00	0.00	0.00
NMNEHC [g/bkW-hr]	0.04	0.03	-0.02	0.06	0.03	0.00	0.03	0.09	0.72	0.05	0.04	0.02	0.01	0.03	0.00	0.00	0.00
THC @15%O2	10.50	10.70	11.30	8.62	7.15	6.25	5.00	4.07	1.88	7.13	10.30	15.80	33.70	46.70	53.00	54.10	53.30
NOx @15%O2	0.15	0.15	0.14	0.16	0.14	0.14	0.15	0.18	0.84	169.00	321.00	402.00	779.00	1000.00	1090.00	1160.00	1190.00
CO @15%O2	171.00	168.00	152.00	127.00	111.00	84.30	49.20	27.00	4.46	1.31	1.43	1.44	2.13	2.69	2.95	3.03	3.05
Wet 2 Dry Scaler	1.24	1.23	1.23	1.23	1.23	1.23	1.23	1.23	1.23	1.23	1.23	1.23	1.23	1.22	1.22	1.21	1.21
15% O2 Factor	0.28	0.28	0.28	0.28	0.28	0.28	0.28	0.28	0.28	0.28	0.28	0.28	0.28	0.29	0.29	0.30	0.30
BS Calc Factor	139.00	139.00	139.00	139.00	139.00	139.00	139.00	139.00	138.00	139.00	139.00	139.00	141.00	142.00	143.00	144.00	146.00

Catalyst 2: Dithering AFR Sweep

	0.95	0.96	0.97	0.98	0.981	0.983	0.985	0.986	0.988	0.99	0.992	0.994	0.996	0.998	1	1.01	1.02	1.03	1.04	1.05
Engine RPM	1799.00	1799.00	1799.00	1799.00	1799.00	1799.00	1799.00	1799.00	1799.00	1799.00	1799.00	1799.00	1799.00	1799.00	1799.00	1799.00	1799.00	1799.00	1799.00	1798.00
Power [kW]	297.50	297.50	297.50	297.40	297.40	297.40	297.50	297.50	297.40	297.50	297.50	297.50	297.50	297.50	297.50	297.50	297.50	297.50	297.50	297.40
Torque [N-m]	1579.00	1579.00	1579.00	1579.00	1579.00	1579.00	1579.00	1579.00	1579.00	1579.00	1579.00	1579.00	1579.00	1579.00	1579.00	1579.00	1579.00	1579.00	1579.00	1579.00
AFR	15.80	15.80	15.90	15.90	15.90	15.90	15.90	16.00	16.00	16.00	16.00	16.00	NaN	16.20	16.30	16.60	16.90	17.10	17.40	17.60
Phi total	1.03	1.03	1.03	1.03	1.03	1.03	1.02	1.02	1.02	1.02	1.02	1.02	NaN	1.01	1.01	0.99	0.97	0.96	0.94	0.93
Air Flow [kg/hr]	1090.00	1070.00	1060.00	1050.00	1050.00	1050.00	1050.00	1050.00	1050.00	1050.00	1050.00	1050.00	NaN	1060.00	1060.00	1080.00	1090.00	1100.00	1110.00	1130.00
Exh Flow [kg/hr]	1150.00	1140.00	1130.00	1120.00	1120.00	1120.00	1120.00	1120.00	1110.00	1120.00	1110.00	1110.00	NaN	1120.00	1130.00	1140.00	1150.00	1170.00	1180.00	1190.00
BMEP [kPa]	1100.00	1100.00	1100.00	1100.00	1100.00	1100.00	1100.00	1100.00	1100.00	1100.00	1100.00	1100.00	1100.00	1100.00	1100.00	1100.00	1100.00	1100.00	1100.00	1100.00
thermal eff	0.33	0.33	0.34	0.34	0.34	0.34	0.34	0.34	0.34	0.34	0.34	0.34	NaN	0.34	0.34	0.35	0.35	0.35	0.35	0.35
BSFC [kJ/kW-hr]	11000.00	10900.00	10700.00	10600.00	10600.00	10600.00	10600.00	10600.00	10600.00	10500.00	10500.00	10500.00	NaN	10500.00	10500.00	10400.00	10400.00	10400.00	10300.00	10300.00
Abs Humidity	0.00	0.00	0.00	0.00	0.00	0.00	0.00	0.00	0.00	0.00	0.00	0.00	0.00	0.00	0.00	0.00	0.00	0.00	0.00	0.00
BSTHC [g/bkW-hr]	0.37	0.42	0.46	0.34	0.39	0.39	0.31	0.22	0.20	0.12	0.02	0.02	NaN	0.08	0.12	0.27	0.37	0.42	0.43	0.43
BS NOx [g/bkW-hr]	0.03	0.01	0.01	0.00	0.00	0.00	0.00	0.00	0.00	0.00	0.01	1.37	NaN	7.35	9.52	17.90	22.20	24.50	25.30	26.20
BS CO [g/bkW-hr]	10.40	6.64	4.00	1.43	1.50	1.28	1.12	0.96	0.51	0.37	0.03	0.02	NaN	0.02	0.02	0.03	0.03	0.03	0.03	0.03
NOx+CO [g/bkW-hr]	10.43	6.65	4.01	1.43	1.50	1.28	1.12	0.97	0.52	0.38	0.04	1.39	#VALUE!	7.37	9.54	17.93	22.23	24.53	25.33	26.23
CH4 [g/bkW-hr]	3.66	2.00	2.52	1.05	1.38	0.75	0.65	0.86	0.56	0.95	1.07	1.52	#VALUE!	1.07	1.59	2.06	2.26	2.22	2.21	0.00
NH3 [g/bkW-hr]	6.32	3.13	3.49	1.33	1.54	0.95	0.74	0.65	0.29	0.27	0.44	0.11	#VALUE!	0.04	0.02	0.01	0.01	0.01	0.01	0.00
Formaldehyde [g/bkW-hr]	0.00	0.00	0.00	0.00	0.00	0.00	0.00	0.00	0.00	0.00	0.00	0.00	#VALUE!	0.00	0.00	0.00	0.00	0.00	0.00	0.00
NMNEHC [g/bkW-hr]	0.05	0.10	0.19	0.05	0.12	0.06	0.07	0.01	0.08	0.39	1.19	0.11	#VALUE!	0.04	0.07	0.08	0.09	0.04	-0.02	0.00
THC @15%O2	45.10	51.70	56.00	41.40	48.50	47.70	38.40	27.20	24.70	15.00	2.86	2.58	6.92	10.30	14.50	34.40	46.80	53.20	54.20	54.10
NOx @15%O2	1.43	0.37	0.25	0.21	0.20	0.19	0.19	0.15	0.16	0.20	0.31	59.60	216.00	321.00	417.00	791.00	983.00	1080.00	1120.00	1160.00
CO @15%O2	720.00	463.00	281.00	102.00	106.00	90.70	79.30	68.50	36.60	26.70	2.27	1.18	1.28	1.43	1.55	2.06	2.23	2.16	2.21	2.21
Wet 2 Dry Scaler	1.24	1.24	1.24	1.23	1.23	1.23	1.23	1.23	1.23	1.24	1.23	1.23	NaN	1.23	1.23	1.23	1.22	1.22	1.22	1.21
15% O2 Factor	0.28	0.28	0.28	0.28	0.28	0.28	0.28	0.28	0.28	0.28	0.28	0.28	0.28	0.28	0.28	0.28	0.29	0.29	0.30	0.30
BS Calc Factor	143.00	142.00	141.00	140.00	140.00	139.00	139.00	139.00	139.00	138.00	139.00	139.00	NaN	139.00	139.00	140.00	141.00	143.00	145.00	147.00

Catalyst 2: Dithering Parameter Sweep

	0Oamp0Hz	05amp01hz	05amp02hz	05amp05hz	05amp10hz	10amp01hz	10amp01hz	10amp05hz	10amp10hz	15amp01hz	15amp02hz	15amp05hz	15amp10hz	20amp01hz	20amp02hz	20amp05hz	20amp10hz
Engine RPM	1.80E+03	1.80E+03	1.80E+03	1.80E+03	1.80E+03	1.80E+03	1.80E+03	1.80E+03	1.80E+03	1.80E+03	1.80E+03	1.80E+03	1.80E+03	1.80E+03	1.80E+03	1.80E+03	1.80E+03
Power [kW]	2.97E+02	2.97E+02	2.98E+02	2.97E+02	2.97E+02	2.98E+02	2.98E+02	2.98E+02	2.98E+02	2.98E+02	2.98E+02	2.98E+02	2.98E+02	2.98E+02	2.98E+02	2.98E+02	2.98E+02
Torque [N-m]	1.58E+03	1.58E+03	1.58E+03	1.58E+03	1.58E+03	1.58E+03	1.58E+03	1.58E+03	1.58E+03	1.58E+03	1.58E+03	1.58E+03	1.58E+03	1.58E+03	1.58E+03	1.58E+03	1.58E+03
AFR	1.60E+01	1.60E+01	1.60E+01	1.60E+01	1.60E+01	1.60E+01	1.60E+01	1.60E+01	1.60E+01	1.60E+01	1.60E+01	1.60E+01	1.60E+01	1.60E+01	1.60E+01	1.60E+01	1.60E+01
Phi total	1.02E+00	1.02E+00	1.02E+00	1.02E+00	1.02E+00	1.02E+00	1.02E+00	1.02E+00	1.02E+00	1.02E+00	1.02E+00	1.02E+00	1.02E+00	1.02E+00	1.02E+00	1.02E+00	1.02E+00
Air Flow [kg/hr]	1.05E+03	1.05E+03	1.05E+03	1.05E+03	1.05E+03	1.05E+03	1.05E+03	1.05E+03	1.05E+03	1.05E+03	1.05E+03	1.05E+03	1.05E+03	1.06E+03	1.06E+03	1.05E+03	1.05E+03
Exh Flow [kg/hr]	1.11E+03	1.11E+03	1.11E+03	1.11E+03	1.11E+03	1.11E+03	1.12E+03	1.12E+03	1.11E+03	1.12E+03	1.12E+03	1.12E+03	1.11E+03	1.12E+03	1.12E+03	1.12E+03	1.12E+03
BMEP [kPa]	1.10E+03	1.10E+03	1.10E+03	1.10E+03	1.10E+03	1.10E+03	1.10E+03	1.10E+03	1.10E+03	1.10E+03	1.10E+03	1.10E+03	1.10E+03	1.10E+03	1.10E+03	1.10E+03	1.10E+03
thermal eff	3.41E-01	3.42E-01	3.42E-01	3.41E-01	3.41E-01	3.41E-01	3.41E-01	3.41E-01	3.42E-01	3.41E-01	3.40E-01	3.41E-01	3.41E-01	3.40E-01	3.39E-01	3.41E-01	3.41E-01
BSFC [kJ/kW-hr]	1.06E+04	1.05E+04	1.05E+04	1.05E+04	1.06E+04	1.06E+04	1.06E+04	1.05E+04	1.05E+04	1.06E+04	1.06E+04	1.06E+04	1.05E+04	1.06E+04	1.06E+04	1.06E+04	1.06E+04
Abs Humidity	3.74E-03	3.80E-03	3.82E-03	3.88E-03	3.90E-03	3.89E-03	3.87E-03	3.72E-03	3.92E-03	3.98E-03	4.07E-03	4.16E-03	4.32E-03	4.41E-03	4.41E-03	4.49E-03	4.52E-03
BSTHC [g/bkW-hr]	2.07E-01	1.69E-01	1.86E-01	2.97E-01	4.46E-01	4.25E-02	8.81E-02	1.43E-01	3.07E-01	3.97E-02	5.82E-02	1.04E-01	2.34E-01	4.37E-02	3.11E-02	6.57E-02	1.51E-01
BS NOx [g/bkW-hr]	4.12E-02	2.01E-02	1.09E-02	7.87E-03	6.49E-03	2.51E-02	9.93E-03	6.41E-03	2.81E-03	2.20E-01	3.22E-02	6.11E-03	1.72E-03	1.45E+00	1.44E-01	7.68E-03	2.73E-03
BS CO [g/bkW-hr]	4.41E-01	5.29E-01	2.32E-01	1.46E-01	2.47E-01	8.92E-01	5.39E-01	3.06E-01	9.50E-02	9.06E-01	7.65E-01	3.31E-01	5.92E-02	1.09E+00	1.01E+00	3.95E-01	9.96E-02
BS CH4 [g/bkW-hr]	3.91E-01	8.61E-01	1.61E+00	7.47E-01	4.17E-02	6.58E-01	1.04E+00	4.59E-01	1.41E+00	2.75E-01	1.07E+00	5.20E+00	1.06E-02	1.01E-01	4.83E-01	5.54E+00	2.20E+00
Formaldahyde [g/bkW-hr]	2.22E-04	0.00E+00	0.00E+00	0.00E+00	0.00E+00	0.00E+00	0.00E+00	0.00E+00	0.00E+00	0.00E+00	0.00E+00	0.00E+00	0.00E+00	0.00E+00	0.00E+00	1.07E-03	0.00E+00
NH3 [g/bkW-hr]	2.39E-01	3.03E-01	1.49E-01	1.52E-01	9.47E-02	4.77E-01	4.43E-01	2.43E-01	4.06E-02	2.83E-01	6.31E-01	2.24E-01	1.36E-02	1.82E-01	3.85E-01	2.25E-01	7.68E-01
Acedeltahyde [g/bkW-hr]	3.41E-03	-7.57E-03	1.13E-02	4.96E-03	3.33E-03	3.94E-03	7.88E-03	2.83E-03	4.96E-03	2.24E-03	1.33E-02	1.84E-02	-4.50E-04	-3.11E-03	3.41E-03	6.17E-03	-2.73E-03
NMNEHC [g/bkW-hr]	7.08E-02	1.50E-01	1.03E-01	5.56E-02	3.35E-02	8.10E-02	2.51E-01	7.14E-02	3.20E-02	4.61E-02	3.73E-01	8.82E-02	5.52E-03	6.69E-02	1.43E-01	1.26E-01	1.26E-01
THC @15%O2	2.56E+01	2.09E+01	2.31E+01	3.70E+01	5.56E+01	5.30E+00	1.10E+01	1.79E+01	3.84E+01	4.96E+00	7.25E+00	1.31E+01	2.93E+01	5.46E+00	3.87E+00	8.20E+00	1.88E+01
NOx @15%O2	1.78E+00	8.69E-01	4.72E-01	3.41E-01	2.82E-01	1.09E+00	4.32E-01	2.79E-01	1.23E-01	9.59E+00	1.40E+00	2.66E-01	7.51E-02	6.31E+01	6.25E+00	3.34E-01	1.19E-01
CO @15%O2	3.13E+01	3.75E+01	1.65E+01	1.04E+01	1.76E+01	6.38E+01	3.85E+01	2.19E+01	6.81E+00	6.47E+01	5.46E+01	2.37E+01	4.25E+00	7.77E+01	7.23E+01	2.82E+01	7.13E+00
Wet 2 Dry Scaler	1.24E+00	1.24E+00	1.24E+00	1.24E+00	1.24E+00	1.24E+00	1.24E+00	1.24E+00	1.24E+00	1.24E+00	1.24E+00	1.24E+00	1.24E+00	1.23E+00	1.24E+00	1.24E+00	1.24E+00
15% O2 Factor	2.77E-01	2.77E-01	2.77E-01	2.77E-01	2.77E-01	2.77E-01	2.77E-01	2.77E-01	2.77E-01	2.77E-01	2.77E-01	2.77E-01	2.77E-01	2.77E-01	2.77E-01	2.77E-01	2.77E-01
BS Calc Factor	1.39E+02	1.39E+02	1.39E+02	1.39E+02	1.38E+02	1.38E+02	1.38E+02	1.38E+02	1.38E+02	1.38E+02	1.38E+02	1.38E+02	1.38E+02	1.39E+02	1.39E+02	1.38E+02	1.38E+02

Catalyst 3: Steady AFR Sweep

lambda	0.95	0.96	0.97	0.98	0.981	0.983	0.985	0.986	0.988	0.99	0.992	0.994	0.996	0.998	1	1.01	1.02	1.03	1.04
Engine RPM	1799	1799	1799	1799	1799	1799	1799	1799	1799	1799	1799	1799	1799	1799	1799	1799	1799	1799	1799
Power [kW]	297.5	297.7	297.7	297.4	297.4	297.4	297.4	297.2	297.3	297.3	297.2	297.3	297.4	297.5	297.5	297.6	297.6	297.6	297.5
Torque [N-m]	1579	1580	1580	1579	1579	1579	1579	1579	1579	1579	1579	1579	1579	1579	1579	1579	1580	1580	1580
AFR	15.4	15.5	15.7	15.8	15.9	15.9	15.9	15.9	16	16	16	16.2	16.2	16.2	16.3	16.6	16.9	17.4	17.6
Phi total	1.05	1.05	1.04	1.03	1.02	1.02	1.02	1.02	1.02	1.02	1.02	1.01	1.01	1	0.998	0.983	0.966	0.939	0.926
Air Flow [kg/hr]	1070	1070	1060	1060	1060	1060	1060	1060	1060	1060	1060	1070	1070	1070	1070	1090	1100	1130	1140
Exh Flow [kg/hr]	1140	1130	1130	1130	1130	1130	1130	1130	1130	1130	1130	1130	1130	1140	1140	1150	1170	1190	1200
BMEP [kPa]	1100	1100	1100	1100	1100	1100	1100	1100	1100	1100	1100	1100	1100	1100	1100	1100	1100	1100	1100
thermal eff	0.324	0.329	0.332	0.336	0.336	0.336	0.338	0.337	0.338	0.339	0.34	0.34	0.341	0.341	0.342	0.343	0.344	0.347	0.347
BSFC [kJ/kW-hr]	11100	11000	10800	10700	10700	10700	10700	10700	10600	10600	10600	10600	10600	10500	10500	10500	10500	10400	10400
Abs Humidity	0.00124	0.00127	0.00129	0.00132	0.00132	0.00132	0.00133	0.00134	0.00134	0.00132	0.00136	0.00135	0.00137	0.00137	0.00139	0.00138	0.00142	0.00142	0.00144
BSTHC [g/bkW-hr]	1.18	1.13	1.09	1.05	1.05	1.04	0.961	0.947	0.74	0.538	0.315	0.627	0.712	0.616	0.646	0.656	0.749	0.746	0.72
BS NOx [g/bkW-hr]	0.532	0.637	0.562	0.351	0.315	0.253	0.0936	0.0703	0.0328	0.0552	1.09	9.19	11.1	10.4	11.5	14.4	19.3	25	26.6
BS CO [g/bkW-hr]	31.5	24.3	15.8	5.4	4.56	3.77	1.21	0.931	0.137	0.0847	0.0792	0.028	0.0282	0.0279	0.0296	0.0313	0.032	0.0311	0.0309
NOx+CO [g/bkW-hr]	32.032	24.937	16.362	5.751	4.875	4.023	1.3036	1.0013	0.1698	0.1399	1.1692	9.218	11.1282	10.4279	11.5296	14.4313	19.332	25.0311	26.6309
CH4 [g/bkW-hr]	3.08914	3.30399	6.22224	2.23862	2.9175	7.1017	2.24739	15.414	4.15947	1.39135	31.4757	11.0356	5.16998	3.87098	3.62829	4.66996	4.04715	2.9136	0.00228
NH3 [g/bkW-hr]	3.93232	3.56722	2.96369	0.95811	1.02412	1.68072	0.42281	1.20951	0.19439	0.11069	0.37957	0.09913	0.04622	0.03178	0.02347	0.02071	0.01635	0.00964	0.0022
Formaldehyde [g/bkW-hr]	0.00417	0.00732	0.01916	0.00884	0.01125	0.00373	0.00053	0	0	0.0013	0	0.00536	0.00021	0.0031	0.00488	0	0.00555	0.00343	3.2E-07
NMNEHC [g/bkW-hr]	0.31204	0.39215	0.72511	0.22822	0.29632	0.41443	0.13293	0.45023	0.08558	0.03905	1.04506	0.31601	0.14768	0.08367	0.12078	0.05214	0.08481	0.05018	0.0005
THC @15%O2	142	138	135	131	131	130	120	118	92.4	67.4	39.4	78.6	89.5	77.3	81.2	82.9	95.2	95.5	92.2
NOx @15%O2	22.2	27.2	24.2	15.2	13.7	11	4.07	3.06	1.43	2.41	47.4	402	486	454	504	633	854	1120	1190
CO @15%O2	2160	1700	1120	385	325	269	86.7	66.6	9.8	6.08	5.67	2.01	2.03	2.01	2.13	2.26	2.33	2.28	2.27
Wet 2 Dry Scaler	1.24	1.24	1.24	1.23	1.23	1.23	1.23	1.23	1.23	1.23	1.23	1.23	1.23	1.23	1.23	1.22	1.22	1.21	1.21
15% O2 Factor	0.278	0.278	0.279	0.278	0.278	0.278	0.278	0.278	0.278	0.279	0.278	0.28	0.281	0.281	0.282	0.286	0.29	0.297	0.301
BS Calc Factor	145	142	141	139	139	139	139	139	139	139	139	139	139	140	140	141	142	145	146

Catalyst 3: Dithering AFR Sweep

	0.95	0.96	0.97	0.98	0.981	0.983	0.985	0.986	0.988	0.99	0.992	0.994	0.996	0.998	1	1.01	1.02	1.03	1.04	1.05
Engine RPM	1.80E+03	1.80E+03	1.80E+03	1.80E+03	1.80E+03	1.80E+03	1.80E+03	1.80E+03	1.80E+03	1.80E+03	1.80E+03	1.80E+03	1.80E+03	1.80E+03	1.80E+03	1.80E+03	1.80E+03	1.80E+03	1.80E+03	1.80E+03
Power [kW]	2.98E+02	2.98E+02	2.98E+02	2.98E+02	2.98E+02	2.98E+02	2.98E+02	2.98E+02	2.98E+02	2.98E+02	2.98E+02	2.98E+02	2.98E+02	2.98E+02	2.98E+02	2.98E+02	2.98E+02	2.98E+02	2.98E+02	2.98E+02
Torque [N-m]	1.58E+03	1.58E+03	1.58E+03	1.58E+03	1.58E+03	1.58E+03	1.58E+03	1.58E+03	1.58E+03	1.58E+03	1.58E+03	1.58E+03	1.58E+03	1.58E+03	1.58E+03	1.58E+03	1.58E+03	1.58E+03	1.58E+03	1.58E+03
AFR	1.54E+01	1.56E+01	1.57E+01	1.59E+01	1.59E+01	1.59E+01	1.60E+01	1.60E+01	1.60E+01	1.60E+01	1.61E+01	1.62E+01	1.63E+01	1.64E+01	1.65E+01	1.67E+01	1.70E+01	1.72E+01	NaN	1.76E+01
Phi total	1.06E+00	1.05E+00	1.04E+00	1.02E+00	1.02E+00	1.02E+00	1.02E+00	1.02E+00	1.02E+00	1.02E+00	1.02E+00	1.01E+00	1.00E+00	9.99E-01	9.94E-01	9.77E-01	9.63E-01	9.52E-01	NaN	9.28E-01
Air Flow [kg/hr]	1.07E+03	1.06E+03	1.06E+03	1.06E+03	1.06E+03	1.06E+03	1.06E+03	1.06E+03	1.06E+03	1.06E+03	1.06E+03	1.07E+03	1.07E+03	1.07E+03	1.08E+03	1.09E+03	1.10E+03	1.11E+03	NaN	1.14E+03
Exh Flow [kg/hr]	1.14E+03	1.13E+03	1.13E+03	1.13E+03	1.13E+03	1.13E+03	1.13E+03	1.13E+03	1.13E+03	1.13E+03	1.13E+03	1.13E+03	1.14E+03	1.14E+03	1.14E+03	1.16E+03	1.17E+03	1.18E+03	NaN	1.20E+03
BMEP [kPa]	1.10E+03	1.10E+03	1.10E+03	1.10E+03	1.10E+03	1.10E+03	1.10E+03	1.10E+03	1.10E+03	1.10E+03	1.10E+03	1.10E+03	1.10E+03	1.10E+03	1.10E+03	1.10E+03	1.10E+03	1.10E+03	1.10E+03	1.10E+03
thermal eff	3.24E-01	3.30E-01	3.34E-01	3.36E-01	3.37E-01	3.37E-01	3.38E-01	3.38E-01	3.39E-01	3.39E-01	3.40E-01	3.41E-01	3.41E-01	3.42E-01	3.42E-01	3.44E-01	3.46E-01	3.46E-01	NaN	3.47E-01
BSFC [kJ/kW-hr]	1.11E+04	1.09E+04	1.08E+04	1.07E+04	1.07E+04	1.07E+04	1.07E+04	1.07E+04	1.06E+04	1.06E+04	1.06E+04	1.06E+04	1.06E+04	1.05E+04	1.05E+04	1.05E+04	1.04E+04	1.04E+04	NaN	1.04E+04
Abs Humidity	1.44E-03	1.41E-03	1.42E-03	1.44E-03	1.49E-03	1.43E-03	1.47E-03	1.47E-03	1.47E-03	1.49E-03	1.51E-03	1.52E-03	1.54E-03	1.54E-03	1.55E-03	1.56E-03	1.60E-03	1.58E-03	1.59E-03	1.59E-03
BSTHC [g/bkW-hr]	1.20E+00	1.12E+00	1.07E+00	8.77E-01	8.76E-01	8.30E-01	7.39E-01	7.33E-01	5.49E-01	4.11E-01	1.94E-01	3.67E-01	4.55E-01	5.51E-01	6.55E-01	8.18E-01	8.14E-01	7.79E-01	0.75	7.18E-01
BS NOx [g/bkW-hr]	4.95E-01	4.49E-01	2.47E-01	1.79E-01	1.70E-01	1.78E-01	1.35E-01	1.52E-01	6.32E-02	5.35E-02	6.27E-01	5.70E+00	8.16E+00	1.05E+01	1.31E+01	1.99E+01	2.24E+01	2.38E+01	25.3	2.52E+01
BS CO [g/bkW-hr]	3.32E+01	2.38E+01	1.52E+01	4.46E+00	4.20E+00	2.88E+00	1.33E+00	1.27E+00	1.90E-01	8.14E-02	5.59E-02	2.73E-02	2.84E-02	2.87E-02	2.92E-02	3.00E-02	2.99E-02	2.98E-02	NaN	2.90E-02
NOx+CO [g/bkW-hr]	3.37E+01	2.42E+01	1.54E+01	4.64E+00	4.37E+00	3.06E+00	1.47E+00	1.42E+00	2.53E-01	1.35E-01	6.83E-01	5.73E+00	8.19E+00	1.05E+01	1.31E+01	1.99E+01	2.24E+01	2.38E+01	#VALUE!	2.52E+01
CH4 [g/bkW-hr]	3.39E+00	3.23E+00	6.17E+00	1.77E+00	2.86E+00	2.65E+00	1.57E+00	9.30E+00	6.53E+00	1.18E+00	9.34E+00	4.22E+00	4.62E+00	5.16E+00	4.96E+00	4.83E+00	3.59E+00	3.62E+00	#VALUE!	6.63E+00
NH3 [g/bkW-hr]	3.67E+00	2.78E+00	4.16E+00	1.17E+00	1.43E+00	8.37E-01	5.02E-01	1.09E+00	5.66E-01	6.43E-02	1.17E-01	3.45E-02	2.52E-02	1.99E-02	1.39E-02	1.22E-02	8.63E-03	8.32E-03	#VALUE!	1.14E-02
Formaldehyde [g/bkW-hr]	3.69E-04	0.00E+00	0.00E+00	0.00E+00	0.00E+00	0.00E+00	0.00E+00	0.00E+00	0.00E+00	2.58E-04	7.26E-03	0.00E+00	3.00E-03	1.13E-03	5.13E-03	1.93E-03	1.49E-03	3.44E-03	0.00E+00	1.49E-03
NMNEHC [g/bkW-hr]	4.43E-01	2.21E-01	3.60E-01	9.07E-02	1.64E-01	1.04E-01	2.72E-02	2.82E-01	4.45E-01	3.80E-02	4.06E-01	5.71E-02	2.51E-01	1.09E-01	4.17E-02	4.96E-02	1.22E-01	5.33E-02	#VALUE!	1.06E-01
THC @15%O2	1.43E+02	1.37E+02	1.31E+02	1.09E+02	1.09E+02	1.04E+02	9.19E+01	9.16E+01	6.85E+01	5.15E+01	2.43E+01	4.63E+01	5.73E+01	6.96E+01	8.27E+01	1.04E+02	1.04E+02	9.97E+01	9.60E+01	9.16E+01
NOx @15%O2	2.06E+01	1.91E+01	1.06E+01	7.78E+00	7.38E+00	7.77E+00	5.87E+00	6.64E+00	2.75E+00	2.34E+00	2.74E+01	2.51E+02	3.59E+02	4.61E+02	5.77E+02	8.81E+02	9.98E+02	1.06E+03	1.12E+03	1.12E+03
CO @15%O2	2.27E+03	1.66E+03	1.07E+03	3.17E+02	3.00E+02	2.06E+02	9.50E+01	9.12E+01	1.36E+01	5.84E+00	4.01E+00	1.97E+00	2.05E+00	2.08E+00	2.11E+00	2.18E+00	2.19E+00	2.18E+00	2.16E+00	2.12E+00
Wet 2 Dry Scaler	1.24E+00	1.24E+00	1.24E+00	1.23E+00	1.23E+00	1.23E+00	1.23E+00	1.23E+00	1.23E+00	1.23E+00	1.23E+00	1.23E+00	1.23E+00	1.23E+00	1.23E+00	1.22E+00	1.22E+00	1.22E+00	NaN	1.21E+00
15% O2 Factor	2.79E-01	2.78E-01	2.78E-01	2.78E-01	2.78E-01	2.78E-01	2.78E-01	2.78E-01	2.78E-01	2.78E-01	2.78E-01	2.80E-01	2.81E-01	2.82E-01	2.83E-01	2.87E-01	2.91E-01	2.94E-01	2.97E-01	3.00E-01
BS Calc Factor	1.45E+02	1.42E+02	1.41E+02	1.40E+02	1.39E+02	1.39E+02	1.39E+02	1.39E+02	1.39E+02	1.38E+02	1.38E+02	1.39E+02	1.39E+02	1.39E+02	1.40E+02	1.41E+02	1.42E+02	1.43E+02	NaN	1.47E+02

Catalyst 3: Dithering Parameter Sweep

	00amp, 00H:	05amp, 01H:	05amp, 02H:	05amp, 05H:	05amp, 10H:	10amp, 01H:	10amp, 02H:	10amp, 05H:	10amp, 10H:	15amp, 01H:	15amp, 02H:	15amp, 05H:	15amp, 10H:	20amp, 01H:	20amp, 02H:	20amp, 05H:	20amp, 10Hz
Engine RPM	1.80E+03	1.80E+03	1.80E+03	1.80E+03	1.80E+03	1.80E+03	1.80E+03	1.80E+03	1.80E+03	1.80E+03	1.80E+03	1.80E+03	1.80E+03	1.80E+03	1.80E+03	1.80E+03	1.80E+03
Power [kW]	2.98E+02	2.98E+02	2.98E+02	2.98E+02	2.98E+02	2.98E+02	2.98E+02	2.98E+02	2.98E+02	2.98E+02	2.98E+02	2.98E+02	2.98E+02	2.98E+02	2.98E+02	2.98E+02	2.98E+02
Torque [N-m]	1.58E+03	1.58E+03	1.58E+03	1.58E+03	1.58E+03	1.58E+03	1.58E+03	1.58E+03	1.58E+03	1.58E+03	1.58E+03	1.58E+03	1.58E+03	1.58E+03	1.58E+03	1.58E+03	1.58E+03
AFR	1.60E+01	1.60E+01	1.60E+01	1.60E+01	1.60E+01	1.60E+01	1.60E+01	1.60E+01	1.60E+01	1.61E+01	1.61E+01	1.60E+01	1.60E+01	1.61E+01	1.60E+01	1.60E+01	1.60E+01
Phi total	1.02E+00	1.02E+00	1.02E+00	1.02E+00	1.02E+00	1.02E+00	1.02E+00	1.02E+00	1.02E+00	1.02E+00	1.02E+00	1.02E+00	1.02E+00	1.01E+00	1.02E+00	1.02E+00	1.02E+00
Air Flow [kg/hr]	1.06E+03	1.06E+03	1.06E+03	1.06E+03	1.06E+03	1.06E+03	1.06E+03	1.06E+03	1.06E+03	1.07E+03	1.07E+03	1.06E+03	1.06E+03	1.07E+03	1.07E+03	1.06E+03	1.06E+03
Exh Flow [kg/hr]	1.13E+03	1.13E+03	1.13E+03	1.13E+03	1.13E+03	1.13E+03	1.13E+03	1.13E+03	1.13E+03	1.13E+03	1.13E+03	1.13E+03	1.13E+03	1.14E+03	1.13E+03	1.13E+03	1.13E+03
BMEP [kPa]	1.10E+03	1.10E+03	1.10E+03	1.10E+03	1.10E+03	1.10E+03	1.10E+03	1.10E+03	1.10E+03	1.10E+03	1.10E+03	1.10E+03	1.10E+03	1.10E+03	1.10E+03	1.10E+03	1.10E+03
thermal eff	3.39E-01	3.39E-01	3.40E-01	3.40E-01	3.40E-01	3.39E-01	3.39E-01	3.39E-01	3.40E-01	3.38E-01	3.38E-01	3.39E-01	3.40E-01	3.37E-01	3.37E-01	3.38E-01	3.39E-01
BSFC [kJ/kW-hr]	1.06E+04	1.06E+04	1.06E+04	1.06E+04	1.06E+04	1.06E+04	1.06E+04	1.06E+04	1.06E+04	1.06E+04	1.06E+04	1.06E+04	1.06E+04	1.07E+04	1.07E+04	1.06E+04	1.06E+04
Abs Humidity	1.57E-03	1.58E-03	1.62E-03	1.64E-03	1.62E-03	1.63E-03	1.63E-03	1.59E-03	1.62E-03	1.65E-03	1.63E-03	1.66E-03	1.60E-03	1.62E-03	1.62E-03	1.62E-03	1.64E-03
BSTHC [g/bkW-hr]	6.54E-01	4.97E-01	4.98E-01	5.03E-01	4.89E-01	4.21E-01	4.06E-01	4.25E-01	4.43E-01	3.52E-01	3.91E-01	4.25E-01	3.45E-01	3.46E-01	3.80E-01	3.79E-01	3.43E-01
BS NOx [g/bkW-hr]	8.59E-02	1.97E-01	1.34E-01	8.65E-02	7.04E-02	4.55E-01	2.10E-01	9.39E-02	6.50E-02	1.23E+00	3.26E-01	9.40E-02	1.06E-01	1.81E+00	4.38E-01	1.04E-01	8.27E-02
BS CO [g/bkW-hr]	8.74E-02	1.75E-01	1.03E-01	7.76E-02	5.83E-02	3.48E-01	1.34E-01	7.71E-02	5.13E-02	5.25E-01	1.74E-01	8.77E-02	6.05E-02	1.19E+00	2.75E-01	9.34E-02	6.29E-02
CH4 [g/bW-hr]	2.19E+00	2.38E+00	1.29E+00	1.37E+00	1.71E-01	2.37E+00	1.61E+00	1.89E+00	5.08E-02	3.94E+00	2.02E+00	5.66E-01	8.62E-02	4.04E+00	3.57E+00	1.90E+00	4.82E-01
Formaldehyde [g/bkW-hr]	0.00E+00	0.00E+00	1.36E-03	4.26E-04	0.00E+00	0.00E+00	7.30E-04	8.29E-04	0.00E+00	0.00E+00	1.36E-03	0.00E+00	4.41E-05	5.12E-04	0.00E+00	0.00E+00	3.79E-04
NH3 [g/bkW-hr]	6.51E-02	1.36E-01	5.58E-02	3.95E-02	2.85E-02	2.17E-01	7.02E-02	4.48E-02	1.42E-02	3.58E-01	1.04E-01	2.26E-02	2.98E-02	6.13E-01	1.96E-01	4.95E-02	9.23E-02
Acetaldehyde [g/bkW-hr]	1.06E-02	3.80E-04	-2.54E-03	5.39E-03	1.58E-03	4.32E-03	1.42E-02	8.22E-03	2.84E-04	7.09E-02	1.57E-03	1.15E-03	7.73E-04	2.87E-02	2.08E-02	8.73E-03	5.31E-03
NMNEHC [g/bkW-hr]	8.53E-02	7.06E-02	2.82E-02	3.03E-02	4.40E-03	4.26E-03	7.63E-02	6.67E-02	4.25E-04	8.44E-02	7.58E-02	1.99E-02	3.43E-03	4.18E-01	2.13E-01	5.10E-02	2.53E-02
THC @15%O2	8.18E+01	6.19E+01	6.21E+01	6.27E+01	6.09E+01	5.22E+01	5.03E+01	5.27E+01	5.50E+01	4.35E+01	4.82E+01	5.24E+01	4.27E+01	4.25E+01	4.67E+01	4.68E+01	4.25E+01
NOx @15%O2	3.75E+00	8.56E+00	5.82E+00	3.76E+00	3.06E+00	1.97E+01	9.08E+00	4.06E+00	2.81E+00	5.28E+01	1.40E+01	4.05E+00	4.58E+00	7.73E+01	1.87E+01	4.45E+00	3.57E+00
CO @15%O2	6.27E+00	1.25E+01	7.32E+00	5.54E+00	4.15E+00	2.47E+01	9.55E+00	5.48E+00	3.65E+00	3.71E+01	1.23E+01	6.20E+00	4.28E+00	8.38E+01	1.94E+01	6.59E+00	4.46E+00
Wet 2 Dry Scaler	1.23E+00	1.23E+00	1.23E+00	1.23E+00	1.23E+00	1.23E+00	1.23E+00	1.23E+00	1.23E+00	1.23E+00	1.23E+00	1.23E+00	1.23E+00	1.23E+00	1.23E+00	1.23E+00	1.23E+00
15% O2 Factor	2.79E-01	2.78E-01	2.78E-01	2.78E-01	2.78E-01	2.78E-01	2.78E-01	2.78E-01	2.78E-01	2.79E-01	2.79E-01	2.78E-01	2.79E-01	2.79E-01	2.78E-01	2.78E-01	2.79E-01
BS Calc Factor	1.39E+02	1.39E+02	1.39E+02	1.39E+02	1.39E+02	1.40E+02	1.40E+02	1.40E+02	1.40E+02	1.41E+02	1.41E+02	1.41E+02	1.40E+02	1.42E+02	1.41E+02	1.41E+02	1.40E+02

Parameters Recorded for Each Test

- Engine RPM
- Power [kW]
- Torque [N-m]
- THC [ppm]
- NOx [ppm]
- O2 [%]
- CO2 [%]
- CO [ppm]
- Jacket Water In [C]
- Jacket Water Out [C]
- Dyno In [C]
- Dyno Out [C]
- ACW In [C]
- ACW Out [C]
- JW Loop Temp [C]
- Spare TC106 [C]
- Oil Sump Temp [C]
- Compressor Out [C]
- Turbine In Temp [C]
- Inlet Air Temp [C]
- Turbine Out Temp [C]
- ACW Loop Supply [C]

- Cat Oil 1 [C]
- Cat Oil 2 [C]
- Cylinder 1 Exh [C]
- Cylinder 2 Exh [C]
- Cylinder 3 Exh [C]
- Cylinder 4 Exh [C]
- Cylinder 5 Exh [C]
- Cylinder 6 Exh [C]
- Cylinder 7 Exh [C]
- Cylinder 8 Exh [C]
- IMAT [C]
- Throttle Temp [C]
- Aftertreatment Inlet [C]
- Aftertreatment Outlet [C]
- Fuel Flow [kg/hr]
- Fuel Temperature [C]
- Spare mA02
- Exhaust Back Pres [kPa]
- Inlet Air Pressure [kPa]
- Fuel Pressure [kPa]
- IMAP [kPa]
- Compressor Pres [kPa]
- Throttle Diff Pres [kPa]

- Spare V05
- Boiler Supply Temp [C]
- Boiler Return Temp [C]
- Jacket Water Flow [LPM]
- Intercooler Flow [LPM]
- Dyno Water Flow [LPM]
- Steam Valve [%]
- Supercharger Speed [%]
- SC IC Ctrl Valve Pos [%]
- Exh Valve Pos [%]
- Air Flow Temp [C]
- Air Flow Diff [kPa]
- Air Flow Static [kPa}
- Inlet Air RH [%]
- Vaisala Temp [C]
- AGA Air Flow [kg/s]
- AmbientAirPress
- DesiredAFR_Final
- ECM_NOx
- EFR_LseriesCmd_Prct
- FuelTemp
- GasDeltaPress
- ManifoldAirPress_kPa

- MassAirFlow_kghr
- ManifoldAirTemp_degC
- NGFlowCmd_Final
- RPM_Setpoint_final
- ThrottlePosition
- UEGO1_Actual_AFR
- UEGO2_Actual_AFR
- UEGO1_O2_Percent
- UEGO2_O2_Percent
- Fuel Control Desired AFR
- AFR Modifier Desired AFR
- UEGO1 Lambda